Copyright Warning & Restrictions

The copyright law of the United States (Title 17, United States Code) governs the making of photocopies or other reproductions of copyrighted material.

Under certain conditions specified in the law, libraries and archives are authorized to furnish a photocopy or other reproduction. One of these specified conditions is that the photocopy or reproduction is not to be "used for any purpose other than private study, scholarship, or research." If a, user makes a request for, or later uses, a photocopy or reproduction for purposes in excess of "fair use" that user may be liable for copyright infringement,

This institution reserves the right to refuse to accept a copying order if, in its judgment, fulfillment of the order would involve violation of copyright law.

Please Note: The author retains the copyright while the New Jersey Institute of Technology reserves the right to distribute this thesis or dissertation

Printing note: If you do not wish to print this page, then select "Pages from: first page # to: last page #" on the print dialog screen

ABSTRACT

BRAINLESS BUT SMART: INVESTIGATING COGNITIVE-LIKE BEHAVIORS IN THE ACELLULAR SLIME MOLD *PHYSARUM POLYCEPHALUM*

by
Subash Kusum Ray

Evolutionary pressures to improve fitness, have enabled living systems to make adaptive decisions when faced with heterogeneous and changing environmental and physiological conditions. This dissertation investigated the mechanisms of how environmental and physiological factors affect the behaviors of non-neuronal organisms. The acellular slime mold *Physarum polycephalum* was used as the model organism, which is a macroscopic, unicellular organism, that self-organizes into a network of intersecting tubules. Without using neurons, *P. polycephalum* can solve labyrinth mazes, build efficient tubule networks, and make adaptive decisions when faced with complicated trade-offs, such as between food quality and risk, speed and accuracy, and exploration and exploitation. However, the understanding of the mechanisms used by *P. polycephalum* in exhibiting such behaviors is very limited. Therefore, the objective of this dissertation is to understand the mechanisms adopted by non-neuronal organisms to explore and exploit resources in the physical environment, using environmental and physiological information.

To this end, the dissertation characterizes the direction and amount of influence between different regions of tubule-shaped *P. polycephalum* cells in binary food choice experiments. The results show that when the two food sources

are identical in quality, the regions near the food source act as the drivers of *P. polycephalum* tubule behavior. Conversely, when one of the food sources is more enriched with nutrients, the regions near the rejected food source were found to drive the tubule behavior. Secondly, a generalized choice-making criterion was formulated to determine the choice-making behaviors of *P. polycephalum*, examine whether sufficient experimental time was given to make a choice, and determine the time point at which a choice was made. The criterion was tested on binary food choice experiments using *P. polycephalum* tubules. The results show that *P. polycephalum* made a choice for the option for the better food option, except when the differences in food quality were low. Moreover, the criterion was found to not determine the choice-making behaviors when the food sources presented were identical in quality. Thirdly, the dissertation investigated whether *P. polycephalum* cells modify their future exploratory behavior using their past foraging experience. The results did not find a strong influence of the past foraging experience on the exploratory networks formed by *P. polycephalum* cells. Finally, *P. polycephalum* exploratory behaviors were examined and compared when the cells were in high-energy versus low-energy physiological conditions. Interestingly, the study found the *P. polycephalum* cells in low-energy conditions show an increased tendency to split themselves into multiple autonomous cells. Additionally, the behavior is shown to increase the fitness of the cell by increasing its foraging efficiency.

BRAINLESS BUT SMART: INVESTIGATING COGNITIVE-LIKE BEHAVIORS IN THE ACELLULAR SLIME MOLD PHYSARUM POLYCEPHALUM

by

Subash Kusum Ray

A Dissertation
Submitted to the Faculty of
New Jersey Institute of Technology
and Rutgers, The State University of New Jersey - Newark
in Partial Fulfillment of the Requirements for the Degree of
Doctor of Philosophy in Biology

Federated Biological Sciences Department

August 2022

APPROVAL PAGE

BRAINLESS BUT SMART: INVESTIGATING COGNITIVE-LIKE BEHAVIORS IN THE ACELLULAR SLIME MOLD PHYSARUM POLYCEPHALUM

Subash Kusum Ray

Dr. Simon Garnier, Dissertation Advisor — Date
Associate Professor of Biological Sciences, NJIT

Dr. Horacio G. Rotstein, Committee Member — Date
Professor of Biological Sciences, NJIT

Dr. Gareth J. Russell, Committee Member — Date
Associate Professor of Biological Sciences, NJIT

Dr. Gregory F. Weber, Committee Member — Date
Assistant Professor of Biological Sciences, University of Indianapolis, IN

Dr. David L. Hu, Committee Member — Date
Professor of Mechanical Engineering and Biology, Georgia Institute of Technology, Atlanta, GA

BIOGRAPHICAL SKETCH

Author: Subash Kusum Ray

Degree: Doctor of Philosophy

Date: August 2022

Undergraduate and Graduate Education:

- Doctor of Philosophy in Biological Sciences,
  New Jersey Institute of Technology and Rutgers University – Newark,
  Newark, NJ, 2022

- Master of Science in Biological Sciences,
  New Jersey Institute of Technology, Newark, NJ, 2014

- Bachelor of Technology in Biotechnology,
  ICFAI University, Dehradun, India, 2012

Major: Biological Sciences

Presentations and Publications:

Ray, Subash K., Abid Haque, Jason Graham, and Simon Garnier, "Physical basis of problem-solving in the acellular slime mold *Physarum polycephalum*", *Animal Society Conference (ABS 2021)*, *Virtual conference*, August 2021.

Ray, Subash K., and Simon Garnier, "Distributed Information transfer in the slime mold *Physarum polycephalum*", *Colloquium Presentation at Federated Department of Biological Sciences*, *NJIT & Rutgers-Newark*, Newark, NJ, May 2021.

Ray, Subash K., Gabriele Valentini, Purva Shah, Abid Haque, Chris R. Reid, Gregory F. Weber, and Simon Garnier, "Distributed information transfer in slime mold *Physarum polycephalum*", *The Association for the Study of Animal Behavior Annual Conference 2019 (ASAB 2019), University of Konstanz & Max-Planck Institute of Animal Behavior,* Konstanz, Germany, August 2019.

Ray, Subash K., and Simon Garnier, "Distributed Information transfer in the slime mold *Physarum polycephalum*", *Research Day at Federated Department of Biological Sciences, NJIT & Rutgers-Newark*, Newark, NJ, May 2019.

Ray, Subash K., Gabriele Valentini, Purva Shah, Abid Haque, Gregory F. Weber, and Simon Garnier, “Information transfer in the slime mold *Physarum polycephalum* membrane during decision-making”, *Animal Society Conference (ABS 2018), University of Wisconsin,* Milwaukee, WI, USA, August 2018.

Ray, Subash K., Gabriele Valentini, Purva Shah, Abid Haque, Gregory F. Weber, and Simon Garnier, “Information transfer in the contractile membrane of slime mold *Physarum polycephalum*”, *Northeast Regional Conference on Complex Systems, Binghamton University,* Binghamton, NY, USA, April 2018.

Ray, Subash K., and Simon Garnier, “Brainless intelligence: the curious case of acellular slime mold *Physarum polycephalum*”, *Young Researchers Workshop: Current trends in kinetic theory, Center for Scientific Computation & Mathematical Modeling, University of Maryland, College Park*, Maryland, USA, October 2017.

Ray, Subash K., Chris R. Reid, Michael Holmes, Tanya Latty, and Simon Garnier, “Relationship between surface object properties and sunlight exposure in nests of meat ants *Iridomyrmex purpureus”, International Congress of Entomology (ICE 2016)*, Orlando, Florida, USA, September 2016.

Ray, Subash K., Chris R. Reid, Michael Holmes, Tanya Latty, and Simon Garnier, “Relationship between surface object properties and sunlight exposure in nests of meat ants *Iridomyrmex purpureus*”, *Social Insect In the North-East Region (SINNERS) at University of Scranton*, Scranton, Pennsylvania, USA, December 2015.

Ray, Subash K., Chris R. Reid, Jason Graham, and Simon Garnier, “What drives an ant colony to choose the shortest path?”, *Social Insect In the North-East Region (SINNERS) at Boston University*, Boston, Massachusetts, USA, June 2015.

Ray, Subash K., Gabriele Valentini, Purva Shah, Abid Haque, Chris R. Reid, Gregory F. Weber, and Simon Garnier (2019) Information transfer during food choice by the slime mold *Physarum polycephalum*. Front Ecol Evol 7:67. https://doi. org/10.3389/fevo.2019.00067.

This work is dedicated to Ma and Baba

ACKNOWLEDGEMENT

First, I would like to thank my Dissertation Advisor, Dr. Simon Garnier. For more than nine years, his dedicated and constant support, mentorship, encouragement, trust, and patience have been the primary guiding voice to get me where I am today both as a scientist and a person. Without his guidance and scientific insight, this dissertation would have been impossible.

I also like to thank the members of my Dissertation Committee: Dr. Horacio Rotstein, Dr. Gareth Russell, Dr. Gregory Weber, and Dr. David Hu for their scientific insights and feedback throughout the Ph.D. process. In particular, I would like to thank Dr. Gregory Weber for his scientific insight, advice, and numerous conversations that helped me think more critically about my work and better understand the cell and molecular aspects of my research. I appreciate the financial support granted to me from the Federated Department of Biological Sciences at NJIT and Rutgers University - Newark, and the National Science Foundation (NSF grant No. IOS-1557610).

I am highly indebted to my undergraduate research assistants, Ms. Purva Shah, Ms. Zainab Shahsamand, Mr. Chukwueloka (Eloka) Anemelu, and Mr. Amogh Sakhvala, and high-school research assistants, Ms. Shayna Turbin and Emma Morin, for their immense hard work, dedication, and meticulousness in helping and performing the experiments.

I thank my many mentors and collaborators: Dr. Chris Reid, Dr. Jason Graham, and Dr. Gabriele Valentini for their continued academic support and timely suggestions and help in making this a better project.

I am thankful to my peers in the NJIT and Rutgers-Newark graduate program for their friendship, academic, and personal support. I would particularly like to thank my lab mates: Mr. Raphael Asfour, Dr. Yohann Chemtob, Ms. Nicole Dykstra, Mr. Abid Haque, Dr. Isabella Muratore, Ms. Courtney Rockenbach, and Dr. Maggie Wisniewska for being amazing colleagues and friends.

Finally, I thank my parents, Ms. Nupur Ray and Mr. Subhrendu Sekhar Ray, my brother and sister-in-law, Mr. Snigdho Kusum Ray and Ms. Priyanka Mukherjee, and my partner, Ms. Swayam Tripathy for their endless and unwavering love, support, strength, and encouragement every day and at every step of this long and challenging journey. Reaching this point seems unfathomable without your support.

TABLE OF CONTENTS

TABLE OF CONTENTS
(Continued)

TABLE OF CONTENTS
(Continued)

LIST OF TABLES

LIST OF FIGURES

LIST OF FIGURES
(Continued)

Figures **Page**

LIST OF FIGURES
(Continued)

LIST OF FIGURES
(Continued)

Figures **Page**

LIST OF FIGURES
(Continued)

LIST OF FIGURES
(Continued)

Figures **Page**

CHAPTER 1

INTRODUCTION

1.1 Background

Organisms are confronted with choices - such as what food to eat, where to live, and when to forage - throughout the course of their lifetime. These choices are essential as each available option of each choice can have a different impact on the fitness of the organism. For example, a food patch may be located at a farther distance relative to another patch; a particular food source may provide better nutrients than another food source; or the microclimatic conditions of a particular environment may provide better growing conditions than another environment. However, the environments inhabited by the organisms and their physiological conditions are heterogeneous and continuously changing. As a result, the range of options available for each choice is seldom available in advance, and the fitness consequences of pursuing each option is difficult to evaluate. Therefore, in order to increase fitness, natural selection has enabled organisms to evolve exploration and exploitation strategies that help make adaptive choices when faced with difficult environmental and physiological conditions.

For example, when organisms forage in patchy and unpredictable environments, they use a random walk based strategy to maximize their search area for resources while minimizing costs associated with exploration (e.g., in wandering albatross *Diomedea exulans* (*1*), spider monkeys *Ateles geoffroyi* (*2*), and blacked-backed jackal *Canis mesomelas* (*3*)). Conversely, when the

resources in the environment are predictable, organisms switch to more energetically efficient, systematic exploratory strategies (e.g., in bumblebees *Bombus impatiens* (*4*), hummingbirds *Phaethornis longirostris* and *Selasphorus rufus* (*5*, *6*), and bison *Bison bison* (*7*)). Similarly, organisms in poor-nutritional conditions increase their exploratory and risk-taking behaviors to increase their chances of discovering food in the environment (e.g., in earthworm *Pumbricus terrestris* (*8*), pigs *Sus domesticus* (*9*), and black garden ants *Lasius niger* (*10*)).

Scientific studies exploring exploration and exploitation in various organisms have primarily focused on “neuronal” or so-called cognitive organisms. These organisms have evolved a neuron-based information processing system that helps them make such choices with ease. However, “non-neuronal” organisms - such as bacteria, fungi, plants, and protists - constitute the vast majority of living species on Earth (*11*), and have existed long before the evolution of neurons (*12*).

Non-neuronal organisms live in complex and changing environments, and hence, are subject to the same challenges as neuronal organisms. For example, non-neuronal organisms must choose between multiple resources of varying quality, search for resources in their environments, select habitats with better microclimatic conditions, adapt to changing environmental and physiological conditions, and respond to multiple and conflicting sources of environmental information. However, the specific mechanisms used by non-neuronal organisms to process environmental and physiological information are not well understood. Therefore, the big question that I am trying to answer is how environmental and physiological factors affect the adaptive behaviors of non-neuronal organisms.

In this dissertation, I used the acellular slime mold *Physarum polycephalum* as a model organism to understand the mechanisms adopted by non-neuronal organisms to explore and exploit resources in the physical environment, using environmental and physiological information.

1.2 *Physarum polycephalum* as a Model Organism

P. polycephalum is a large, single-celled, multi-nucleated protist, belonging to the phylum Amoeboazoa and class Myxogastria. *P. polycephalum* is closer to the animal-fungal clade than compared to green plants (*13*). It inhabits shady, cool, and moist areas of temperate forests, and is primarily found in Australia, Europe, North America, and Japan. The life cycle of *P. polycephalum* is composed of multiple life stages that include plasmodia, fruiting body, and spores. The cell achieves a large, macroscopic size when in the plasmodium and fruiting body stage, and therefore, can be observed by an unaided eye. In this stage, the cell moves by extending pseudopods in an amoeba-like fashion to explore its environment, hence referred to as “multi-headed” (which translates to polycephalum in Latin). The exploratory search front of the cell advances in a dense fan-like shape, followed by an interconnected network of tubules (*14*), where the protoplasm (containing cytoplasm, organelles, nutrients, and signaling molecules) flows in a rhythmic back-and-forth manner called shuttle-streaming (*15*, *16*). In the presence of abundant food, the plasmodia are capable of covering an area exceeding 900 cm^2 and moving up to a speed of 5 cm/hr (*14*). When under nutritional stress and light irradiation, the plasmodia form fruiting bodies called

sporangium that contain haploid spores of the organism. The haploid spores can get dispersed widely into different environments using wind or water currents. When the spores find hospitable habitats, they germinate to form microscopic myxamoebae. The myxamoebae are motile and can reproduce asexually. Moreover, when two strains of myxamoeba of different mating types meet, they fuse to form a diploid *P. polycephalum* plasmodia.

Despite lacking a neuron-based information processing system, *P. polycephalum* can demonstrate complex behaviors. For example, a *P. polycephalum* cell can find the shortest path to connect two food sources in a complex labyrinth maze (*17*). Tero et al. (2010) found that *P. polycephalum* is capable of forming adaptive networks that have efficiency, cost, and fault tolerance similar to those found in human-made structures (*18*). While exploiting multiple food sources of varying quality, *P. polycephalum* can achieve its intake target (2:1 protein to carbohydrate ratio), by allocating a precise amount of biomass to each food source based on its nutrient composition (*19*). In additiona, *P. polycephalum* can: 1) solve complex optimization problems that are challenging for computer programs (*20*); 2) anticipate periodic events (*21*); 3) avoid previously exploited areas by using its extracellular slime trail (*22*); 4) habituate to a repeated irrelevant stimulus (*23*, *24*); and even 5) make economically irrational choices that before were considered a by-product of a neuron-based decision-making system (*25*).

Additionally, *P. polycephalum* can integrate information from multiple and conflicting sources, and solve problems by making complicated trade-off decisions. For example

, in Latty and Beekman (2010), when an attractive resource (e.g. high-quality food source) was placed in a repellent environment (e.g. bright-lit area), *P. polycephalum* chose the higher quality food source only when it was five times higher in concentration than the lower quality food source (*26*). Similarly, *P. polycephalum* has been observed to achieve trade-offs between risk and efficiency (*27*). When half of the region between two diagonally placed food sources was illuminated with light, *P. polycephalum* avoided the shortest path to join the food sources. The food sources were joined such that, the light exposure of the tubule was reduced, but the light was not completely avoided, as it might overly elongate the network (*27*). *P. polycephalum* cells are also subject to other well-studied trade-offs in cognitive sciences, such as between speed and accuracy while making foraging decisions (*28*), and between exploration and exploitation when foraging in unpredictable environments (*29*).

Figure 1.1 *P. polycephalum* plasmodia grown on 1% agar solution in a Petri plate (Ø = 10 cm, *H* = 1.5 cm) with oatmeal flakes as food embedded in the agar gel.

P. polycephalum is a unique and novel model organism, which combines the experimental tractability of a macroscopic unicellular organism with the emergent, complex behaviors of multi-cellular organisms. Its behavior can be seen with the naked eye, and choice-making strategies can be observed in real-time (*30*). *P. polycephalum* is readily available and easy to culture, manipulate (it can be fashioned into different shapes and sizes), and control (such that past

experience, nutritional state, and extraneous information do not confound the results). Moreover, the complete genome of *P. polycephalum* was recently sequenced (*31*), and studies have shown that *P. polycephalum* is accessible to genetic manipulations (*32*, *33*). All these qualities, coupled with its ability to demonstrate incredible problem-solving behaviors, make *P. polycephalum* an ideal system for the detailed study of cognitive-like capabilities in a non-neuronal organism.

1.3 Objective

The goal of this dissertation is to understand the mechanisms used by *P. polycephalum* in using information from the environment and physiological state to explore and exploit resources in the physical environment. To achieve this, I along with my collaborators, have tried answering four broad questions, with each question forming a chapter of this dissertation. The details are as follows:

1) **How does *P. polycephalum* process information when choosing between two food sources?**

The role of this chapter is to understand the flow of information between different regions of a *P. polycephalum* tubule when the cell is choosing between two food sources. I tested *P. polycephalum* tubules in two different food choice conditions, i.e., a symmetric food choice condition and an asymmetric food choice condition. In the symmetric food choice condition, the two food sources presented to the cells were identical in quality. Whereas, in the asymmetric food choice condition, one of

the food sources was more enriched with nutrients than the other. I used the information-theoretic tool of transfer entropy to measure the amount and direction of information flow between different regions of a tubule. I observed that in the symmetric food choice conditions, the tubule regions near the two food sources acted as the information source, and the regions in the middle were information destinations. However, contrary to our expectation, in the asymmetric food choice condition, I observed the tubule regions near the rejected food source acted as the sources of information, and the tubule region near the chosen food source acted as the destination of the information. In summary, I found that in the symmetric food choice condition, the regions near the two food sources acted as the driver of *P. polycephalum* tubule behavior, and in the asymmetric food choice condition, the regions near the rejected food source acted as the drivers of the cell behavior.

2) Could there be a generalized criterion to decide whether *P. polycephalum* made a choice to exploit available resources?

The objective of this chapter is to formulate a generalized criterion that can be used across different experimental frameworks to a) determine whether *P. polycephalum* can choose the best resources when presented with an option between two alternatives, b) examine whether the experimental time allotted was sufficient to make a choice, and c) determine the time point when the cell made the choice. The criterion formulated in this chapter tested the null hypothesis that the relative difference in foraging effort distributed by *P. polycephalum* cells towards the most rewarding resource would be proportional to the relative

difference in quality between the available resources. I tested this criterion by placing *P. polycephalum* tubules in binary food choice experiments with varying quality of the resources. The criterion found that the tubule chose the better resource, except in the case when the difference in quality between the resources was too small. In this case, the experimental time period was found to be insufficient for the tubules to make a choice. Moreover, the criterion did not determine choice-making in *P. polycephalum* tubules when the food sources presented were identical in quality.

3) Can *P. polycephalum* integrate past foraging experience in its future exploration strategy?

In this chapter, I investigated whether *P. polycephalum* modifies its exploratory behavior in response to the frequency of food sources encountered in its past. I conducted experiments with different distribution of food sources, and then studied the subsequent exploratory network formed by the *P. polycephalum* cells. Three different *P. polycephalum* network properties were measured, namely, Sparsity (i.e., a measure of scatteredness of the network), Isotropy (a measure of angular spread of the network), and rate of exploration (i.e., a measure of showing the rate of growth of the network). In this study, I did not find a strong influence of the past foraging environment in any of the network properties.

4) How does *P. polycephalum* explore its environment when in different physiological states?

The role of this chapter was to explore and compare the difference in exploratory behavior of *P. polycephalum* cells, when in a high-energetic and a low-energetic states. I created *P. polycephalum* cells in the high-energetic state by providing cells access to food before measuring their behavior. Conversely, created low-energetic states by removing the cell's access to food 24 hours before measuring their exploratory behavior. Interestingly, I found that cells in low-energetic or starved states split into multiple autonomous subunits to explore their environment. Moreover, using a conceptual agent-based model, I show that the property of starved cells to split into multiple autonomous units, increases the chances of at least one cell finding food in their environment. Such an adaptive strategy of splitting oneself to survive harsh physiological environments has not been observed in any organism before.

CHAPTER 2

HOW DOES *P. POLYCEPHALUM* PROCESS INFORMATION WHEN CHOOSING BETWEEN TWO FOOD SOURCES?

Originally published in *Frontiers in Ecology and Evolution*:

Ray, S.K., Valentini, G., Shah, P., Haque, A., Reid, C.R., Weber, G.F., and Garnier, S. (2019). Information transfer during food choice in the slime mold *Physarum polycephalum*. Frontiers in Ecology and Evolution, 7:67.

2.1 Introduction

In order to develop, survive and reproduce, all living organisms have to make decisions regarding what resource to exploit, which microclimate to inhabit, when to forage in an environment, etc. Therefore, natural selection has led to the evolution of information processing capabilities in living systems that help them make adaptive choices in the face of complex and changing environmental conditions. The majority of the studies on decision-making has focused on organisms with a neuron-based information processing system, and it is only recently that researchers have started investigating non-neuronal organisms in the context of decision-making (see (*34*) and (*12*) for full review). Non-neuronal organisms - like plants, bacteria, fungi, and protist - constitute a majority of living species on Earth and do not possess cells and organs dedicated to integrating information from their multiple sensory systems. These organisms have existed long before the evolution of neuronal organisms (*12*) and, despite lacking neurons, have the capability to process information in order to exploit their environment in a non-random, adaptive fashion. For example, *Escherichia coli* bacteria have been shown to select the best of multiple resources of varying quality (*35*).

Rhodospirillum and *Rhodobacter* bacteria (*36*), *Dictyostelium discoideum* protists (*37*), *Phytophthora capsici* oomycetes (*38*) actively move toward locations with microclimates more favorable to their development. Moreover, *Paenibacillus dendritiformis* bacteria (*39*, *40*), *Abutilon theophrasti* plants (*41*), *Phanerochaete velutina* fungi (*42*), *Dictyostelium discoideum* protists (*43*) make compensatory decisions when faced with multiple conflicting sources of environmental information. However, little is known about the mechanisms by which non-neuronal organisms integrate multiple, sometimes conflicting sources of information when navigating their environment in search for better living conditions.

The acellular slime mold *Physarum polycephalum* has recently emerged as a model system for studying information processing and problem-solving in non-neuronal organisms (*30*, *44*). *P. polycephalum* is a unicellular, multi-nucleated protist that can cover an area of over 900 cm^2 (*14*) and move up to a speed of 5 cm/hour (*45*). Despite lacking neurons, *P. polycephalum* shows complex decision-making behaviors. For example, it can solve labyrinth mazes (*17*); form adaptive networks balancing efficiency, cost and fault tolerance, similar to those found in man-made structures (*18*); solve complex optimization problems (*20*); anticipate periodic events (*21*); avoid previously exploited areas by using its extracellular slime trail as an externalized memory (*22*); habituate to repeated irrelevant stimuli (*23*); and even make economically irrational decisions that were previously deemed a by-product of neuronal decision-making only (*25*). Combined with its macroscopic scale and its experimental tractability, the cognitive-like abilities of *P.*

polycephalum make it a unique model organism to investigate the mechanisms of problem-solving in non-neuronal systems.

Previous studies have suggested that the problem-solving abilities of the slime mold *P. polycephalum* are driven by a coupled-oscillator based sensorimotor system present in its membrane (*46*, *47*). Indeed, *P. polycephalum's* membrane is composed of multiple rhythmically contractile regions that lead to the emergence of a complex pattern of contraction-relaxation cycles at the organism level. The contractions occur about once every 60-120 seconds (*48*) and result from the activity of the actomyosin protein networks that comprise the cell cytoskeleton (*49*). The membrane contraction-relaxation cycles are coordinated at the organismal level such that they cause the protoplasm[1] to flow rhythmically back and forth throughout the cell (*50*), a phenomenon called shuttle streaming. The individual contractile regions change their contraction intensity in response to both the quality of the local environment (*51–54*) and the contraction intensities of the neighboring regions (i.e., the coupling between the neighboring contractile regions) (*46*, *52*). Previous studies have found that the contraction intensities in the slime mold *P. polycephalum* can change both in frequency (*46*, *52*) and amplitude (*55*). When a region of a *P. polycephalum* encounters an attractive (e.g., a food source) or a repulsive (e.g., bright areas) stimulus in the local environment, the contraction intensity of the region increases or decreases, respectively. The coupling between the neighboring regions triggers a change in the pattern of membrane contractions

[1] Protoplasm: is the sol-like substance flowing within a *P. polycephalum* cell. The protoplasm contains the cell cytoplasm, organelles, nutrients and signaling molecules.

throughout the cell, followed by the movement of the cell towards attractive and away from repulsive stimuli (*46*, *52*, *54*). Therefore, this coupling is a potential mechanism for transferring information about the quality of the local environment to distant regions of the cell.

This information processing mechanism in *P. polycephalum* is part of the broader class of distributed decision-making mechanisms present in numerous biological systems (*56*). Decision-making in these systems is decentralized (i.e., without a leader or a pre-designed blueprint), with different parts of the system changing their behavior based on information extracted from the local environment and/or transferred from neighboring parts (*57*). Information transfer between the parts is achieved via repeated interactions and enables the system to collectively integrate information about the environment and generate a response at the level of the group. For example, (*58*) showed that local visual interactions in schools of golden shiner fish (*Notemigonus crysoleucas*) allow individuals informed about the location of a resource to steer the entire group toward it. Non-neuronal organisms have also been observed to process information and solve problems in a distributed fashion (reviewed in (*34*)). For example, in *Arabidopsis thaliana* plants, information about a herbivore attack on a leaf is transferred to the undamaged parts through the transfer of molecular Ca^{2+} signals (*59*). This information is subsequently used by the undamaged parts to activate their defense responses against herbivory.

Our objective in this study is to investigate the distributed information transfer between different contractile regions in *P. polycephalum*, in the presence

of an attractive stimulus (i.e., a food source). To this effect, we recorded the contraction-relaxation pattern of a straight tubule-shaped cell of *P. polycephalum* connected on both ends to two food sources. We tested two experimental conditions: a symmetric condition in which both food sources were identical in their nutrient concentration, and an asymmetric condition in which one food source was more concentrated with nutrients than the other one. We measured the contractile behavior of different parts on the tubule while the cell was integrating and processing information about the food sources. Finally, we used a model-free, information-theoretic tool known as transfer entropy to measure the relative influence of the contraction-relaxation pattern of each tubule regions on the others.

The concept of transfer entropy is built upon the theoretical concept of Shannon entropy (*60*). Shannon entropy (hereafter simply referred to as entropy) is a measure that quantifies the degree of uncertainty in predicting the value of a random variable. For example, consider the thickness of a region of a *P. polycephalum* as a random variable determined by the cyclical pattern of contractile behavior of that region. In a condition with complete lack of contractions, i.e., constant thickness over time and no cycle, entropy is precisely zero, independent of the particular thickness value. When the cycles are more variable, i.e., changing in either frequency or amplitude over time, the thickness of the *P. polycephalum* region is characterized by high uncertainty and therefore high entropy. We can take a step further and look at how the entropy of different regions of a *P. polycephalum* are related to each other. Transfer entropy is a tool that measures the reduction in uncertainty in the future values of a focal random

variable when we take into consideration its past values as well as the current values of another random variable (*61*). It is the entropy in common between the present of one variable and the future of the other. Due to this directionality in time, it can be interpreted as the directed transfer of information between these two variables. In our case, it measures the reduction in uncertainty of the future thickness values of a focal region given knowledge of the current thickness of a different region. Conceptually, transfer entropy quantifies the direction and amount of predictive information between two dynamical processes (*62*). Although it is not a measure of causality, as it can lead to false positives, it can identify causal interactions when present. For this reason, transfer entropy has been used to infer leader-follower relationships in bats (*63*) and zebrafishes (*64*), to study animal-robot interactions (*65*), neural connections in the brain (*66*, *67*), decision-making in agent collectives (*68*) as well as information transfer between financial time-series (*69*).

Several attempts to characterize information transfer in *P. polycephalum* have been made before (*46*, *52*, *55*, *56*), but none of them relied on a formal definition of information and formal tools to characterize its dynamics. Information theory provides us with a toolbox that we use here to quantify the direction and amount of information transferred between different contractile regions of *P. polycephalum* when choosing between two food sources. We find that the direction of information transfer in a *P. polycephalum* tubule differs with the food choice condition presented and the amount of information transferred is inversely proportional to the distance between the contractile regions along a *P.*

polycephalum tubule. Our results provide a characterization of information transfer in *P. polycephalum*, which can inform and guide the design of future experiments for understanding the functioning of this organism, and contribute to a more general understanding of the role of information and its fundamental processes - storage, transfer and modification (*70*) - in other distributed computing systems.

2.2 Materials and Methods

2.2.1 Biological Material

The acellular slime mold *P. polycephalum* is a protist (phylum Amoebozoa, class Myxogastria) that inhabits shady, cool and moist areas of temperate forests. In its vegetative or "plasmodium" stage, it exists as a macroscopic cell with a large number of nuclei freely floating within the protoplasm, without any cellular plasma membrane separating them. The plasmodium moves through its environment by extending and retracting multiple tubular extensions (referred to as pseudopods) in an amoeba-like fashion (Figure 2.1A). As a consequence of this feature, it is referred to as the multi-headed (*polycephalum* in Latin) slime mold.

For our experiments, *P. polycephalum* stocks were obtained from Carolina Biological Supply Company® and cultured in Petri plates (ø = 10 cm, H = 1.5 cm) in a dark environment with a controlled temperature of 26°C. Each Petri plate was filled with a water solution with 1% w/v (weight/volume) non-nutrient agar to provide a gel-like, moist substrate, and 5% w/v blended oat flakes (Quaker Oats Company®) as food. Laboratory stocks were recultured on a weekly basis using new, 5% w/v oat-agar plates.

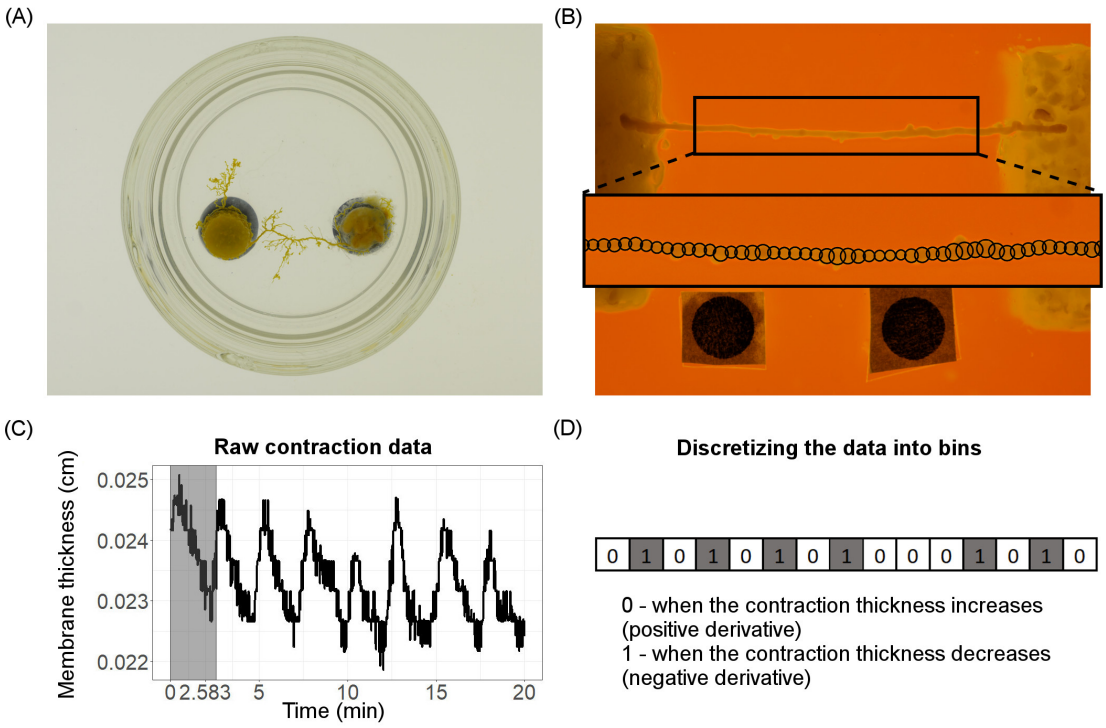

Figure 2.1 A) Picture of the setup used to make the tubule-shaped cells of *P. polycephalum*. B) Straightened tubule of *P. polycephalum* placed between 2 food sources (10% w/v oat-agar block on the *left* and 2% w/v oat-agar block on the *right*). The two black dots (Ø = 0.3 cm) at the bottom of the image were used as reference points and scale for the image analysis. Outset - Contractions were measured at 50 equidistant locations along the length of the tubule (shown by black circles along the tubule axis). C) The contractile behavior observed at the 25th contractile location along the tubule axis. D) Discretized version of the raw data used in calculating the transfer entropy. A value of 0 or 1 is assigned when the contractions increase or decrease, respectively, in time. Derivatives for the first 15 time steps of the raw data shown in C).

2.2.2 Experimental Setup

We studied information transfer during food choice in tubule-shaped cells of *P. polycephalum*. *P. polycephalum* tubules were obtained using the following procedure. Two agar blocks - an agar-only block and a 5% oat-agar block (or food agar) - were placed above the surface of a pool of water using a support (Figure

2.1A). The two agar blocks were separated by a distance of approximately 4 cm. A *P. polycephalum* biomass of approximately 0.5 g was placed on top of the agar-only block and allowed to grow tubular extensions on the water surface. After about 18-24 hours, *P. polycephalum* had formed a tubule network extending between the agar-only and food-agar blocks. Tubules of 2.5 cm in length were cut from the network, straightened, and placed between two food sources in the final experimental setup (Figure 2.1B). The final experimental setup was a Petri plate (Ø = 6 cm, H = 1.3 cm) with a substratum of 1% w/v non-nutrient agar that provided a gel-like, moist base. Two food blocks were embedded in the non-nutrient agar substrate separated by a distance of 2 cm (Figure 2.1B). The tubule was arranged on the two food blocks such that equal lengths of tubule interacted with food at each end. The *P. polycephalum* tubule was presented with two food choice treatments. In the first treatment, two identical food sources with 10% oat-agar were placed at each tubule end (hereafter referred to as the symmetric food choice condition). While in the second treatment, a 10% and 2% oat-agar food block were placed at the left and right tubule end, respectively (hereafter referred to as the asymmetric food choice condition).

The contractile behavior of the *P. polycephalum* tubule was recorded with high-resolution time-lapse photography using a Panasonic® Lumix GH4 camera fitted with an Olympus® M.Zuiko Digital ED 60mm macro lens. Images were captured every second for a total of 9999 seconds (or approximately 2 hours and 45 minutes, the maximum authorized by the camera in this configuration). In order to capture high-resolution images of the tubule, we recorded only the portion of the

experimental setup between the two food sources where the tubule lies the camera was zoomed in to the tubule to the closest extent possible. The experimental setup was illuminated from below using an LED panel (www.superbrightleds.com®) to allow the recording of high-definition tubule edges. As *P. polycephalum* is sensitive to and avoids UV and short wavelength visible light, we placed a 610 nm long-pass filter (Newport Corporation®) between the experimental setup and the LED panel. Previous studies have shown that *P. polycephalum* is not sensitive to wavelengths of light passing through this filter (*50*).

The use of 610 nm light filter made the slime mold growth on the food source appear indistinguishable from the food block background by the computer vision software. Therefore, we visually inspected the experimental setup at the end of the experiment to record the final food choice of the *P. polycephalum* tubule. When a distinguishable amount of biomass aggregation was visually observed on the left or right food source, the final choice was recorded as *left* or *right* choice, respectively. In the case in which the relative *P. polycephalum* biomass growth on the two food sources was visually indistinguishable, the final outcome of the experiment was recorded as *undecided*.

The contractile behavior of the tubules was measured using a dedicated, computer vision script written in MATLAB®. For each time-lapse picture, the script detects the tubule edges, extracts it from the background, and measures the tubule thickness at 50 equally spaced locations along the length of the tubule (Figure 2.1B outset). The script positions a circle at each location and adjusts their diameters to match the thickness of the tubule location. Over the course of the

experiment, changes in the circles' diameters at each tubule location captures the contractile behavior of the tubule. Figure 2.1C shows the typical form of raw data that we obtained and used for the analysis. The contractile behavior of the tubule was measured within a centrally located 1.6 cm long segment, i.e., we disregarded 0.2 cm of tubule section on each side as the overlapping of tubule with the food sources did not allow us to reliably track its contractions.

2.2.3 Data Preprocessing

As the tubule contracts over time, its thickness sampled at each location varies and produces a noisy, cyclical signal as shown in Figure 2.1C. To reduce the effects of noise, we filtered our raw data using a LOWESS smoothing algorithm (*71*). In our analysis, we varied the smoothing span, i.e., the fraction of data used to locally estimate the smoothed signal, between 0% (no smoothing) and 1% of the raw data. The smoothing span we use to filter raw data is given in Section 2.3.1 and the rationale behind choosing a value is explained in the section below (Section 2.2.4). Finally, we discretize the filtered signals sampled at each of the 50 locations of the tubule and obtain a set of 50 binary time series (one for each location). For each signal, we compute the derivative in time and construct a time series $X = \{x_1, \ldots, x_n\}$ (see Figure 2.1D) by assigning a value of $x_i = 0$ when the tubule thickness increases at time i (i.e., positive derivative) or a value of $x_i = 1$ if the tubule thickness decreases at time i (i.e., negative derivative).

2.2.4 Metrics

Final Tubule Choice

A one-sample proportionality test with Yates' continuity correction (*72*) was used to determine whether the tubules had a statistically significant preference for either of the two food sources. Under the null hypothesis (i.e., no preference for either of the two food sources) we expect the theoretical proportions of choosing either of the two food sources to be equal. However, the theoretical proportion of the undecided cases cannot be calculated as it would require knowing the exact decision-making mechanism. The undecided cases is nonetheless an essential piece of information indicating when *P. polycephalum* could not express a preference for either of the food sources, and therefore should not be discarded from the analysis. As a consequence, half of the undecided experimental trials were counted towards the left food source and the other half towards the right food source. This ensured that a lack of choice in one or more trials was represented in the final outcome of the analysis.

Transfer Entropy

Our analysis of information transfer underlying food choice by the slime mold *P. polycephalum* is based on the notion of *transfer entropy* introduced by Schreiber (*61*). Transfer entropy, $T_{Y \to X}$, is an information-theoretic measure that quantifies the exchange of information originating from a process Y and directed toward a process X. In our analysis, process X and Y correspond to a pair of oscillatory signals generated by the contractile behavior of the tubule at two different locations

and discretized as explained in Section 2.3. Transfer entropy $T_{Y\to X}$ from a location Y on the tubule toward a location X is given by

$$T_{Y\to X} = \sum_{x_{i+1},\, x_i^{(k)},\, y_i} p\left(x_{i+1},\, x_i^{(k)},\, y_i\right) \log_2 \frac{p(x_{i+1},\, y_i \mid x_i^{(k)})}{p(x_{i+1} \mid x_i^{(k)})\, p(y_i \mid x_i^{(k)})}. \tag{1.1}$$

In Equation 1.1, $p(\cdot)$ represents the empirical probability of a certain event (e.g., $x_i = 1$) estimated from the time series X and Y while $x_i^{(k)} = \{x_{i-k+1},\, x_{i-k+2}, \ldots, x_i\}$ represents the k-history of X at time i and is given by the k consecutive values of the time series preceding and including x_i. In other words, transfer entropy provides a measure of the amount of information that we gain about the contractile behavior of the tubule at location X from knowledge of the same behavior at location Y given the history of X. All computations of transfer entropy were performed using package *rinform-1.0.1* (*73*) in R version 3.4.3 (*74*).

Based on transfer entropy, we then define different aggregation measures to study the dynamics of information transfer. We consider the *total transfer entropy* TTE over all locations of the *P. polycephalum* tubule defined as

$$TTE = \sum_{1 \le x,\ y \le 50,\ x \ne y} T_{Y_y \to X_x}, \tag{1.2}$$

i.e., the sum of transfer entropy over all pairs of locations x and y on the tubule. We use TTE as a target measure to find the parameters that optimize and improve

the quality of information transfer measurements in the food choice experiments. Specifically, we calculated TTE for different combinations of parameters, namely history length k and LOWESS smoothing span. The combination of k and LOWESS span that maximizes TTE is used in the computation of *net transfer entropy* $NTE(x)$ values described in detail below.

We define the *net transfer entropy* $NTE(x)$ as a measure for the study of information transfer as a function of the location $x \in \{1, \ldots, 50\}$ of the tubule

$$NTE\ (x) = \sum_{1 \le y \le 50,\ y \neq x} T_{X_x \to Y_y} - \sum_{1 \le y \le 50,\ y \neq x} T_{Y_y \to X_x}. \tag{1.3}$$

$NTE(x)$ computes the difference between outgoing information and incoming information for a particular location of the *P. polycephalum* tubule. That is, the difference between total information transferred from location x towards any other location $y \neq x$ of the tubule (outgoing information) and the total information transferred to location x from any other location $y \neq x$ of the tubule (incoming information). Positive values of $NTE(x)$ indicate that location x is a *source* of predictive information about the system. Negative values of $NTE(x)$, indicate instead that location x is an information *destination*. $NTE(x)$ as defined above is a variation of the standard, pairwise net transfer entropy

$$NTE_{X \to Y} = T_{X \to Y} - T_{Y \to X}, \quad \text{if } T_{X \to Y} > T_{Y \to X}, \tag{1.4}$$
$$NTE_{X \to Y} = |\, T_{X \to Y} - T_{Y \to X} \,|, \text{ if } T_{X \to Y} < T_{Y \to X},$$

between a pair of processes and (cf. (*64*)). We use $NTE_{X\to Y}$ between a pair of locations x and y of the tubule to determine and visualize the flow of information across the tubule as a network and gain insight into the orientation of the information flow. We do so by grouping locations on the tubule in 5 sets of ten (i.e., {1, 2, …,10}, …, {41, 42, …, 50}). For each pair of groups, the total net transfer entropy was calculated as the sum of contributions of $NTE_{X\to Y}$ between all pairs of locations belonging to the two groups.

We computed all measures defined above considering also an artificially created dataset that we used as the *control* to define a reference level of zero transfer of information. We do so by computing transfer entropy $T_{Y\to X}$ between pairs of locations x and y whose time series X and Y have been collected from two different experimental trials (i.e., two different tubules). As the experimental trials are independent of each other, there is no real transfer of information happening across the two tubules. The results computed in this way allow us to discriminate between information transfer generated by intrinsic noise in our experimental procedure and actual information transfer happening among the tubule regions during an experiment. Additionally, by pairing signals collected by two different experimental trials, we effectively augment the size of the control dataset with respect to the actual number of trials (e.g., $42 \cdot 41$ for the asymmetric treatment with 42 trials). All results discussed in Sections 3.1 and 3.3 are reported at the net of the same measures computed over the control dataset based on 252 random pairs of trials. In Section 2.3.2., the results computed using the control dataset are visualized separately.

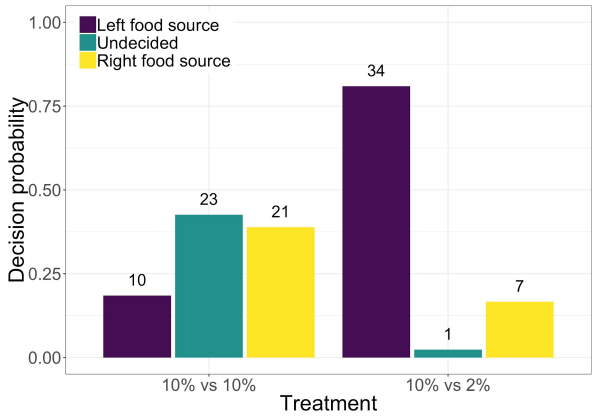

Figure 2.2 Distribution of final decisions (i.e., left food source, undecided, or right food source) taken by *P. polycephalum* tubules for the symmetric food choice condition with two 10% w/v oat-agar blocks (54 experimental trials with both left and right food sources being 10% w/v oat-agar food block) and the asymmetric food choice condition with 10% w/v and 2% w/v oat-agar blocks (42 experimental trials with left food source being 10% w/v oat-agar food block and right being 2% w/v oat-agar food block).

2.3 Results

We performed two series of experiments (or treatments) where the quality of the food source placed on the left side of the tubule was kept constant with a 10% w/v oat-agar block and varied that of the food source placed on the right side of the tubule with either 10% w/v (i.e., the symmetric food choice condition) or 2% w/v oat-agar blocks (i.e., the asymmetric food choice condition). Figure 2.2 shows the distributions of the final decisions of the *P. polycephalum* tubules over the different experimental trials. In the symmetric treatment, *P. polycephalum* does not show a significant preference for either of the two food sources (proportionality test: p = 0.1696, 54 trials) with a large number (23 out of 54) of experimental trials concluding in an undecided state. However, in the asymmetric treatment, *P. polycephalum* shows a significant preference (proportionality test: p = 4.896e - 05,

42 trials) for the left block composed of 10% w/v oat-agar over the right block with 2% w/v oat-agar. This result is consistent with the findings from a previous study by Latty and Beekman (*26*), which showed that *P. polycephalum* has a significant preference for the more nutrient concentrated food option when given a choice between two food sources with different nutrient concentrations.

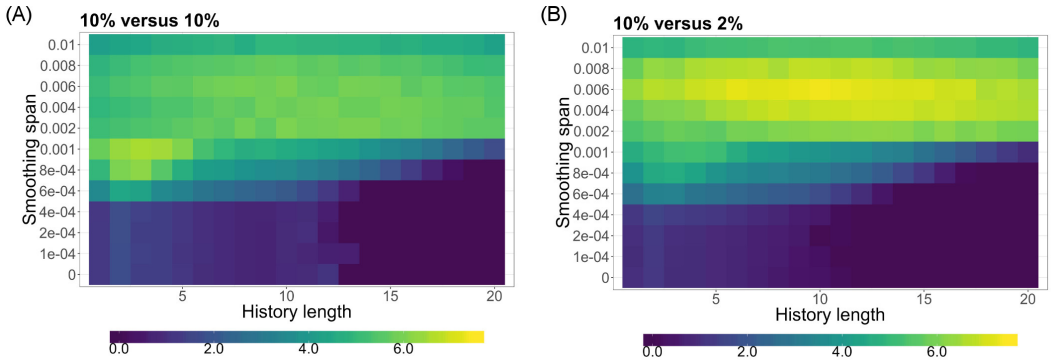

Figure 2.3 Total transfer entropy (TTE) as a function of the history length ($k \in \{1, \ldots, 20\}$) and of the LOWESS smoothing span (smoothing span $\in \{0.0001, \ldots, 0.01\}$). A) The symmetric food choice condition with two 10% w/v oat-agar blocks where *TTE* is maximized for history length k = 3 and smoothing span 0.001. B) The asymmetric food choice condition with 10% w/v and 2% w/v oat-agar blocks where TTE is maximized for history length k = 10 and smoothing span of 0.006.

2.3.1 Analysis of the Parameter Space

For both treatments, we calculated the total transfer entropy averaged over all experimental trials as a function of the history length k and of the LOWESS smoothing span. We performed the same calculations for the control dataset and computed the difference between the real results and the control ones. Figure 2.3 shows the distribution of total transfer entropy ($TTE;$ adjusted to that of the control dataset) over the parameter space. The landscapes of TTE in the two experimental treatments are similar to each other, however, the particular parameters that

maximize TTE differ. In the symmetric food choice condition, TTE is maximized for history length k = 3 and smoothing span 0.001 (see Figure 2.3A). In the asymmetric food choice condition instead, TTE is maximized for history length k = 10 and smoothing span of 0.006 (see Figure 2.3B). While the accuracy of these parameter configurations is subject to the number of experimental trials, their values provide us with a good representation of information transfer occurring within the tubules.

2.3.2 Information Sources and Destinations

To understand how *P. polycephalum* process information during the food choice experiments, it is imperative to investigate where information is generated or gathered from the environment (i.e., source) and to which locations of the system it is transferred (i.e., destination). We examined the net transfer entropy as a function of the location on the *P. polycephalum* tubule. Figure 2.4 shows the results of our analyses for both experimental treatments and their control datasets arranged by the final decision of the *P. polycephalum* tubule. In the symmetric food choice condition with two 10% w/v oat-agar blocks, the net transfer entropy is symmetrically distributed around the center of the tubule (i.e., locations 25-26) with the extremities of the tubule characterized by positive values of NTE and the middle section characterized by negative values independently from the final food choice (cf. Figure 2.4A and 2.4B). Additionally, for both final food choices, the values of net transfer entropy were similar along the length of the tubule (in the range between -0.025 and 0.05 bits). However, in the asymmetric food choice condition, NTE is positive for locations on the *P. polycephalum* tubule that is

opposite to the chosen food source and negative for locations in the proximity of this source. Note that the scale of the y-axis in Figures 2.4A, B is different, with the NTE values being higher in the tubule regions near the chosen food source when the final choice was the 2% oat-agar food block (upper limit of the y-axis is approximately 0.4 bits) relative to the case when the tubule choice was the 10% oat-agar food block (upper limit of the y-axis is approximately 0.1 bits). Similarly, the regions near the rejected food source show lower NTE values when the tubule choice was 2% oat-agar food block (lower limit of the y-axis is approximately -0.3 bits) than the case when the choice was 10% oat-agar food block (lower limit of the y-axis is approximately -0.05 bits). In Figure 2.4C, we aggregated the results of all experimental trials by inverting the order of the tubule locations for all trials where the tubule chose the right food source and half of the trials recorded as undecided. This allows us to visualize the results of NTE for all trials independently from the nutrient concentration of the food source chosen by the *P. polycephalum* tubule. While in the symmetric food choice condition information originates at the extremities of the tubules (i.e., from the tubule regions near the two food sources) and flows towards the center without a noticeable correlation with the final food choice (i.e., left), whereas in the asymmetric food choice condition, information originates at the opposite side of the chosen food source and flows towards the tubule region in its proximity. That is, when a more nutrient-rich food option is available, the contractile dynamics of the tubule in the proximity of the chosen food source are anticipated by those at the opposite extremity.

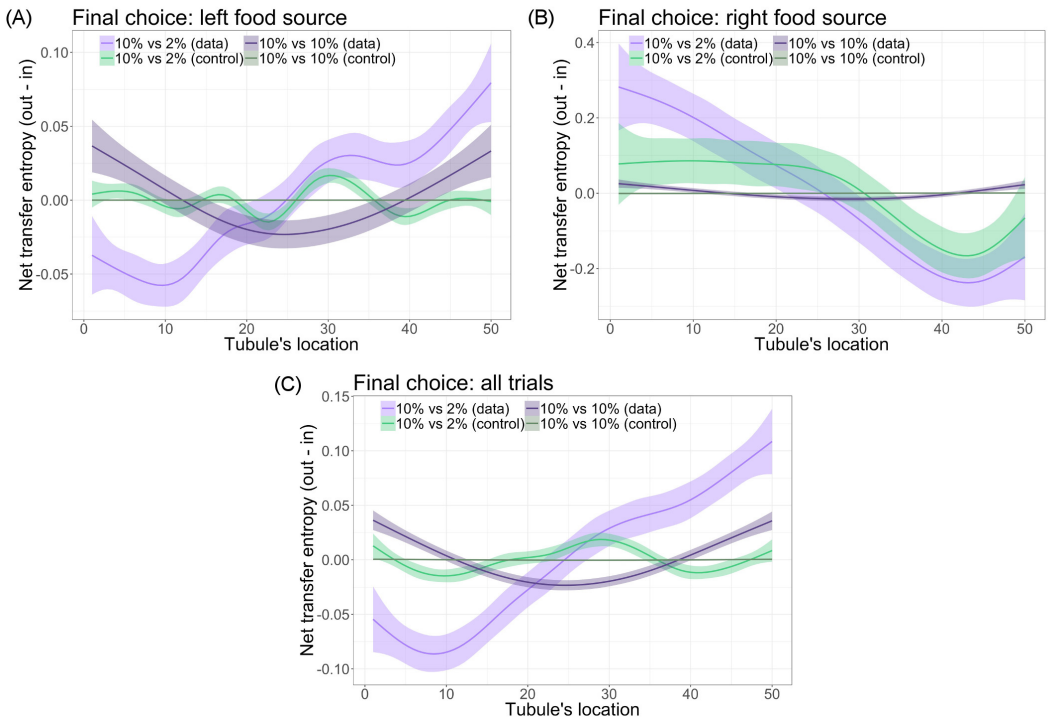

Figure 2.4 Net transfer entropy at the contractile locations along the length of the tubule ({1, …, 50}) for A) trials with final choice being the left food source, B) trials with final choice being the right food source, and C) all trials such that the chosen food source is on the left and rejected food source on the right. Parameters: 10% w/v versus 10% w/v (k = 3, smoothing span 0.001), 10% w/v versus 2% w/v (k = 10, smoothing span 0.006).

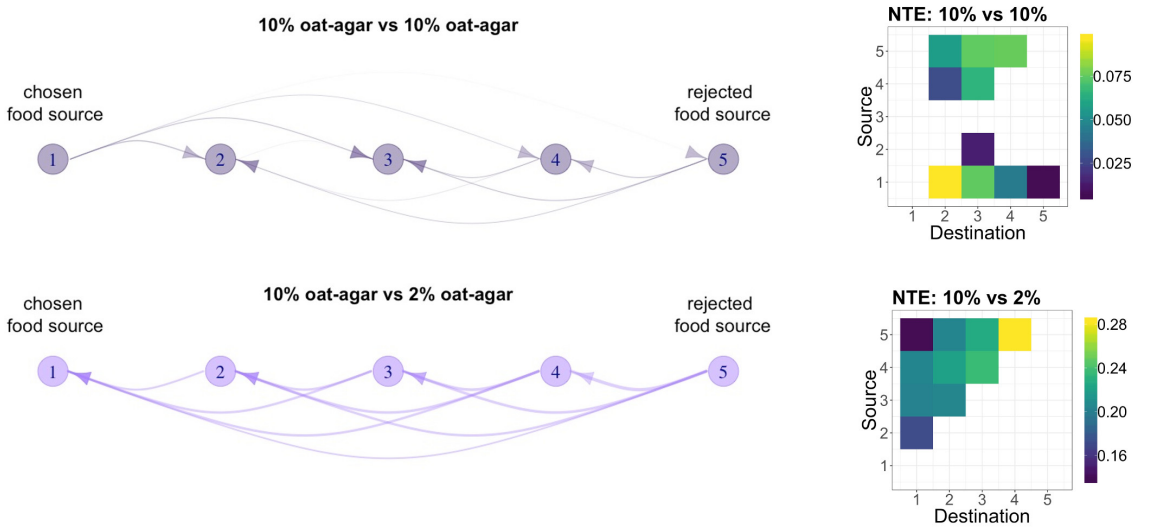

Figure 2.5 Networks and their adjacency matrix of information flow between groups of adjacent locations (i.e., 1 = {1, 2, …, 10}, …, 5 = {41, 42, …, 50}) on the *P. polycephalum* tubule constructed from net transfer entropy averaged over all experimental trials. The orientation of the tubule in each trial is adjusted so that the final choice of the tubule is always on the left side of the network (i.e., vertex 1); edge width is proportional to the net transfer entropy. Parameters: 10% w/v versus 10% w/v (k = 3, smoothing span 0.001), 10% w/v versus 2% w/v (k = 10, smoothing span 0.006).

2.3.3 Information Flow Network

Finally, we look at the direction and amount of information flow within the tubules of the slime mold *P. polycephalum* during the food choice experiment. Measurements were coarse-grained to obtain a simpler and clearer picture of information transfer. Adjacent locations on the *P. polycephalum* tubule were binned into five groups of ten locations each (i.e., we equally divided the tubule into 5 sub-segments or regions). Figure 2.5 shows the total net transfer entropy between these portions of the tubule averaged over all experimental trials and corrected with the results of the control dataset. As in the previous section, we reversed the orientation of the tubules in all experimental trials where the final

choice was the right food source and in half of the trials recorded as undecided. As a consequence of this, the left side of the networks (i.e., vertex 1) represents the extremity of the tubule in the proximity of the chosen food source regardless of its nutrient concentration. Likewise, the right side of the networks represents the extremity that is next to the rejected food source. Both the symmetric and asymmetric treatments show well-defined networks of information flow. However, the resulting network topologies are significantly different between the two food choice conditions. The symmetric food choice condition, shown in the top panel of Figure 2.5, is characterized by a flow of information originating from both extremities (i.e., vertex 1 and vertex 5) of the tubule and converging towards its center (i.e., vertex 3). As also shown by the corresponding adjacency matrix, the topology defined by the edges is approximately symmetric with respect to the center of the tubule. In contrast, in the asymmetric food choice condition, shown in the bottom panel of Figure 2.5, is characterized by a flow of information originating at the extremity of the tubule in contact with the rejected food source and directed towards the opposite extremity. As shown by the corresponding adjacency matrix, for each group of locations $1 < i \leq 5$, there are edges $i \rightarrow j$ connecting the group to all groups $j < i$ on its left. In both experimental conditions, the absolute values of net transfer entropy represented by the adjacency matrices in Figure 2.5 are inversely proportional to the distance between two regions of the tubule. Moreover, their amount differs between conditions: in the asymmetric food choice condition, the tubule transfers an amount of information (0.2092 ± 0.038 bits) that is approximately four times the amount transferred during the symmetric food choice

condition (0.0537 $\pm$ 0.0297 bits). That is, more information is transferred across the tubule when there is a contrast in the concentration of nutrients between the two available food options.

2.4 Discussion

We studied the relative influence between the contractile regions of a *P. polycephalum* tubule while it was choosing between two food sources. The tubule was presented with two food choice conditions, which were either symmetric or asymmetric in nutrient concentrations. We studied information transfer across the tubule by measuring the change of thickness at 50 equidistant locations and computing the transfer entropy between each of them.

Our results show that *P. polycephalum* does not have a significant preference for either of the food options in the symmetric food choice condition, while it has significant preference for the more nutrient-rich option in the asymmetric food choice condition. We showed that the difference in food qualities affects information transfer between the contractile regions of *P. polycephalum*. In the symmetric food choice condition, the tubule locations near each of the two food sources act as the information sources while those near the center of the tubule act as information destinations. Information transfer is symmetrically distributed around the center of the tubule. These trends are similar regardless of the food source chosen by the tubule at the end of the experiment. Conversely, in the asymmetric food choice condition, the tubule locations near the chosen food source, regardless of the food source quality, act as the destinations of information

while those in the proximity of the rejected food act as the information sources). Therefore, the tubule sub-regions near the rejected food source transfer information towards the sub-regions near the chosen food source. Additionally, the amount of information transfer was found to be inversely proportional to the distance between the sub-regions, similar to the results obtained in the symmetric food choice condition. Interestingly, the amount of information transferred between the tubule regions in the asymmetric food choice condition was four times higher than that of the symmetric condition.

Transfer entropy measures the amount of directed predictive information flow (or information transfer) between two processes, but establishing a causal relationship between the behaviors requires additional considerations (*62*). Therefore, values calculated in our study captures the net transfer of predictive information at each location (Figure 2.4) and between different sub-regions (Figure 5) along the *P. polycephalum* tubule but, based on our results, we cannot claim yet a causal relationship between the behaviors of different locations and sub-regions. However, the *P. polycephalum* tubule is a continuous system and all the locations that we observed are physically connected to each other and constantly interacting with one another through physical forces and chemical exchanges. Therefore, we preliminarily conclude that our results about information transfer capture causal interactions between physically adjacent locations. The existence of a causal relationship between the locations along the tubule will be formally tested in future experiments by physically intervening or perturbing the contractile behavior at a given location.

While our work indicates the occurrence of information transfer between contractile regions of the tubule, the precise medium of the information being transferred remains unknown. In view of this, it is important to note that the organism tested were reacting to external food stimuli. Although the information transfer that we observed in this study dominantly originates from the end of the *P. polycephalum* tubule in proximity to the lower nutrient concentrated food source, it would be naïve to neglect the apparent role that food has in stimulating and promoting the contractile behavior (*46*, *52*, *54*, *55*). Food-containing vesicles both stimulate local changes in intracellular signal transduction and are degraded to yield sugars and amino acids that fuel all cellular functions. For example, the contraction-relaxation cycles of the membrane that generate protoplasmic flow involves dynamic rearrangements of actin cytoskeleton and signaling that require ATP (*75*) and Ca^{2+} (*76*), both of which are derived from food (*77*, *78*). By this reasoning, information flow should originate from nutrient-rich food sources. While local contraction intensity may be increased by food stimuli, we suggest that the long-range coordination of the contractile behavior across the *P. polycephalum* (*50*) is influenced by the contractile behavior at the tubule end with lower nutrient concentrated food source. Information transfer in the form of molecular stimuli originating from the food source and related signal transduction events were not measured in the current work. Yet, this stimulus clearly drives the observed changes in contractile behavior patterns and is likely to represent the primary medium of information acquisition. Future work will be directed toward determining

the precise physicochemical signaling that is initiated by foods of differing quality and their impact to oscillatory regulation and ultimately decision-making in *P. polycephalum*.

Previous studies have shown that when a *P. polycephalum* cell interacts with an attractive substance, the cell regions located in the vicinity of the substance acts as the information source and the regions located away from the attractive substance act as the information destination (*46*, *52*, *55*). Moreover, these studies show that the information transfer occurs via changes in contraction intensities that can be in the form of changes in frequency or amplitude. Our results do not indicate whether the information transfer occurs by increasing or decreasing the contraction frequency and/or amplitude. However, the results show that the tubule regions acting as information sources and destinations varied with respect to the food choice conditions presented to the *P. polycephalum* tubule. Additonally, this imbalance in the localized nature of predictive information with certain regions of the organism covering a more prominent role than the others is a reminiscent of the control kernel in yeast-cell regulatory networks (*79*) or of informed individuals playing leadership roles in a school of fishes (*58*).

The two food choice conditions used in our study presented the *P. polycephalum* tubule with two different decision-making challenges. As the direction and amount of information transfer differed in the two treatments, this opens the question of whether the information transfer in *P. polycephalum* changes relative to the decision-making problem faced by the cell. The experiment we suggest to test this behavior in detail is to progressively increase the quality of the

lower concentrated food source and compare the effects on the direction and amount of information transfer.

Finally, our analysis does not provide details about the dynamics of information transfer during the course of the experiment. A refined examination during various stages of decision-making may find information transfer relationships more specifically pertaining to food detection, nutrient transfer, and/or final decision execution. Experiments should be conducted for a longer period of time which would permit to repeat a similar analysis but at different phases of the experiment.

CHAPTER 3

COULD THERE BE A GENERALIZED CRITERION TO DECIDE IF *PHYSARUM POLYCEPHALUM* MADE A CHOICE TO EXPLOIT AVAILABLE RESOURCES?

3.1 Introduction

Physarum polycephalum is a large, unicellular, multi-nucleated protist (phylum Amoebozoa, class Myxogastria) that inhabits shady, cool, and moist areas of temperate forest. When in the vegetative or plasmodial stage of its life cycle, the *P. polycephalum* moves in its environment by extending pseudopods in an amoeba-like fashion. The cell can extend multiple pseudopods to explore its environment, and is referred to as multi-headed (i.e., translates to *polycephalum* in Latin). *P. polycephalum*, without the help of a nervous system, can find the shortest path through a labyrinth maze (*17*), form efficient transport networks (*18*), solve complex optimization problems (*20*), anticipate periodic events (*21*), habituate to irrelevant environmental stimuli (*23*), and avoid previously exploited areas by using its extracellular slime trail (*22*). Additionally, numerous studies have claimed that *P. polycephalum* is capable of choosing the most rewarding option when presented with a set of multiple alternatives (*25*, *26*, *28*, *29*, *80*). However, the criteria used to determine such choice-making behaviors are either not generalizable to studies using different experimental designs or are ambiguous and open to other interpretations.

For example, Latty and Beekman (2010) used a criterion that considered *P. polycephalum* to make a choice for a resource when the cell moved its entire biomass towards the resource by the end of the experimental time period (*26*).

Moreover, in the cases when *P. polycephalum* allocated biomass to multiple resources, the authors designated them as “undecided”. When the authors used this criterion to determine whether *P. polycephalum* cells chose the best option when presented with two food sources of varying quality, they observed the choice of the more nutrient-rich option in >95% of the replicates. In the remaining <5% of the experimental replicates, the cells were undecided. Lastly, the cells did not choose the less nutrient-rich option in any of the experiments. Since the cells moved their entire biomasses exclusively towards the more nutrient-rich food source, the study demonstrated *P. polycephalum’s* capability to choose the most rewarding food option when given a choice between two alternatives. Nonetheless, the criterion used in this study was specific to the experimental framework employed, and might not apply to studies with different experimental designs. In particular, when using the criterion above, the experimental time period needs to be long enough to allow the cells to move their entire biomasses towards a particular resource. However, the foraging behavior of *P. polycephalum* cells is highly variable between the cells of the same (*80*) and different (*81*) strains. As a consequence, the time taken by *P. polycephalum* cells to make a choice could be unpredictable and vary with the changing complexities of different experimental environments. Therefore, it could make it challenging to design experiments comprising sufficient time periods that allow *P. polycephalum* to choose between a given set of options. Accordingly, we argue that in Latty and Beekman (2010), the replicates in which *P. polycephalum* allocated its biomass towards multiple resources were not necessarily undecided, but instead, the cells were in the

process of choosing between resources. As a result, the experimental time period was not long enough for these cells to move their entire biomass towards some resource in the environment.

Alternatively, Reid et al. (2016) and Vogel et al. (2018) used a criterion that compared the distribution of biomass on different resources to determine choice-making in *P. polycephalum* (*29*, *80*). In particular, these studies considered *P. polycephalum* cells to make a choice for a resource when the cells distributed a majority of their biomass towards the resource repeatedly and more often than predicted by chance alone. These studies examined the choice-making behaviors in *P. polycephalum* by introducing the cells into an experimental setup comprising two environments of varying quality (i.e., the environments differed in the number of food sources in Reid et al. (2016); and the concentration of an attractant in Vogel et al. (2018)). The studies tested the null hypothesis that the proportion of replicates distributing a majority of biomass towards an option due to chance is 0.5. The authors found that *P. polycephalum* cells demonstrated a preference for the more rewarding environment in both studies. However, the significant deviation in proportion from the null hypothesis does not necessarily indicate a choice made by a *P. polycephalum* cell. The reason is that the above criterion does not differentiate between a situation when *P. polycephalum* explores resources relative to their qualities and when the cell is choosing an option over multiple alternatives. Suppose *P. polycephalum* cells are presented with two environments of different quality, and the cells are exploiting both resources by distributing their biomass in proportion to the relative quality of each resource. We would expect the

proportion of replicates with a majority of biomass distribution towards the higher quality option to be equivalent to the relative quality between the environments, and that the proportions would deviate from 0.5. As a result, in such a situation, the above criterion would designate such biomass distribution as a choice for the higher quality option, when in reality, the cells were exploiting both resources. The *P. polycephalum* would be considered to choose an environment when the proportion of replicates distributing a majority of biomass towards the particular environment is greater than its relative quality.

Therefore, in this study, we devise an aggregate criterion that determines if 1) *P. polycephalum* cells can choose the most rewarding option (will be referred to as the "better resource" from here onwards) when presented with a choice between two resources, and 2) examines if the experimental time period was sufficient for the cells to express their choice-making behavior. Our choice-making criterion tests the null hypothesis that the relative difference in foraging effort (i.e., amount of biomass and time) distributed by *P. polycephalum* cells towards the most rewarding resource would be proportional to the relative difference in quality between the available resources. In this criterion, we first make aggregate measurements of the relative difference in foraging effort invested by *P. polycephalum* cells on the better resource, over the experimental time period, and across all experimental replicates. And then, we compare the measurement results to the relative difference in quality between the resources. When the value of the relative difference in foraging effort exceeds the relative difference in quality between the food sources, the cells will be considered as having chosen the better

resource. Whereas, when the relative difference in foraging effort plateaus to a value equivalent to, or lesser than, the relative difference in quality between the food sources, we will consider the cell to not have chosen the better resource. Moreover, if the value of the relative difference in foraging effort does attain a value that is lesser than the relative difference in quality, we will conclude that the *P. polycephalum* cells were not given sufficient time to evaluate the options to make choices between the resources.

We test this criterion to explore the choice-making capabilities in tubule-shaped *P. polycephalum* cells. We introduce a *P. polycephalum* tubule to binary food choice experiments, where both ends of the tubule are connected to a food source. We test the tubule in multiple food choice conditions, by progressively increasing the quality of the lower concentration food source with each experimental condition. Next, we use our choice-making criterion to a) determine if the *P. polycephalum* tubules chose the better resource, b) examine if the experimental time period dedicated to the experiments was sufficient to make a choice, and c) estimate the time point at which the cells made the choice on aggregate.

3.2 Materials and Methods

3.2.1 Biological Material

In our experiments, we used *P. polycephalum* when it was in the plasmodium stage of its life cycle. At this stage, the cell is large enough to be observed with an unaided eye (can cover an area up to several hundred square centimeters (*14*))

and can move up to a speed of 5 cm/hr (*45*). In this study, we obtained *P. polycephalum* cultures from Carolina Biological Supply® (Burlington, North Carolina). The cells were cultured in Petri plates (Ø = 10 cm, *H* = 1.5 cm) containing water solution of 1% w/v (weight/volume) non-nutrient agar and 5% w/v blended rolled oats (Quaker Oats Company®). The laboratory *P. polycephalum* stocks were recultured into new Petri plates biweekly and maintained at 26°C under dark conditions.

3.2.2 Experimental Setup and Protocol

We studied the choice-making criterion in tubule-shaped *P. polycephalum* cells. The tubule-shaped cells were obtained using the following procedure. We placed two agar blocks, one non-nutrient agar-only block, and one 5% oat-agar (i.e., food agar) block, right above the surface of a pool of water using supports. Next, we introduced a *P. polycephalum* mass (approx 0.5 gm) on the surface of the non-nutrient agar block. Within a few hours, the *P. polycephalum* cell could be observed extending tubular pseudopods on the water surface. The cell formed a tubular network encompassing the non-nutrient and food agar block after 18 - 24 hours since the introduction of *P. polycephalum* into the setup. We cut a tubule of length 2.5 cm from the cell network (i.e., an edge from the tubular network), and placed it between the two food sources in the final experimental setup. The final experimental setup consisted of 1% w/v non-nutrient agar solution poured in a Petri plate (Ø = 6 cm and *H* = 1.3 cm). Two food agar blocks of concentrations, given in Table 3.1, were embedded into the agar. The agar blocks were placed such that the inner edge of the two blocks was separated by a distance of 2 cm. The *P.*

polycephalum tubule was carefully introduced to the setup, such that equal lengths of the tubule interacted with the two food sources. Table 3.1 shows the different food choice conditions, the relative quality of the poorer food source, and the number of experimental replicates conducted for each condition.

Table 3.1 OUTLINE OF THE EXPERIMENTAL TREATMENTS TO TEST THE CHOICE-MAKING CRITERION

Condition Number	Food choice condition (w/v oat-agar concentration)	Relative quality of the poorer food source	Relative difference between the food sources (or the choice-making threshold)	Number of replicates
1	10% vs 1%	0.1	0.82	68
2	10% vs 2%	0.2	0.67	42
3	10% vs 4%	0.4	0.43	49
4	10% vs 6%	0.6	0.25	22
5	10% vs 8%	0.8	0.12	48
6	10% vs 10%	1.0	0	52

3.2.3 Data Collection

The experiments were recorded using Panasonic® Lumix GH4 camera fitted with an Olympus® M.Zuiko Digital ED 60mm macro lens. The camera took a picture every second for a period of 9999 seconds (or approx 2 hours and 45 minutes, which was the maximum capacity allowed by the camera). The cameras were placed in a manner that the more enriched food source (i.e., the better resource) always appeared on the left-hand side of the image. In order to capture high-

definition images of the *P. polycephalum* tubule, the setup was illuminated from below with an LED panel (www.superbrightleds.com®) fitted with a 610 nm long-pass light filter (Newport Corporation®). Studies have shown that *P. polycephalum* is unreceptive to wavelengths of light passing through this filter (*50*).

3.2.4 Relative Difference in Foraging Effort on the Better Resource

We studied the relative difference in the foraging effort by measuring the aggregate proportion of occurrences of higher biomass growth on the better resource as a function of the experimental time period. First, we visually inspected the experimental images at 8 equidistant time points along the length of the experiment, and recorded the food source showing a distinguishable biomass growth by the *P. polycephalum* tubule. Next, we used this information to construct a discrete, binary time series showing the success or failure of the tubule to aggregate more biomass on the better resource (will be referred to as the "success time series" from here onwards). In particular, at each time point, when a distinguishable amount of *P. polycephalum's* biomass growth was observed on the better resource, we considered it a "success" denoted by a value of 1. Whereas, when the tubule showed a distinguishable biomass growth on the inferior resource or when the amount of growth on both the food sources was indistinguishable (i.e., the case of being "undecided"), the cases were considered a "failure" (assigned a value of 0). Moreover, in the condition where the tubule was offered a choice between food sources that were identical in quality (i.e., the 10% vs 10% food choice condition in Table 3.1), we considered a success as the case when a distinguishable biomass growth was observed on the left food source. This

exercise was repeated for all experimental replicates across the experimental conditions, and was conducted by an individual who was not involved in any other parts of this study.

We fitted the success time series with a generalized linear mixed effects model (GLMM) using a binomial error distribution and logit link function. In this model, we treated the food choice conditions, time points, and an interaction between the food choice conditions and time points as fixed effects. Moreover, each experimental replicate was treated as a random effect. We used the relative quality of the poorer food source values as the inputs to the model for the different food choice conditions tested. The choice-making capabilities of the *P. polycephalum* tubule were examined using the probability of success estimates (i.e., the probability of observing distinguishable growth on the better resource) predicted by the model. The analysis was conducted in R version 4.1.2 (*82*), using the "lme4" package (*83*).

3.2.5 Relative Difference in Quality Between the Food Sources

The relative difference in quality (will be referred to as the "choice-making threshold") was used as the threshold to determine whether the *P. polycephalum* tubules made a choice for the better resource (discussed in detail in the next section). The choice-making threshold for the different food choice conditions is given in Table 3.1, and the values were calculated using the Equation 3.1:

$$Choice - making\ threshold = \frac{Absolute\ difference\ in\ food\ quality}{Total\ sum\ of\ the\ food\ qualities} \qquad (3.1)$$

3.2.6 Choice-making Criterion

In order to determine whether *P. polycephalum* tubule made a choice for the better resource, we compared the probability of success estimates to the choice-making threshold, for each food choice condition. The choice-making threshold provides an estimate of the probability of success values when the *P. polycephalum* tubule is choosing the better resource according to the null hypothesis (i.e., the relative number of occurrences of higher biomass growth on the better resource is proportional to the relative difference in qualities between the presented food options). Therefore, we consider *P. polycephalum* tubule to make a choice for the better resource when the probability of success reaches a value that is greater than the choice-making threshold.

Figure 3.1 shows a schematic description of the choice-making criterion used in this study. The criterion compares the lower limits of the 95% confidence intervals (will be referred to as “lower confidence interval” from here onwards) of the probability of success estimates to determine the tubule choice. Such that, when the lower confidence interval exceeded the choice-making threshold, *P. polycephalum* tubules will be considered to choose the better resource. The comparison of the lower confidence interval to the choice-making threshold ensures that a significant majority of the probability of success estimates (i.e., 97.5% of the estimates) is above the choice-making threshold. Moreover, the choice-making time point is defined as the time point when *P. polycephalum* made a choice for the better resource. The choice-making point was calculated as the

time point corresponding to the intersection point between the lower confidence interval and the choice-making threshold.

In contrast, when the lower confidence interval is below the choice-making threshold, the cells will be considered to not have chosen the better resource. Additionally, in such cases, the shape of the probability of success estimates was used to determine if the *P. polycephalum* tubules were given sufficient experimental time to make the choice. In particular, when the probability of success estimates become constant (or plateaus) by the end of the experimental time period, this implies that the *P. polycephalum* tubule has reached the final probability of success state for the particular food choice condition. And therefore, the cell was given sufficient time to evaluate the options and make a choice. In contrast, when the shape of the probability of success estimates does not plateau, this implies that the *P. polycephalum* is still in the process of choosing between the food sources and has not reached the final probability of success state for the given experimental condition.

3.3 Results

We used a GLMM model using binomial error distribution and logit link function to analyze the relationship between the food choice conditions (i.e., the relative quality of the poorer food source), time points, and interaction between the food choice conditions and time points, on the probability of observing distinguishable growth on the better resource (i.e., the probability of success). We found that, when holding all the predictor variables constant, ~~then~~ for every 1 unit increase in the

time points, the odds ratio (OR) of the probability of success increased by a factor of 1.8924 (95% CI: 1.57 to 2.21, $p < 2e\text{-}16$). In other words, across all the food choice conditions the probability of success increased with the increase in experimental time (see Figure A.1 of the *Appendix*). The food choice conditions had a positive but a nonsignificant effect on the odds ratio of the probability of success (OR = 1.7612, $p = 0.197$, see Figure A.2 of the *Appendix*).

Importantly, the predictor variable comprising the interaction between the food choice condition and time points had a significant effect on the odds ratio of the probability of success (OR: -1.2882, CI: -1.77 to -0.99, $p < 2.98e\text{-}12$, Figure 3.2). The results show that when the relative quality of the poorer food source is low (i.e., when the difference in the relative quality of the food source is high), the probability of success increases at a higher rate over the experimental time period. In contrast, at high values of the relative quality of the poorer food source, the probability of success increases at a lower rate. In other words, when the relative quality of the poorer food source decreased, the *P. polycephalum* was observed to aggregate a distinguishable amount of biomass on the better resource more frequently, with the increase in the experimental time period. The model diagnostics and performance are given in Figures A.3 and A.4, of the *Appendix*, respectively.

Next, we compared the lower confidence interval values of the probability of success estimates and the choice-making threshold to determine whether the *P. polycephalum* tubule made a choice for the better resource. Table 3.2 details the results of the analysis. The results show that the *P. polycephalum* was able to

choose the better resource in all but the 10% vs 8% food choice condition. The results can also be corroborated with Figure 3.2, showing the lower confidence intervals not exceeding the choice-making threshold in the 10% vs 8% food-choice condition. Lastly, when the tubules demonstrated a choice for the better resource, we calculated the time point at which the tubules made the choice. The results of the analysis are also shown in Table 3.2. Finally, in the 10% vs 10% food choice condition, the choice-making criterion determines the choice-making point to be at time points < 1, suggesting the non-applicability of the criterion when the food choices presented are identical in quality.

3.4 Discussion

We devised a choice-making criterion that determines whether *P. polycephalum* is capable of choosing the most rewarding option when given a choice between two sources, examines whether the *P. polycephalum* was given sufficient experimental time to make the choice, and obtains the time point at which the choice was made. The choice-making criterion tested the null hypothesis that the relative difference in the foraging effort (i.e., the amount of biomass and time) by *P. polycephalum* in moving towards the most rewarding resource would be proportional to the relative difference in quality between the available resources. We tested the criterion on *P. polycephalum* tubule in binary food choice experiments, with the quality of the inferior food source varying progressively with each experimental condition. We examined the foraging efforts in the terms of proportion of occurrences of higher biomass growth on the better resource over the experimental time period. The

results show that *P. polycephalum* cells made a choice for the better food source in each of the experimental conditions but the 10% vs 8% food choice conditions. Moreover, the choices made by the tubule were inconclusive in the 10% vs 10% food choice conditions.

Table 3.2 SUMMARY OF THE APPLICATION OF THE CHOICE-MAKING CRITERION ON THE CHOICE-MAKING BEHAVIORS OF *P. POLYCEPHALUM* TUBULES

Food choice condition (w/v oat-agar concentration)	**Relative quality of the poorer food source**	**Choice-making threshold**	**Choice (Yes or No)**	**Choice-making point**
10% vs 1%	0.1	0.82	Yes	6.57
10% vs 2%	0.2	0.67	Yes	6.34
10% vs 4%	0.4	0.43	Yes	6.45
10% vs 6%	0.6	0.25	Yes	7.16
10% vs 8%	0.8	0.12	No	Not enough experimental time
10% vs 10%	1.0	0	Yes	NA

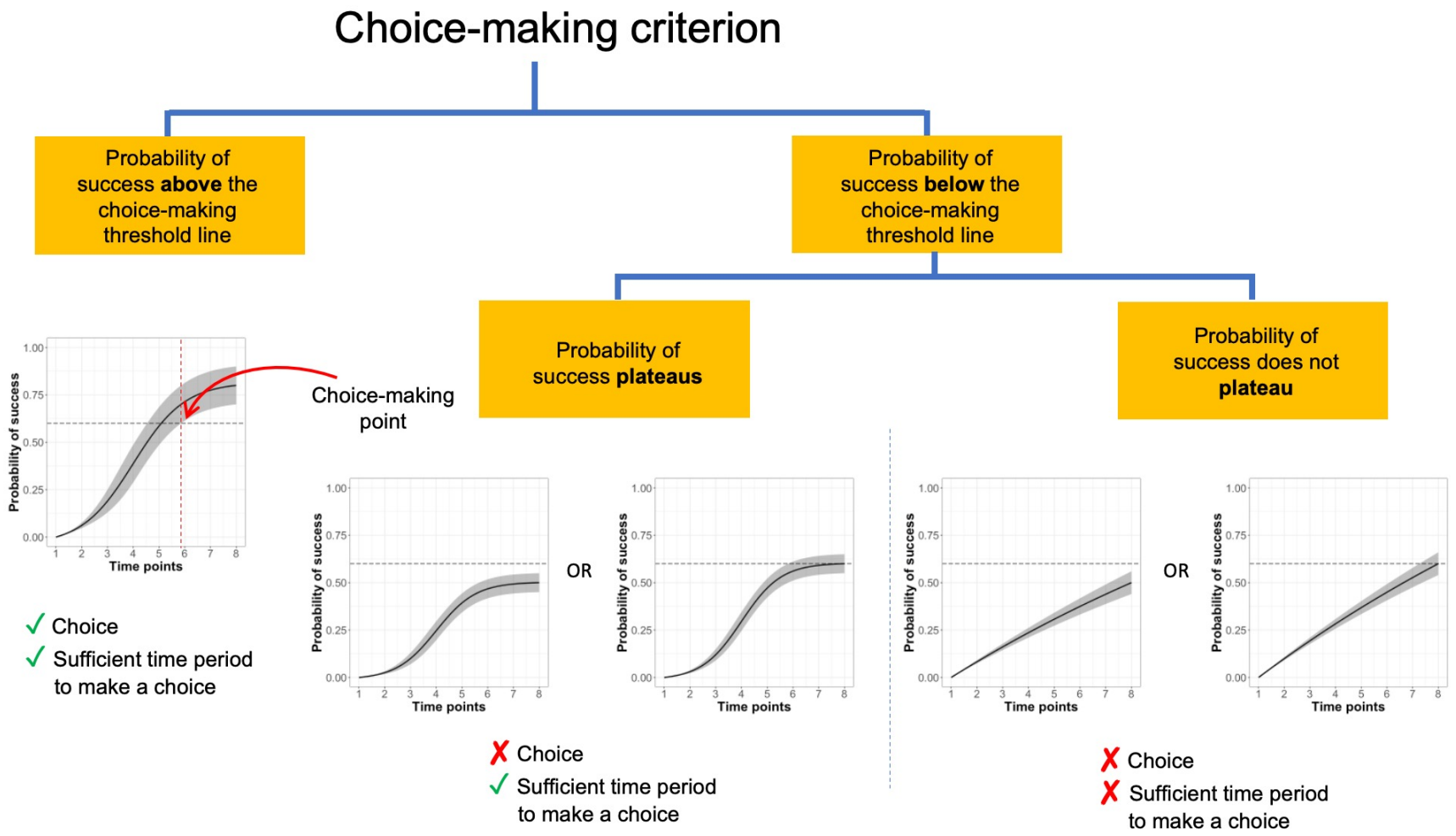

Figure 3.1 Choice-making criterion used to determine tubule choices and the sufficiency of experimental time period to make food choices. The dotted line in the plots represents the choice-making threshold and was calculated using the formula given by Equation 3.1. The solid black line represents the mean estimate of the probability of success, and the gray envelope represents the confidence interval of the estimate. Note: The trends and values of the choice-making criterion and probability of success used are for example purposes only.

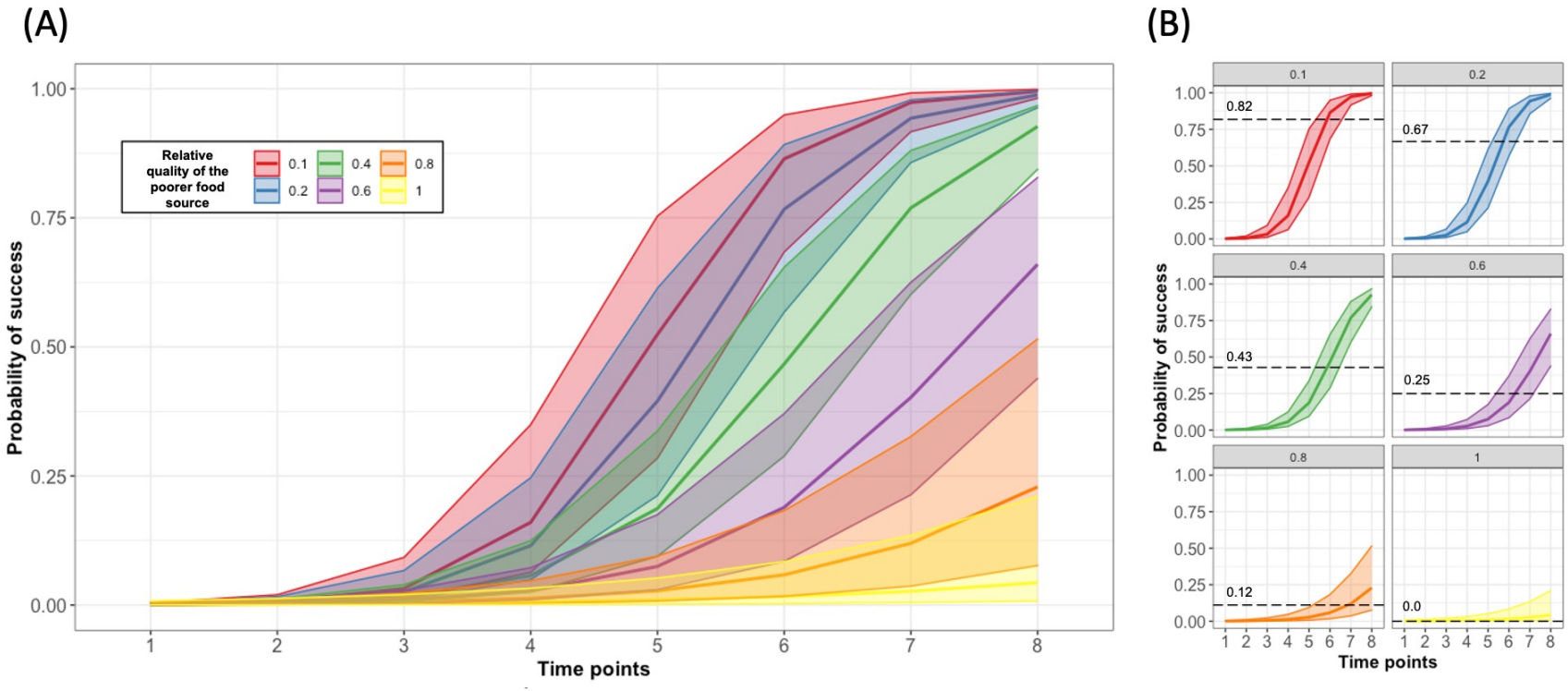

Figure 3.2 Plot of the Probability of Success as a function of the Time points, for each experimental food-choice condition. The data were analyzed using a generalized mixed effects model (GLMM) with binomial error distribution and logit link function. The food-choice condition was inputted into the model as the relative quality of the poorer food source. The colored lines represent the probability of success (i.e., the probability of observing distinguishable growth on the better resource) as predicted by the GLMM model, for each food choice condition. The semi-transparent envelope around the curves represents the 95% confidence interval of the fit. A) Shows the probability of success estimates for all the food choice conditions. B) Shows the probability of success estimates for different food choice conditions. The food choice condition is stated in the title of each plot. The horizontal dotted lines represent the choice-making threshold for the particular food choice condition, and the values are shown by the numbers placed right above the lines.

In this study, we used a strain of *P. polycephalum* cells that have previously been observed to show growth in the surface area that was in proportion to the qualities of the environment (*29*, *84*). However, there could be a *P. polycephalum* strain that allocates a differential amount of biomass toward resources, while not showing any difference in the net surface area coverage. In such a scenario, the criterion used in this study would not work. Therefore, to examine the choice-making behaviors of *P. polycephalum* in such situations, we propose an alternative criterion that measures the biomass distribution on the resources. And then use the precise biomass measurements to examine whether the distribution of the biomass on the better resource is significantly different from the expected distribution suggested by the null hypothesis.

Since the lower confidence interval in the 10% vs 10% food choice scenario cannot achieve a value that is below zero, any proportion of occurrences of higher biomass growth on the left food source will show a choice as made for the particular resource. Moreover, our choice-making criterion only deciphers choice-making behaviors when *P. polycephalum* cells are presented with options varying in a single attribute (i.e., food quality in this study). Our future work will be directed towards expanding the choice-making criterion to determine choice-making when the options available to the *P. polycephalum* cell are identical in quality and when the options vary in more than a single attribute.

CHAPTER 4

CAN *PHYSARUM POLYCEPHALUM* USE INFORMATION FROM ITS PAST TO DIRECT ITS FUTURE FORAGING BEHAVIORS?

4.1 Introduction

Natural selection has enabled living organisms to exploit information from their past history to better survive and reproduce in challenging environmental conditions. Foraging organisms have been observed to integrate information from their past experiences, and use the information to adapt their future foraging behaviors (*85*–*87*). This allows organisms to increase their foraging efficiency by decreasing search time and energy expenditure for discovering resources in the environment (*88*, *89*). For example, bumble bees *Bombus spp* (*90*, *91*), hummingbirds *Phaethornis longirostris* and *Selasphorus rufus* (*5*, *6*), tamarin monkeys *Saguinus mystax and Saguinus fuscicollis* (*92*), and bison *Bison bison* (*7*) adopt a non-random, goal-directed movement towards patches where they encountered high-quality and replenishable food sources in their past. Conversely, wildebeest *Connochaetes taurinus* and caribous *Rangifer tarandus granti* (*93*), and grizzly bears *Ursus actos* (*94*) avoid revisiting patches with non-replenishable food sources, and instead, focus their foraging activity on other unexplored patches in the environment. Moreover, honey bees *Apis mellifera* (*95*), golden shiner fish *Notemigonous crysoleucus* (*96*), macaques *Macaca arctoides* (*97*), and Risso's dolphin *Grampus griseus* (*98*) adapt the timing of their foraging trips to the spatiotemporal distribution of food sources encountered in their past foraging efforts.

In all these examples, the organisms used a specialized information processing organ, i.e., a nervous system, to adapt their foraging behaviors in response to their past experiences. However, life on Earth is primarily composed of organisms that are “non-neuronal”, which have existed long before the evolution of neurons (*12*). Yet, most of the studies investigating the influence of past experience on foraging have primarily focused on neuronal organisms, seemingly ignoring a large portion of life on Earth.

Non-neuronal organisms - such as bacteria, fungi, plants, and protists - lack a specialized organ for information processing, and yet many studies have shown that they can use information from their past to inform their future foraging behaviors. For example, *Escherichia coli* bacteria can detect the temporal pattern of nutritional changes in their local environment, and use this information to predict the future occurrences of a fitness-limiting nutrient (i.e., maltose) (*99*). Similarly, they can compare the quality of their local environment on a temporal scale and use this information to navigate towards attractive resources in the environment (*100*, *101*). *Mucor* and *Aspergillus* spp. of fungi release chemical inhibitors that repel the fungal hyphae, preventing them from revisiting previously explored areas (*102*). Furthermore, clonal plants *Potentilla reptans* and *P. anserina* based their choice of placing a new rooting ramet (ramets are stem extensions that help a plant forage for resources from an environment where it is rooted) on the quality of the new environment as well as the quality of the environments encountered by older ramets (*103*).

While we have recorded examples of how non-neuronal organisms can exploit information from their past history to inform their future foraging behaviors, our understanding of the mechanisms involved is very poor. Therefore, in order to understand these mechanisms, we are using the acellular slime mold *Physarum polycephalum* as a model organism.

P. polycephalum is a macroscopic, unicellular, multi-nucleated protist (phylum: *Amoebozoa*, class: *Myxogastria*) that lives in dark, cool, and moist areas of temperate forests. *P. polycephalum* can extend multiple pseudopods to explore its environment, hence referred to as “multi-headed” (i.e., translates to polycephalum in *Latin*). The exploratory search front of *P. polycephalum* advances in a dense fan-like shape, followed by a network of interconnected tubules (*14*), where the protoplasm (containing cytoplasm, organelles, nutrients, and signaling molecules) flows in a rhythmic back-and-forth manner called shuttle streaming (*16*). *P. polycephalum*, without the help of a single neuron, can exhibit complex problem-solving behaviors, such as finding the shortest path in a labyrinth maze (*17*), forming adaptive networks with properties similar to those found in human-made structures (*18*), solving complex nutritional challenges (*19*), anticipating periodic events (*21*), and making irrational decisions similar to organisms with neurons (*25*). Moreover, *P. polycephalum* has been shown to have “internal” memory that helps the cell to habituate to repeated innocuous stimuli from the environment (*23*), and “external” memory in the form of extracellular slime that repels the cell from repeated exploration of the same area (*22*). In essence, the macroscopic size of the organism combined with the experimental tractability and

problem-solving capabilities, make *P. polycephalum* an excellent model organism to understand the mechanisms used by non-neuronal organisms to exploit past information to direct future foraging behaviors.

In a previous study by Latty and Beekman (2009), the authors showed that *P. polycephalum* could modify its network morphology depending on the quality of the recently exploited environment (*104*). When grown in a high-quality food patch of 10% quality (i.e., 10% oat-agar weight/volume), *P. polycephalum's* subsequent foraging network was dense and localized, presumably in an attempt to maximize resource exploration in regions neighboring the high-quality food source. In contrast, *P. polycephalum* grown in a low-quality food patch (i.e., 1% oat-agar weight/volume) built a subsequent network that was sparse and thinly scattered in an effort to explore a larger area for food. These different exploratory strategies employed by the *P. polycephalum* cell were interpreted as adaptive responses induced by the organism's recent experience of foraging environment quality. However, the study did not investigate the influence of foraging in environments with multiple and patchily distributed resources on the subsequent exploratory behavior of *P. polycephalum*.

In this study, we examine how *P. polycephalum* alters its exploratory behavior in response to the experiences of foraging in environments with varying distribution of food sources. By predictably changing the number of food sources encountered by a *P. polycephalum* cell, we examine how the subsequent exploratory behavior is modified by the cell, in order to maximize resource acquisition in the experimental environment. We hypothesize that as the number

of food sources encountered by a *P. polycephalum* cell decreases, the cell would increasingly engage in an exploratory strategy that helps detect resources in the far reaches of the experimental setup. To test our hypothesis and characterize the exploratory behavior, we quantify the *P. polycephalum* exploratory behavior by defining 3 morphological metrics: *Sparsity*, *Isotropy*, and *Rate of exploration*.

Sparsity is a measure that quantifies how thinly scattered or sparsed is an exploratory network formed by *P. polycephalum*. That is, when the exploratory network formed by *P. polycephalum* is thinly dispersed and distributed, then the network will have high *Sparsity*. Conversely, an exploratory network that is dense and concentrated will have a low *Sparsity*. We expect that with decreasing number of food sources encountered by *P. polycephalum*, the *Sparsity* of the subsequent cell network would increase. This expectation is based upon the results of the study conducted by Latty and Beekman (2019), as discussed above. Specifically, when the cell encounters a lower number of food sources, a *P. polycephalum* cell would have an increased tendency to leave the current environment and explore resources that might be available in the far reaches of the experimental setup. Thereby forming a network that is highly scattered and thinly distributed.

Isotropy is the measure that quantifies the angular distribution of the exploratory network formed by *P. polycephalum*. That is, when the exploratory network formed by *P. polycephalum* is growing equally in all directions (i.e., growing “isotropically” in all directions), then the network will have a high *Isotropy*. Conversely, an exploratory network growing in very few directions (i.e., growing “anisotropically”), the network will have a low *Isotropy*. We expect that with

decreasing number of food sources encountered by *P. polycephalum*, the *Isotropy* of the subsequent cell network would decrease. Our expectation is based on the results of previously conducted simulation-based studies, which showed that organisms adopting a straighter, unidirectional path are more successful at finding better resources away from their current foraging environment (*105*–*107*). Moreover, organisms such as prairie rattlesnake *Crotalus viridis viridis* (*108*), sharks (i.e., *Galeocerdo cuvier*, *Alopias vulpinus*, and *Carchahinus melanopterus*) (*109*), and eagle owls *Bubo bubo* (*110*) have been observed to use straighter paths having low sinuosity when exploring environments that are located at increased distances.

Rate of exploration is a measure defined as the speed at which *P. polycephalum* explores (or moves) in the open arena. We expect that with decreasing number of food sources encountered by *P. polycephalum*, the rate of exploration would increase. This expectation is based on previous simulation studies showing that organisms attempting to move away (or disperse) from a low-quality environment will efficiently discover new high-quality environments by moving quicker (i.e., making rapid movements) from their current environment (*105*, *107*). Such exploratory patterns have been previously observed in eagle owls *Bubo bubo* (*111*) and goats *Capra hircus* (*112*).

4.2 Materials and Methods

4.2.1 Biological Material

We used *P. polycephalum* in the plasmodium stage of its life cycle, where the cell is large enough to be observed with the naked eye. In that stage, the cell can move in space up to a speed of 5 cm/hr (*45*) and can cover an area up to several hundred square centimeters (*14*).

We obtained *P. polycephalum* cultures from Carolina Biological Supply® (Burlington, North Carolina). It was cultured in Petri plates (Ø = 10 cm, *H* = 1.5 cm) containing water solution of 1% w/v (weight/volume) non-nutrient agar (referred to as blank agar in the rest of the document) and 5% w/v blended rolled oats (referred to as food agar in the rest of the document). We used rolled oats manufactured by Quaker Oats Company®. *P. polycephalum* stocks were recultured onto new Petri plates twice every week and maintained at 26°C under dark conditions.

4.2.2 Experimental Setup

To investigate how *P. polycephalum* modifies its foraging behavior in response to the distribution of food sources encountered, we tested cells in the experimental setup shown in Figure 4.1A. The setup is composed of 3 different sections, namely: 1) a starting site, 2) a food track, and 3) an open arena. The boundary wall of the setup was 0.2 cm in thickness and 0.9 cm in height. The setup was 3d printed using MakerBot® PLA filament. The starting site was a 1.5 cm by 1.5 cm space where we introduced the *P. polycephalum* cell to the setup. The food track was a 1 cm wide and 6 cm long passage that connected the starting site to the open arena. The food track contained a varying number of food sources (dimensions 1

cm in length, 0.1 cm in width, and 0.5 cm in height) depending on the experimental condition as given in Table 4.1 (see also next section). Since *P. polycephalum* feeds on the nutrients available on the surface of their foraging environment (*113*), the upper 1 cm x 0.1 cm (or 0.1 cm^2) surface of the food sources were only available to the cell to forage. The open arena was a 10 cm wide and 6 cm long space where a *P. polycephalum* was free to form an exploratory foraging network after exiting the food track.

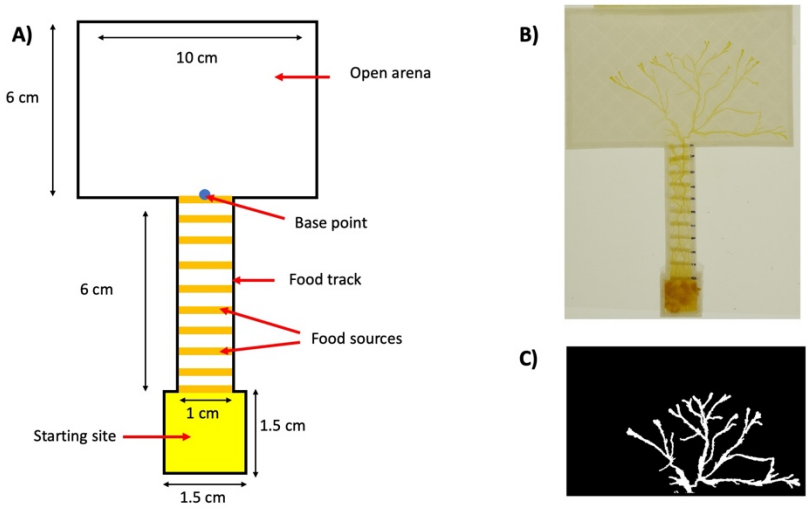

Figure 4.1 A) Picture of the experimental setup used in the experiments. The details about the setup are described in the text. B) An example last image of an experiment with 11 food sources (Condition No. 4 in Table 4.1), and C) shows the final explored area image of the given example experiment.

4.2.3 Experimental Protocol

The experimental setup was filled with blank agar solution to a height of 0.5 cm. We began our experiments by carefully extracting 300 ± 5 mg of *P. polycephalum* biomass from our lab stocks and placing it at the starting site. When detached from the main cell, the biomass fragments begin to act as independent cells within a few

minutes after extraction (*114*). In each experimental condition, a food agar block was placed right at the entrance of the food track in order to motivate the *P. polycephalum* cell to begin exploring the experimental setup. The experimental setup was covered with a transparent acetate sheet. Since *P. polycephalum* is photophobic, we conducted the experiments in a dark chamber for a period of 48 hours. The temperature of the experimental chamber was maintained at 26 °C, which has been observed to be the optimal temperature for cell growth in our lab cultures. The experiments were stopped once an edge from the *P. polycephalum* network contacted one of the three boundaries of the open arena that were not attached to the food track.

The experiments were recorded using a Panasonic® Lumix GH3 camera fitted with Lumix® G Varia 14-140mm f/3.5-5.6 II lens. The camera took a picture once every 5 minutes, while an LED panel placed below the setups illuminated the experiments. The LED panel switched on for a period of 10 seconds while the camera took a picture, but at all other times, experiments were kept under dark conditions.

Table 4.1 OUTLINE OF THE EXPERIMENTAL CONDITIONS

Condition No.	Experimental Conditions (i.e., the no. of food sources offered to *P. polycephalum*)	No. of replicates
1	1	16
2	3	35
3	6	33
4	11	36
5	21	18

4.2.4 Image Segmentation

We processed and segmented the experimental images to extract different morphological features of *P. polycephalum* exploration using a custom-written computer vision script in MATLAB®. First, the script requires a user to manually select 4 corners of the open arena to create a mask that removes the background regions (i.e., the regions other than the open arena) of the experimental setup. Then, the script computes a threshold to segment the *P. polycephalum* network using a reference image and the last experimental image. The reference image was defined as an image with no *P. polycephalum* growth in the open arena. We chose the reference image to be the image taken one before the first image showing *P. polycephalum* growth in the open arena. The last experimental image was the image where a part of the *P. polycephalum* cell came in contact for the first time with one of the three boundaries of the open arena that were not attached to the food track. To calculate the threshold, we first converted the background and last experimental image from RGB (i.e., Red Green Blue) to HSV (Hue

Saturation Value) color space, as *P. polycephalum* showed the highest contrast in the saturation (i.e., S) channel of this colorspace. Next, we subtracted the saturation channel of the background image from the saturation channel of the last image. We used this differenced image to obtain a threshold that could be used to get a binary image with white pixels representing the *P. polycephalum* cell and black pixels representing the other regions in the open arena. We tried different methods using trial and error to get the best segmented image. The best result was produced by taking the difference image, setting all the pixels with negative values to 0, and normalizing the pixel values between 0 and 1. Then, from the resulting image, the threshold was calculated as the elbow point of the image histogram (Figure 4.1C). Lastly, to get the binary images of *P. polycephalum* for each experimental image, the script used the calculated threshold on the image resulting from the difference in the saturation channels of the focal and reference image.

We used these binary images to create a new set of binary images that showed the area visited or explored by *P. polycephalum* until each experimental time step. That is, in each experimental image, if a pixel in the open arena was visited by a *P. polycephalum* cell at the current time step or in the past, then that pixel appeared as white in the binary image. From here onwards, we use the terms “explored area” and “explored area image” when referring to the total area explored until each experimental time step and the binary image showing the pixels visited by *P. polycephalum*, respectively. The different morphological metrics measured

to understand the exploratory behavior of *P. polycephalum* were calculated using the explored area image.

4.2.5 Morphological Metrics to Quantify *P. polycephalum* Exploratory Behavior

We computed three different metrics to investigate the performance of *P. polycephalum* in response to its past foraging experience. The metrics are discussed in detail below:

1) ***Sparsity*** is the measure that defines how thinly scattered or distributed an exploratory network formed by *P. polycephalum* is. *Sparsity (S)* was calculated for each explored area image using Equation 4.1:

$$S = 1 - \frac{C_S}{C_N} \tag{4.1}$$

with C_N representing the circumference of the explored area by a *P. polycephalum* cell, and C_S representing the circumference of a semi-circle having the same surface area as that of the *P. polycephalum* exploratory network. In other words, if *P. polycephalum* explored systematically each and every portion (or pixel) of the open arena, then the cell would have allocated all its biomass into a shape that resembled a semi-circle with a circumference C_S.

As per Equation 4.1, a *Sparsity* value of 1 represents a network that is maximally sparsed. Conversely, a value of 0 represents a network that is maximally dense.

2) ***Isotropy*** is defined as a measure of the angular distribution of *P. polycephalum* biomass in the open arena. We used an information-theoretic tool called Jensen-Shannon Divergence (i.e., JSD) to measure the *Isotropy* in *P. polycephalum* growth in the open arena. JSD is the measure of the symmetric distance between two probability distributions (*115*). The concept of JSD is based upon another information-theoretic measure called Kulback-Leibler Divergence (i.e., KLD) or relative entropy. The JSD between two discrete probability distributions *P(x)* and *Q(x)*, defined over the same probability space *X* is given by:

$$JSD(P(x)||Q(x)) = \frac{1}{2}D_{KLD}(P(x)||M(x)) + \frac{1}{2}D_{KLD}(Q(x)||M(x)) \quad (4.2)$$

Where, quantity $M(x)$ is the vector mean of $P(x)$ and $Q(x)$, such that $M(X) = \frac{1}{2}(P(x) + Q(x))$. $D_{KLD}(A(x)||B(x)$ is the KLD measuring the divergence of the distribution $B(x)$ from the distribution $A(x)$, over the same probability space X (*116*), and is given by:

$$D_{KLD}(A(x)||B(x)) = \sum_{x\varepsilon X} A(x) \log \frac{A(x)}{B(x)} \quad (4.3)$$

When the JSD between two distributions is 0, then the two distributions are identical (i.e., having a statistical distance of 0 between the two distributions). Whereas, a JSD value of 1, means that two distributions are maximally different from one another.

To measure *Isotropy*, for each explored area image, we first divided the open arena into 180 sectors, with each sector subtending a 1° angle at the *base point*. The *base point* was defined as the point in the middle of the food track right at the entrance of the open arena (Figure 4.1A). Next, we calculated the proportion of *P. polycephalum* biomass occurring in each of the sectors. We then calculated the JSD between the distribution of the biomasses in the different sectors and the expected distribution if the *P. polycephalum* biomass was uniformly distributed among all the sectors (i.e., 1/180 parts or 0.5556% of the total biomass found in each sector). Therefore, when the JSD of an explored area is 0, then the growth of the *P. polycephalum* is completely isotropic (i.e., the biomass is equally distributed in all the sectors), i.e., the exploratory network has high *Isotropy*. In contrast, a JSD of value 1 would mean the *P. polycephalum* growth is completely anisotropic (i.e., the *P. polycephalum* is growing in only 1 sector in the open arena), i.e., the exploratory network has low *Isotropy*.

3) ***Rate of exploration*** is a measure defined as the rate at which *P. polycephalum* explores or moves in the open arena. This was calculated by taking the difference of the explored area between two consecutive experimental images, from the time the *P. polycephalum* first appears in the open arena until the end of an experiment.

4.2.6 Statistical Analyses

The *Sparsity, Isotropy,* and *Rate of exploration* were analyzed separately using a combination of a linear model and/or nonlinear least squares models. The details of the analyses are given below and were performed in R version 4.1.2 (*82*). We used the model diagnostics plots (Q-Q plot and standardized residuals vs fitted value) and the "DHARMa" package in R to test for the model performance (*117*) for all our analyses.

Sparsity

To investigate the influence of environments with a different number of food sources on *Sparsity*, we examined the change in *Sparsity* values as a function of the explored area for each experiment. In order to account for the behavior of *Sparsity* reaching an upper asymptote at high explored area values (see *Appendix* Figures B.1 – B.5), we fitted an asymptotic nonlinear least square model for each experimental data separately. The model was of the form:

$$Y = a - (a - b) * e^{(-c * X)} \quad (4.4)$$

Where, Y is the dependent variable (i.e., *Sparsity* in our analysis) and X is the independent variable (i.e., explored area in our analysis). The parameter a represents the upper asymptote of the model (i.e., the maximum achievable Y value) and was set to a value of 1. This is because we expect the *P. polycephalum* exploratory network to be maximally thin and dispersed (i.e., *Sparsity*

approximating a value of 1) as the explored area of the network tends to infinity. The parameter b represents the value of Y when X = 0, and in our model, the value of b was set to 0, as we expect *Sparsity* to be 0 when there is no *P. polycephalum* growth in the open arena. Next, the parameter *c* represents the relative rate at which Y reaches an upper asymptote with increasing X. In our analysis, c represents the rate of change of *Sparsity* towards the upper asymptote (it will be referred to as the rate of change of *Sparsity* from here onwards) as a *P. polycephalum* cell explores more of the open arena. The model parameter c was kept free and fitted to each experimental data separately. We tried a combination of transformations on the independent variable to find the best visual fit to our data. We found that a square root transformation on the independent variable produced the best fit (see *Appendix* Figures B.1 – B.5). Lastly, we analyzed the rate of change in *Sparsity* as a function of an increasing number of food sources encountered by *P. polycephalum* using a linear model.

Isotropy

To investigate the influence of different foraging environments on *Isotropy*, we first examined the change in JSD values as a function of explored area for each experiment. The change in JSD did not show any consistent pattern across different experiments (see *Appendix* Figures B.8 – B.12 for raw data). Therefore, we only considered the JSD in the final image, as it shows the overall exploratory behavior of *P. polycephalum* throughout the experimental time period (i.e., it shows everything visited by *P. polycephalum* during an experiment). We analyzed the

JSD in the final explored area image (will be referenced as “Final JSD” from here onwards) as a function of an increasing number of food sources encountered by *P. polycephalum* in the past using a general linear model.

Rate of exploration

To investigate the influence of different foraging environments on the *Rate of exploration*, we examined the change in the *Rate of exploration* as a function of time. The change in *Rate of exploration* didn’t show a consistent pattern across experiments (see *Appendix* Figures B.15 – B.19 for raw data), and therefore, we analyzed the mean *Rate of exploration* as a function of an increasing number of food sources encountered by *P. polycephalum* using a general linear model.

4.3 Results

4.3.1 Sparsity Analysis

To understand the influence of environments with a different number of food sources on the *Sparsity* of the *P. polycephalum* exploratory network, we first examined the rate of change of *Sparsity* as a function of the explored area for each experiment. *Sparsity* initially increases with increasing explored area by the *P. polycephalum* cell, and then reaches an upper asymptote at high explored area values (see *Appendix* Figures B.1 – B.5). Additionally, this trend was corroborated by the positive parameter *c* values (i.e., the rate of *Sparsity* reaching an upper asymptote of values 1 in Figure 4.2) estimated for all experimental replicates across different experimental conditions.

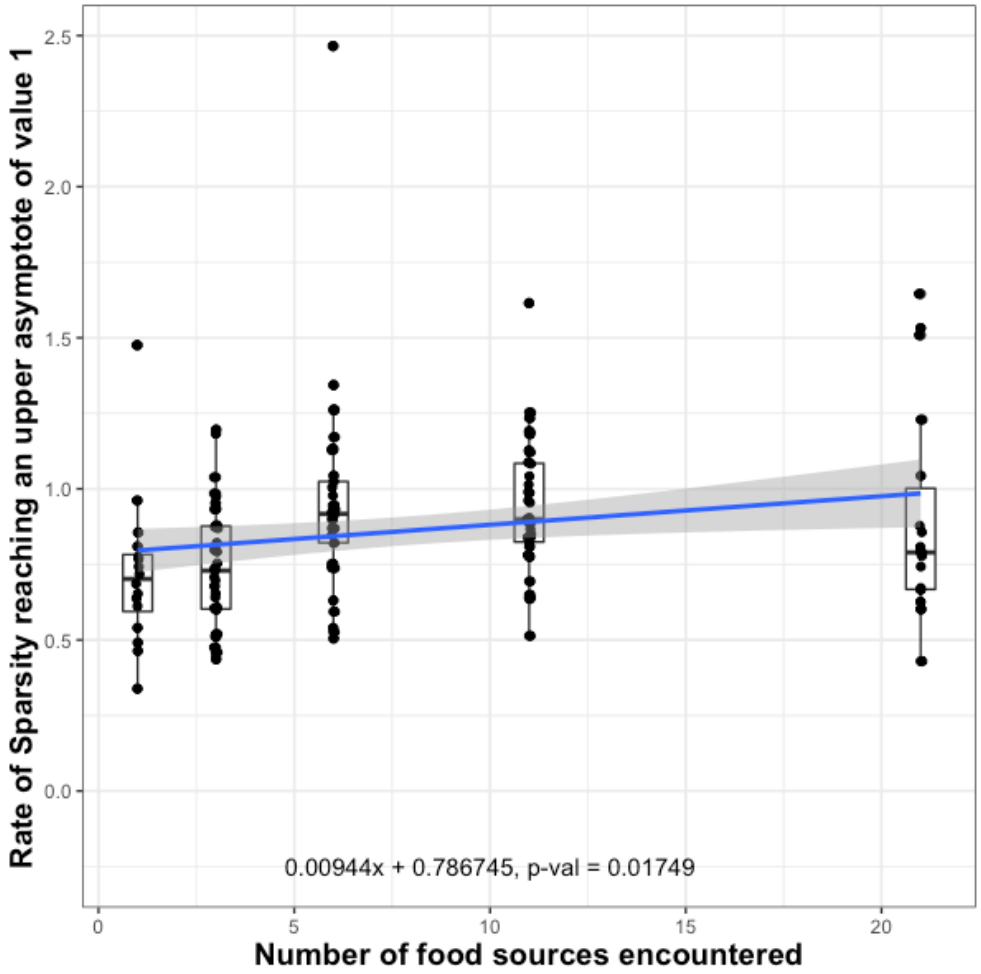

Figure 4.2 Plot of the Rate of *Sparsity* reaching an upper asymptote of value 1 (i.e., the rate of change of *Sparsity*, or the parameter *c* in Eq. 4.4) vs Number of food sources encountered in the past. Higher values of the rate of change of *Sparsity* show that a *P. polycephalum* reaches the upper asymptote faster than the values that are lower. The solid blue line represents the best linear model fit to the data (R^2 = 0.04081, $F_{1,136}$ = 5.787, and p = 0.01749) and the semi-transparent envelope represents the 95% confidence interval of the fit. The fitted regression model equation is given at the bottom of the figure (*x* is the number of food sources encountered).

Next, we examined the rate of change of *Sparsity* as a function of the number of food sources encountered in the past using a linear model (Figure 4.2). The best-fitted regression model was *0.00944x + 0.786745* (where *x* is the number

of food sources encountered). Overall, the regression was found to be statistically significant (R^2 = 0.04081, $F_{1,136}$ = 5.787, and p = 0.01749). The model diagnostics and performance are shown in *Appendix* Figures B.6. and B.7, respectively.

While the results of a linear model fit show the relationship between the rate of change of *Sparsity* and the number of food sources encountered to be significant, the increase in the rate of change of *Sparsity* with every additional food source encountered is extremely low (i.e., the effect size was found to be 0.00944, or a ~ 0.9% increase in the rate of change of *Sparsity* with every additional food source encountered). Moreover, the R-squared value of the model was found to be extremely low (i.e., a value of 0.04081). This means that there are other factors that significantly influenced the rate of change of *Sparsity* of a *P. polycephalum* exploratory network. Therefore, taking into account the low effect size and R-squared value, we conclude that our analysis did not find any strong influence of the number of food sources encountered in the past on the rate of change of *Sparsity*.

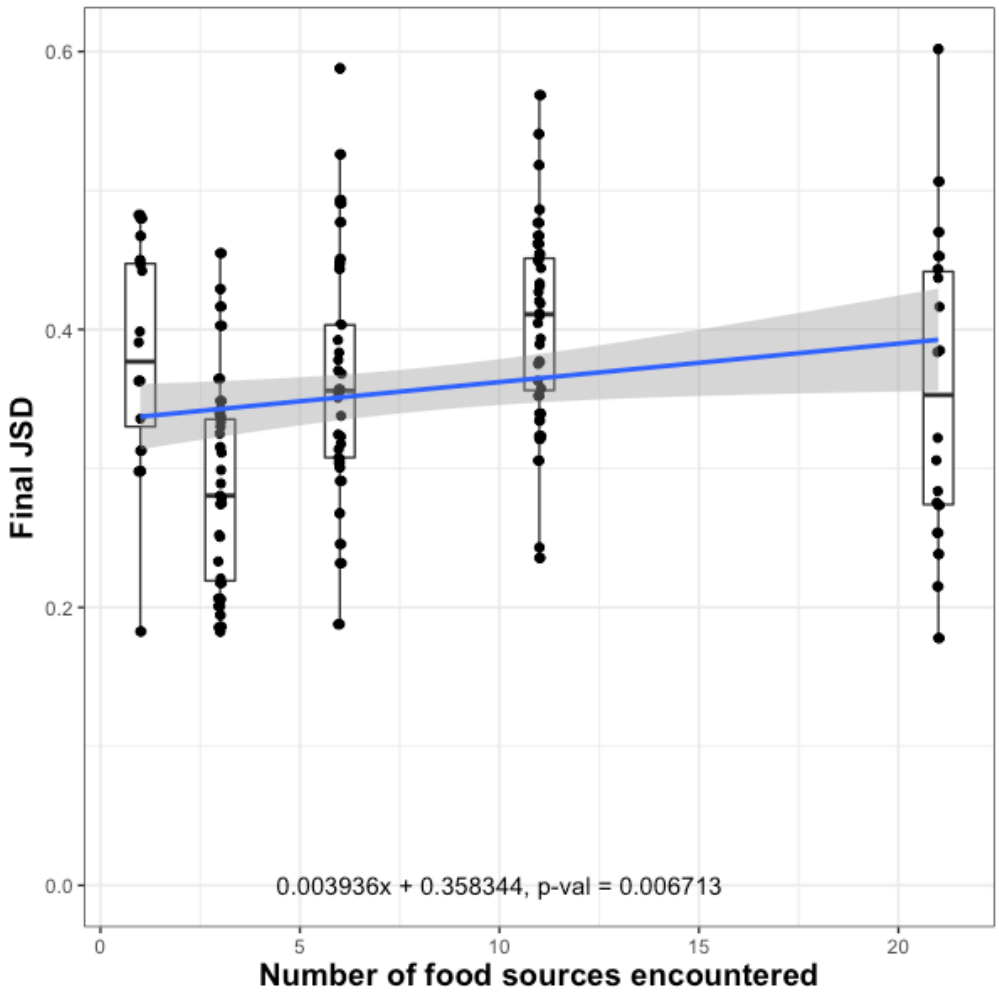

Figure 4.3 Plot of the Jensen-Shannon Distance (JSD) vs Number of food sources encountered in the past. Higher JSD values represent low *Isotropy* in the *P. polycephalum* exploratory network, and vice-versa. The solid blue line represents the best linear model fit to the data (R^2 = 0.05279, $F_{1,136}$ = 7.579, and p = 0.006713) and the semi-transparent envelope represents the 95% confidence interval of the fit. The fitted regression model equation is given at the bottom of the figure (*x* is the number of food sources encountered).

4.3.2 Isotropy Analysis

To understand the influence of environments with a different number of food sources on the *Isotropy* of the *P. polycephalum* exploratory network, we examined the JSD in the final image (i.e., Final JSD) as a function of the number of food sources encountered in the past. We found the relationship to be best described

by a linear regression model (Figure 4.3) of form 0.003936x + 0.358344 (where *x* is the number of food sources encountered). The regression was found to be statistically significant (R^2 = 0.05279, $F_{1,136}$ = 7.579, and p = 0.006713). The model diagnostics and performance are shown in *Appendix* Figures B.13 and B.14, respectively.

The results show that with the increase in the number of food sources encountered in the past, the JSD of the exploratory *P. polycephalum* network increases (i.e., *Isotropy* decreases). However, the model showed the increase in JSD to be extremely small (i.e., JSD increases by a factor of 0.003936 or by ~0.4% with each additional food source encountered by the cell). Moreover, the fitted model showed an extremely low R-squared value (i.e., a value of 0.05279), suggesting that other factors were more influential in explaining the variability in the JSD values than the number of food sources encountered by the *P. polycephalum* in its past. In essence, given the extremely low effect size and R-squared values of the fitted model, we conclude that the isotropy of *P. polycephalum* networks are not strongly influenced by the number of food sources encountered in the past.

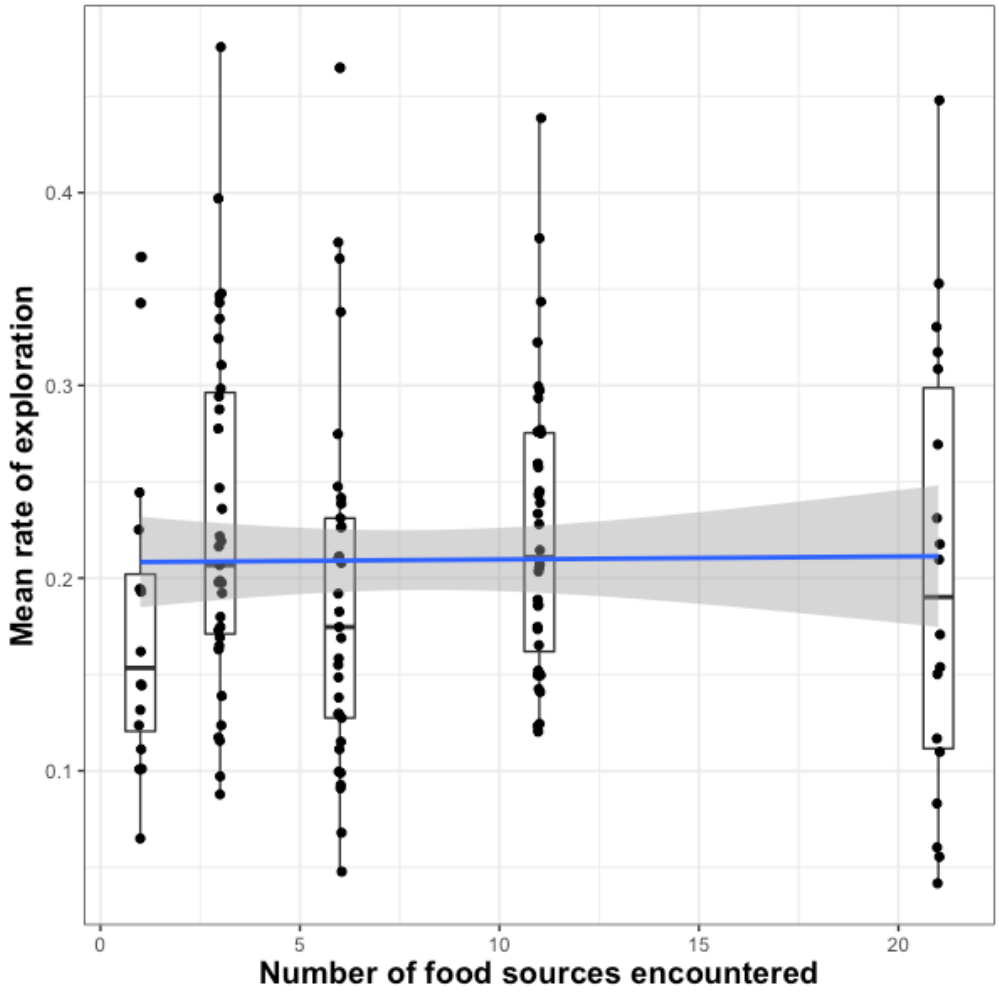

Figure 4.4 Plot of the Mean rate of exploration vs Number of food sources encountered in the past. The solid blue line represents the best linear model fit to the data (R^2 = 0.0001511, $F_{1,136}$ = 0.01382, and p = 0.9066) and the semi-transparent envelope represents the 95% confidence interval of the fit. The results show the relationship between the mean rate of exploration and the number of food sources encountered in the past was not statistically significant.

4.3.3 Rate of Exploration

To understand the influence of environments with a different number of food sources on the *Rate of exploration* of the *P. polycephalum* exploratory network, we examined the mean *Rate of exploration* as a function of the number of food sources encountered in the past. The results are shown in Figure 4.4 (see *Appendix*

Figures B.20 and B.21 for model diagnostics and performance, respectively), and we found that the relationship between the mean *Rate of exploration* and the number of food sources encountered in the past is not significant ($R^2 = 0.0001511$, $F_{1,136} = 0.01382$, and $p = 0.9066$). Therefore, we conclude that the mean *Rate of exploration* of the *P. polycephalum* exploratory network is not influenced by the number of food sources encountered in the past.

4.4 Discussion

We studied the exploratory strategy adopted by *P. polycephalum* in response to the experiences of foraging in environments with a varying number of food sources. We introduced a *P. polycephalum* cell to experimental environments with a different number of food sources, and examined the subsequent exploratory behavior. The exploratory behavior was quantified using 3 morphological metrics, namely: *Sparsity*, *Isotropy*, and *Rate of exploration*. We hypothesized that with decreasing number of food sources encountered by a *P. polycephalum* in the past, the cell would increasingly adopt an exploratory strategy that helps detect resources in the far reaches of the experimental setup. We expected an increase in *Sparsity* and *Rate of exploration* and a decrease in *Isotropy*. However, our results did not validate our hypothesis. In particular, our results did not find support for any changes in *Sparsity*, *Isotropy*, and *Rate of exploration* as a function of the number of food sources encountered in the past (Figures 4.2 - 4.4).

Although *P. polycephalum* cells were introduced to experimental conditions of varying qualities - the number of food sources offered to a cell ranged from 1 to

as many as 21 (Table 4.1) -, it is highly possible that each of the experimental conditions was deemed as “low-quality” by the cell. Previous studies that observed changes in *P. polycephalum* foraging behavior in response to environments with different qualities, introduced a *P. polycephalum* cell in experimental setups that provided a higher quantity of food in relation to the cell size, as compared to the proportions used in this study. For example, Reid et al (2016) examined the exploration-exploitation trade-off in *P. polycephalum* using an experimental setup that comprised a food track with dimensions and number of food sources similar to the experimental conditions used here (*29*). However, the authors introduced a *P. polycephalum* biomass that weighed 25 ± 5 mg (i.e., < 1/10th or 10% of the biomass used by us) to conduct their experiments. Similarly, Latty and Beekman (2009) tested the exploitation performance of *P. polycephalum* cells weighing 27 ± 2 mg in environments comprising 4 food agar disks (with quality similar to ours) each having a diameter of 1.5 cm (*104*). Specifically, the authors provided food sources to a *P. polycephalum* cell having a surface area (*P. polycephalum* only feeds on the nutrient available on the surface of their environment (*113*)) similar to that used in our experiments (i.e., a combined surface area of 1.76 cm^2 in Latty and Beekman (2009) vs. 2.1 cm^2 of a maximum combined surface area in Condition No. 5 in Table 3.1). But, the cells weighed < 10% of the *P. polycephalum* weight introduced in our study. Therefore, it is likely that in our experiments, none of the experimental conditions provided a *P. polycephalum* with enough nutrients that could enable the cell to explore regions neighboring the food track, in an effort to maximize resource acquisition within the experimental environment. As a result,

the cell might have adopted an exploratory behavior that would help discover resources in the far reaches of the experimental environment, thereby showing no differences in the morphological metrics measured in the study.

Previous studies exploring the problem-solving behaviors of *P. polycephalum* neither justified their decision of using a cell of a particular size to conduct their experiments, nor explored the *P. polycephalum's* problem-solving performance with changing cell sizes. Moreover, the amount and metric of *P. polycephalum* cells used in the studies were highly variable across different studies. For example, in a study by Reid et al. (2013), the authors introduced a *P. polycephalum* cell measured in square centimeters (used 3 cm^2 of *P. polycephalum*) into a setup containing two food-agar disks of diameter 1.2 cm each (i.e., with a surface area of 1.13 cm^2) located at a distance of 4 cm from the *P. polycephalum* inoculation site (*118*). Conversely, Dussutour (2010) used a setup that placed the food sources at the same distance from the *P. polycephalum* inoculation site as Reid et al. (2013), but introduced a cell that weighed in grams (i.e., weighing 0.014 gm) and food-agar disks with diameters of 2.0 cm (i.e., a surface area of 3.14 cm^2) (*19*). Similarly, Smith-Ferguson et al. (2021) introduced *P. polycephalum* of length < 5 mm into setups containing food disks of a diameter of 2.0 cm (i.e., a surface area of 3.14 cm^2) (*119*). In essence, the studies introduced *P. polycephalum* cells into setups that were similar in terms of food quality and structure but the amount of biomass used was incomparable, as the studies used different metrics to measure *P. polycephalum* biomass. Therefore, our results combined with the inconsistencies in *P. polycephalum* biomass size used in the

previous studies necessitate the need to establish a standard and explore the role of cell size in the problem-solving capabilities of *P. polycephalum*. Our future work will involve repeating the experiments as conducted in this study, but using *P. polycephalum* biomass weighing 10% of that used here (i.e., biomass weighing similar to that used by Reid et al. (2016) (*29*) and Latty and Beekman (2009) (*104*), described in the paragraph before). Additonally, we will investigate the changes in exploratory behavior as a function of the *P. polycephalum* biomass weight.

Our experimental framework provides an excellent testbed to understand the influence of past foraging experiences on the future exploratory behaviors of *P. polycephalum*. Since *P. polycephalum* can simultaneously grow in multiple directions to forage in their environment, it could be difficult to examine and quantify the exploratory behavior of *P. polycephalum* in response to the quality of their foraging environment. However, our experimental setup (Figure 4.1A) overcomes this problem by limiting the scope of directions that could be adopted by a *P. polycephalum* cell to search for resources in the experimental environment. Moreover, the *Sparsity* and *Isotropy* morphological metrics, devised in this study, provide a standardized measure of scatteredness and directionality, respectively, of a *P. polycephalum* exploratory network. These metrics provide values that are normalized between 0 and 1, thereby, making it possible to compare the metrics between cell networks at different stages of an experiment. Lastly, the *Rate of exploration* metric used in this study provides a good measure to compute the speed of exploration of a cell over time, and has been used frequently to understand the exploratory behaviors in different organisms, such as, in juvenile

starlings *Sturnus vulgaris* (*120*), frogs *Xenopus tropicalis* (*121*), rats *Rattus rattus* (*122*), and mycorrhizal fungi belonging to Glomeraceae and Claroideoglomeraceae families (*123*).

CHAPTER 5

HOW DOES *P. POLYCEPHALUM* EXPLORE ITS ENVIRONMENT WHEN IN DIFFERENT PHYSIOLOGICAL STATES?

5.1 Introduction

Exploring the environment is an important activity performed by organisms to improve fitness. For example, exploration helps organisms discover new food sources (*124–126*), find habitats with better microclimates (*127*, *128*), detect competitors (*127*, *129*), seek refuge from predators (*130*, *131*), etc. Conversely, exploration may result in fitness costs by exposing organisms to predators (*132*, *133*), and demanding high energy and time investments (*134–137*). Previous studies have shown that organisms, across taxa, employ exploration strategies that help them better explore their environments while minimizing costs from various risks. For example, the great tit *Parus major* and blue tit *Parus caeruleus* preferentially forage on food patches that provide high prey biomass and are located at distances closer to their nest, in order to optimize the prey delivery rate to their nestlings (*138*). The white-faced saki monkeys *Pithecia pithecia* exploit patches with highly productive food sources at the cost of traveling a longer distance, to minimize intragroup competition and maintain intergroup dominance over useful resources (*139*). Moreover, non-neuronal organisms, such as plants in tussock tundra, differentiate the exploitation (in the terms of timing, location, and chemical form) of a limiting nutrient (i.e., soil nitrogen) in their environment, to avoid competition with the heterospecifics (*140*). However, when faced with heterogeneous and changing environmental and physiological conditions, the

costs and benefits of an exploration strategy changes. For example, in summers juvenile Atlantic salmon *Salmo salar* forage during the day, despite increased predation risks from avian predators, as they have high escape responses caused by a high metabolic rate. However, this strategy is detrimental to the fitness of juvenile salmon in the winter as their metabolic rate drops, thereby causing slower escape responses from the predators (*141*).

In order to adapt to changing conditions, organisms, therefore, switch or change their exploration strategies to increase fitness. For example, when resources in the environment are sparse and unpredictable, organisms may use a correlated random walk based strategy (e.g., Brownian walks (*142*, *143*), and Lévy flights and walks (*1*, *3*, *144*, *145*)) to search for food sources in the environment. Studies have shown that such movement strategies increase an organism's chances of locating a food patch by maximizing the exploratory area for resources while minimizing the mean distance traveled during exploration (*142*, *143*, *146*). However, when the resources are predictable, they switch to more direct, energetically efficient, and systematic foraging strategies (*147–149*). For example, bumblebees *Bombus impatiens* use repeatable, shortest, and energetically less expensive paths when foraging in patches with renewable resources (*4*). Similarly, organisms change their exploration strategies in response to variations in their energetic states. Studies show that when organisms are in a low-energy state (e.g., after a period of starvation), they increase their exploratory activity and risk-taking behaviors, compared to their high-energy counterparts, in order to increase their chances of discovering food sources (see Moran et al. (2021) (*150*) for a full

review). For example, the earthworm *Lumbricus terrestris* in starved conditions preferentially foraged in environments comprising more profitable resources, but involved increased risks from predation and desiccation, more frequently than compared to the earthworms in good nutritional condition (*8*). Likewise, piglets *Sus domesticus* in starved conditions showed riskier foraging behaviors (i.e., foraging at the cost of being accidentally crushed by mothers), in order to increase the frequency and time period of obtaining food (*9*). Furthermore, organisms can switch their exploration strategies to increase fitness in response to the presence or absence of a predator (*151–153*), changing environmental conditions of their home range (*154*, *155*), and managing costs of inter-or intraspecific competition (*156*, *157*).

In the aforementioned examples, the organisms functioned as single units (or individuals) that changed their behavior or movement patterns, to adapt to the changing environmental and physiological conditions. Nevertheless, in nature, there are organisms that are capable of fragmenting (or splitting) themselves into multiple autonomous subunits during reproduction in order to ensure the continued survival of their gene pool. For example, bacterial cells (e.g., *Escherichia coli* (*158*), and *Prosthecomicrobium* (*159*)), fungi (e.g., *Penicillium marneffei* (*160*), *Trachipleistophora extenrec* (*161*), *Pneumocystis* spp. (*162*)), and protists (e.g., *Opalina* spp. (*163*), *Dictyostelium discoideum* (*164*) are capable of splitting a single parent cell into two equal daughter cells using the process of binary fission. Bacterial cells (e.g., *Hyphomicrobium vulgare* (*165*), *Pelodictyon clathratiforme* (*166*), *Rhodomicrobium vannielii* (*167*)), fungi (e.g., *Candida albicans* (*168*),

Yarrowia lipolytica (*169*), and *Saccharomyces cerevisae* (*170*)), and cnidaria (e.g., *Carybdea marsupialis* (*171*), *Paraconularia crustula* (*172*)) are capable of splitting themselves into a small daughter cell and a larger parent cell using the process of budding.

Studies investigating splitting as an adaptive strategy to survive in difficult environments have only been studied in organisms capable of producing multiple spores. In particular, when organisms - such as, bacterias, fungi, protists, and plants - encounter harsh environmental and physiological conditions, the organisms split themselves into multiple spores (a metabolically dormant and stress-resistant form of an organism), which helps both survival in harsh environmental and physiological conditions and dispersal to favorable environments (*173*–*176*). For example, segmented filamentous bacteria *Candidatus* spp. form multiple spores in response to unfavorable environmental conditions (*177*, *178*) and are capable of dispersing to favorable environments via horizontal host transmission (*179*). The fungi *Apiocrea chryosperma* produce multiple spores (or conidia) in response to environments lacking food sources that are dispersed to different environments by wind currents (*180*). The plants of species *Ulota* spp. form multiple spores when under harsh environmental conditions and are capable of dispersal by wind currents to search for environments with suitable habitats (*181*). Once a spore encounters a hospitable environment, it germinates to transform into a growing organism. The spores could disperse in different directions in the environment, thus, resulting in an increase in the chances of at least one of the spores discovering a favorable habitat (*182*).

Since the spores are clonal subunits of the organism, the increase in survival chances of one spore is equivalent to the increase in survival chances of the whole organism.

Although sporulating organisms are capable of splitting and finding favorable environments, the spores produced are sedentary and are dependent on passive mechanisms (such as, dispersal by wind or water currents, or living hosts) to explore for suitable habitats. To the best of our knowledge, there is no existing literature investigating the adaptive exploration strategies in organisms, which split in response to harsh environmental or physiological conditions and actively explore environments in search of more suitable environments.

Here, we show that the acellular slime mold *Physarum polycephalum* is capable of splitting into multiple autonomous subunits and changing its movement pattern in order to increase its chances of survival when faced with stressful physiological conditions. *P. polycephalum* is a single-celled, multinucleated protist (phylum: *Amoebozoa*, class: *Myxogastria*). It inhabits cool, dark, and moist areas of temperate forests. *P. polycephalum* can move up to a speed of 5 cm/h (*45*) and grow up to a size of several hundred square centimeters (*14*). *P. polycephalum* moves by extending pseudopods in an amoeba-like fashion. It can spread multiple pseudopods to probe its environment, and therefore, is referred to as “multi-headed” (polycephalum in *Latin*). The search front of *P. polycephalum* advances in a dense fan-like shape. This is followed by a network of interconnected tubules (*14*), where the protoplasm (containing cytoplasm, organelles, nutrients, and signaling molecules) flows in a characteristic back-and-forth manner called shuttle-

streaming (*16*). Despite lacking neurons, *P. polycephalum* can demonstrate complex problem-solving behaviors, such as solving labyrinth mazes (*17*); forming networks with properties similar to human-made networks (*18*); solving complex optimization problems (*20*); anticipating periodic events (*21*); habituating to repeated innocuous environmental stimuli (*23*); avoiding previously explored areas using its extracellular slime (*22*); and, making irrational decisions that were previously believed to be a by-product of neuron-based decision-making (*25*).

In this study, we measure and compare the exploratory activity of *P. polycephalum* cells in two different physiological conditions: a high-energy condition (i.e., fed cells) in which a *P. polycephalum* cell was supplied with a food source before recording its exploratory behavior, and a low-energy condition (i.e., starved cells) in which a *P. polycephalum* cell was starved for 24 hours before recording the exploratory behavior. We observed that the starved cells split sooner and into more autonomous subunits than the fed cells. In order to understand the foraging advantages of the splitting behaviors, we devise a conceptual model to understand whether the splitting behavior of starved cells increases the chance of at least one autonomous subunit discovering food sources in the environment. We hypothesize that the exploration strategy of splitting into multiple autonomous subunits will increase the chances of the organism to locate food sources in their environments, and therefore, increase the chances of survival of the organism.

5.2 Materials and Methods

5.2.1 Biological Material

In our experiments, we used *P. polycephalum* when it was in the plasmodium stage of its life cycle. At this stage, the cell is large enough to be observed with an unaided eye (can cover an area up to several hundred square centimeters (*14*)) and can move in space up to a speed of 5 cm/hr (*45*). We obtained cultures of *P. polycephalum* from Ward's Science® (Rochester, New York). We cultured *P. polycephalum* in Petri plates (dimensions of the plates used throughout this study were: $Ø$ = 10 cm, H = 1.5 cm) at 26 °C and under dark environmental conditions. The Petri plates were filled with water solution of 1% w/v (weight/volume) non-nutrient agar and 5% w/v blended rolled oats (Quaker Oats Company®). *P. polycephalum* stocks were recultured onto new Petri plates every alternate day.

5.2.2 Experiments to Understand the *P. polycephalum* Exploratory Behavior in Fed versus Starved Cell Conditions

Experimental Protocol

We studied the exploratory behavior of *P. polycephalum* in two different physiological conditions i.e., a high-energy condition (i.e, fed cells) and a low-energy condition (i.e., starved cells). To create the fed cells, *P. polycephalum* was grown on food-agar Petri plates (containing a solution of 1% w/v non-nutrient agar and 5% w/v blended oats) for a period of 48 hours before the beginning of our experiments. In contrast, we created the starved cells by extracting *P. polycephalum* from food-agar Petri plates and placing them on blank agar

(containing a solution of 1% w/v non-nutrient agar) for a period of 24 hours before the start of our experiments.

The experimental protocol to study the exploratory activity of *P. polycephalum* was the same for both the experimental conditions. The experiments were conducted on Petri plates filled with a solution of 1% blank agar to a height of 0.6 cm. We measured 150 ± 5 mg of *P. polycephalum* biomass, of either fed or starved cells, and placed it at the center of the experimental Petri plates (number of replicates (or n) = 30 for the fed cell conditions, and n = 31 for the starved cell condition). When *P. polycephalum* fragments are removed from the main cell, the individual fragments start functioning as independent cells within a few minutes after separation (*114*). Since *P. polycephalum* is photophobic, we conducted the experiments in a dark chamber for a period of 24 hours. The temperature of the experimental chamber was maintained at 26 °C, which has been observed to be the optimal temperature for cell growth in our lab cultures.

Data Collection and Analysis

We recorded the exploratory activity of the cells using a Panasonic® Lumix GH3 camera fitted with Lumix® G Varia 14-140mm f/3.5-5.6 II lens. Pictures were taken once every 5 minutes for a period of 24 hours. The experimental setup was illuminated using an LED panel placed underneath the experimental plates. The LED panel would switch on for a period of 10 seconds every 5 minutes while the camera took a picture of the experiment. At all other times, experiments were conducted under dark conditions.

The exploratory behavior of *P. polycephalum* was extracted using a custom-made script written in R version 4.1.2 (*82*). The script processed each experimental image and extracted different exploratory characteristics of *P. polycephalum* cell growth, as given below:

1) *Number of cells*: is the total number of autonomous *P. polycephalum* cells in an experimental image.

2) *Surface area of the cells*: calculated as the amount of area covered by each autonomous cell(s) in an experimental image.

3) *Total surface area of the cells*: calculated as the sum total of the surface area covered by all the cell(s) in an experimental image.

4) *Total explored surface area*: defined as the total surface area that has been visited by the *P. polycephalum* cell(s) till each experimental time point.

5) *Total newly explored surface area*: defined as the new surface area explored in an experimental image that was not visited by the *P. polycephalum* cell(s) previously.

6) *Normalized newly explored surface area*: defined as the total new surface area explored by per unit surface area of the cell(s). It was calculated as the newly explored surface area of the cells divided by the surface area of the cells.

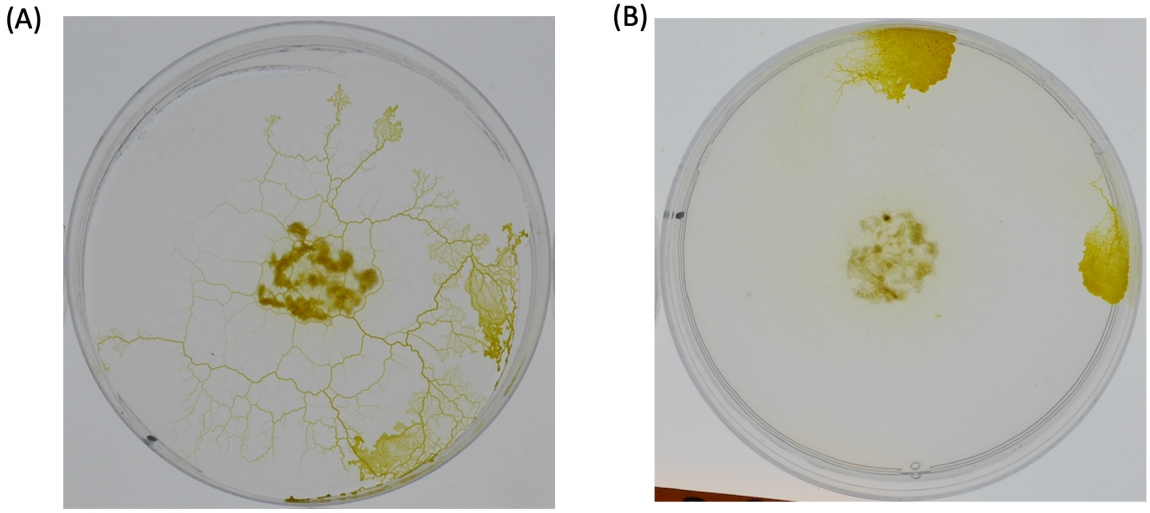

Figure 5.1 Final experimental images from A) High-energy condition (i.e., fed cells), and B) Low-energy condition (i.e., starved cells).

5.2.3 Agent-based Model

We studied the exploration strategy of the *P. polycephalum* when in fed versus starved physiological conditions using an agent-based model coded in Julia programming language version 1.7 (*183*). The purpose of this model was not to reproduce the *P. polycephalum* cell behaviors observed in the experiments, but to generally understand the fitness advantages of splitting in *P. polycephalum*. In particular, we used the model to investigate whether the splitting of *P. polycephalum* cells into autonomous subunits could potentially help increase the foraging success of the cell to find food in the environment. Foraging success was quantified by the time taken by the cells to find the first food in the environment.

Model Setup

The spatial units of the model were in centimeters (cm) and time units were in minutes (min). The simulation arena comprised a circular grid of radius 5 cm with a mesh (or pixel) size of 0.005 cm along the horizontal and vertical axis. The simulations were run for a maximum of 1440 minutes (or 24 hours) with a time-step size of 1 minute. *P. polycephalum* cells were represented as circular "agents", and all the agents were initially located with the center of mass positioned at the center of the arena.

Simulation Environments

In order to test the foraging success of splitting in different environmental conditions, we created three different simulation environments that differed in the probability profiles of finding food in the arena. Each profile assigned a different number to each pixel of the arena, and these numbers represented the probability of finding food at the location. The description of the probability profiles is as follows:

1) *No food scenario*: represents an environment where the probability of finding food at each pixel location is 0. This scenario is meant to understand the behavior of the agents when there is no food in the environment.

2) *Increasing probability profile*: is an environmental scenario where the probability of finding food increases as a function of distance from the center of the simulation arena (Figure 5.2). In particular, this probability profile represents an environment where the chances of *P. polycephalum* cells discovering food sources increase when they explore regions of the simulation arena located away from the starting location. The probability of finding food at a pixel location was calculated using Equation 5.1:

$$Probability\ of\ finding\ food\ at\ a\ location = 1 - \frac{e^{-0.15*x^2}}{\sum_{x=0}^{N} e^{-0.15*x^2}} \quad (5.1)$$

In this equation, *x* represents the distance of a pixel from the center of the simulation arena. Figure 5.2 shows the probability landscape at different pixel locations in the arena. The probability of finding food at each pixel location was normalized, such that the total sum of the probability of finding food in the whole arena equals a value of 1.

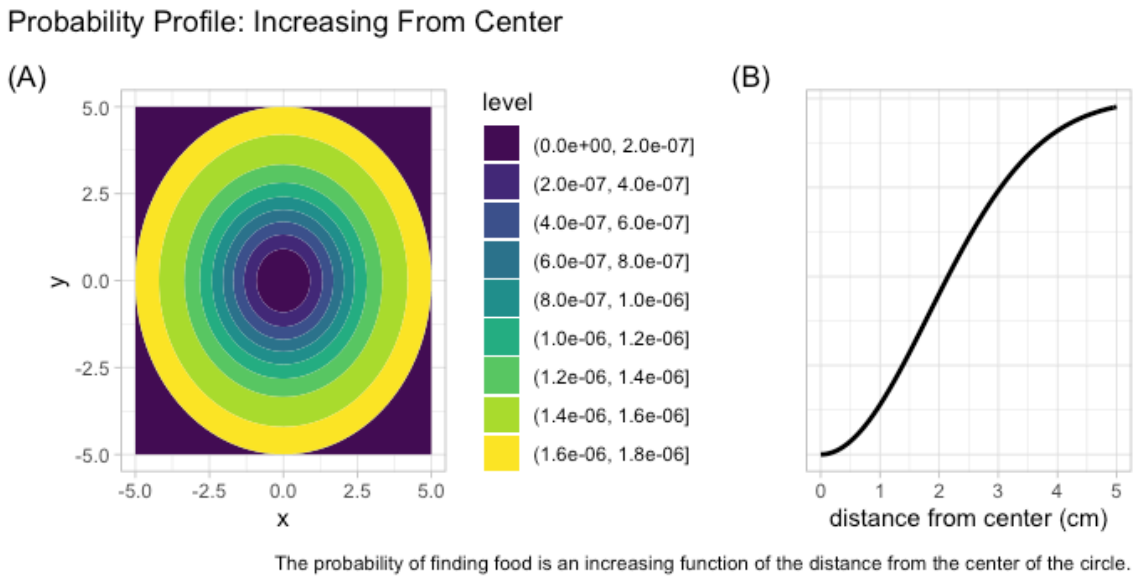

Figure 5.2 Increasing probability profile of the simulation arena. A) Shows the heatmap of the probability of finding food at different pixel locations on the arena. B) Shows the trend of the probabilities as a function of distance from the center of the arena. The probability of finding food at every pixel location was calculated using Equation 5.1. The sum of all the probabilities at the different location in the arena add up to a value of 1.

3) *Decreasing probability profile*: is an environmental scenario where the probability of finding food decreases as a function of distance from the center of the simulation arena (Figure 5.3). In particular, this probability profile represents an environment where chances of *P. polycephalum* cells discovering food sources are high when they explore regions neighboring the starting locations. The probability of finding food at a pixel location was calculated using the Equation 5.2:

$$Probability\ of\ finding\ food\ at\ a\ location = \frac{e^{-0.15*x^2}}{\sum_{x=0}^{N} e^{-0.15*x^2}} \quad (5.2)$$

Similar to the *increasing probability profile*, *x* represents the distance of a pixel from the center of the simulation arena in Equation 5.2. Figure 5.3 shows the probability landscape at different pixel locations in the arena. Moreover, the probability of finding food at each pixel location was normalized, such that the sum total of the probability of finding food in the whole arena equals a value of 1.

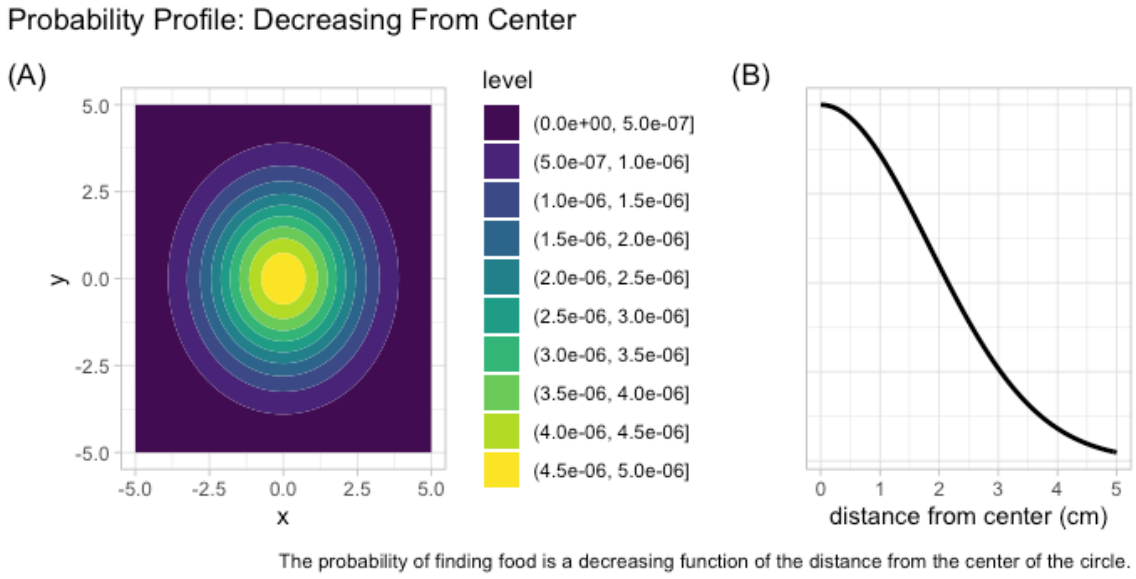

Figure 5.3 Decreasing probability profile of the simulation arena. A) Shows the heatmap of the probability of finding food at different pixel locations on the simulation arena. B) Shows the trend of the probabilities as a function of decreasing distance from the center of the arena. The probability of finding food at every pixel location was calculated using Equation 5.2. The sum of all the probabilities at the different locations in the arena adds up to a value of 1.

Simulation experiments

At each time step, an agent moved and foraged for food in the simulation arena using the following procedure. We first computed a movement direction for each agent by generating a random number from a circular uniform distribution. Then,

we moved the agent in the direction suggested by the random number with a distance calculated by multiplying the speed of movement with the length of each time step. The speed of movement was an input parameter in our simulation (given in Table 3.1). Next, at each of the pixels traversed by the agent in the particular time step, we generated a random number from a binomial distribution with a probability of success given by the probability of finding food at the respective pixel locations. When the random number generates a value of 1 (i.e., success) at any of the pixels traversed, we consider the agent to have found food. Whereas in the cases when the number generated was all 0's (i.e., failure), we considered the agent to have found no food. The simulations were run for a maximum time of 1440 minutes, or until the time when any of the agents in the simulation found their first food. We used the total biomass area of the cells (i.e., the combined area of the agents), the number of biomass (i.e., the number of agents), and speed as the input parameters for each simulation experiment. The values of the parameters are given in Table 5.1.

The simulation was run for 7x8x7 = 392 unique parameter combinations, for each of the probability profiles. Moreover, in order to account for random variation, 30 simulations were run for each parameter combination. For each experiment in the increasing and decreasing probability profiles, we recorded the time taken to find the food as the output. On the contrary, in the no food scenario we recorded the proportion of area covered by the agents as the output.

We expected the time taken to find food to decrease with the increase in the number of biomass in the simulation arena with an increasing probability

profile. Conversely, we expected the time taken to find food to increase with the increasing number of biomass in the arena with the decreasing probability profile. In addition, in both the probability profiles, we expected the time taken to find food to decrease with the increase in total biomass area of the cells and speed of cell movement.

Table 5.1 VALUES OF THE DIFFERENT MODEL PARAMETERS

Parameter	Values used
Number of biomass (i.e., number of autonomous cells)	1 to 8
Total biomass area of the cells (cm^2)	2, 4, 6, 8, 10, 12 & 14
Speed (cm/min)	0.10, 0.15, 0.20, 0.30, 0.50, 0.80, & 1.00

Statistical analysis

We used a generalized linear model (GLM) with beta error distribution and logit link function to analyze the influence of number of biomass, total biomass area, and speed on the time taken to find food. We entered the number of biomass, total biomass area, speed, the interaction between number of biomass and total biomass area, number of biomass and speed, and total biomass area and speed as fixed effects in our model. The analyses were conducted separately for the increasing and decreasing probability profiles The analysis was performed in R version 4.1.2 (*82*) using the “glmmTMB” r package (*184*).

5.3 Results

5.3.1 Experiments to understand the *P. polycephalum* exploratory behavior in fed versus starved cell conditions

In order to understand the exploratory behavior of *P. polycephalum* in the fed vs starved conditions, we measured and compared different characteristics of *P. polycephalum* cell growth in the two physiological conditions, as shown in Figure 5.4.

Figure 5.4A shows the mean number of *P. polycephalum* cells over the course of the experimental time period. The results show that the fed cells remain undivided for the most part of the experiments (i.e., the mean number of cells has a value of 1 across different replicates), and splits only after ~20 hours from the beginning of the experimental time period (Figure 5.1). The mean number of cells at the end of the experiments was found to be 1.20 cells. In contrast, the starved cells on average split after ~12 hours (will be referred to as the "starved cell splitting point" from here onwards), and they split into more number of cells than compared to the fed cells (Figure 5.1). Moreover, the splitting in the *P. polycephalum* cells increased over time, and the mean number of cells at the end of the experiments was found to be 1.8 cells. In summary, the starved cells show a tendency to split sooner and into greater number of autonomous cells than compared to the fed cells.

Figure 5.4B shows the mean surface area of the *P. polycephalum* cells over time. The results show that during the time period before the starved cell splitting point, the cells in both conditions increased in surface area. However, the mean

surface area was higher in the starved cells. In addition, in the latter half of the experiments, the mean surface area of the fed cells increased to reach a maximum cell surface area but then decreased at the experimental time period > 20 hours (i.e., coinciding with the time period when fed cells showed splitting). The mean surface area of the starved cells decreased after the starved cell splitting point. In summary, the undivided starved cells had a higher mean surface area than the fed cells during the experimental time periods before the starved cell splitting point, and the mean surface area of both the cells decreased with the increase in splitting of *P. polycephalum* cells.

Figure 5.4C shows the mean total surface area of the cells over time. Similar to the results in the mean surface area of the cells (Figure 5.4B), the starved cells showed a higher mean total surface area than compared to the fed cells in the experimental time period before the starved cell splitting point. In addition, in the experimental time period after the starved cell splitting point, the total surface area of the starved cells decreased. This shows that the starved cells after splitting became denser and concentrated more biomass into the autonomous cells.

Figure 5.4D shows the mean total explored surface area over time. The results show that during the time period before the starved cell splitting point, the starved cells explored more surface area of the experimental arena than compared to the fed cells. However, during the time period post the starved cell splitting point, the total surface area explored was higher in the fed cells. A similar trend was observed in the mean newly explored surface area data (Figure 5.4E), with starved

cells exploring more new areas before the starved cell splitting point and fed cells exploring more new areas in the latter time periods.

However, when the new surface area explored was normalized to the respective *P. polycephalum* cell sizes (Figure 5.4F), the starved cells explored more new surface areas of the experimental arena than compared to the fed cells, during a majority of the time periods both before and after the starved cell splitting point. This shows that the starved cells show a higher propensity to explore more surface area than the fed cells. Additionally, the lower total and newly explored area (shown in Figures 5.4D and E) in the starved cells could be due to the lower total surface areas (shown in Figure 5C) of the starved cells, causing the cells to overall explore less area of the experimental environment.

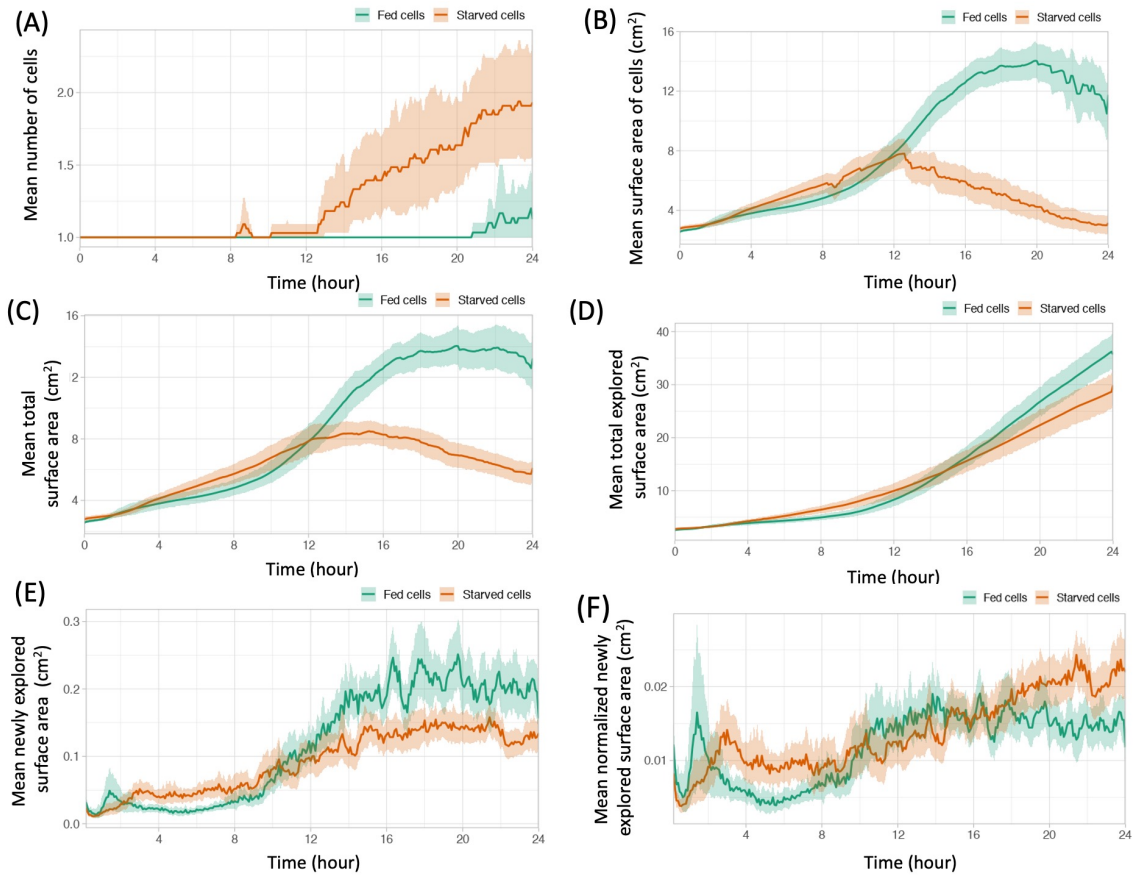

Figure 5.4 Different characteristics of the *P. polycephalum* cells exploration in the fed and starved conditions (referred to as fed and starved cells, respectively), across all experimental replicates, over the experimental time period of 24 hours. A) Mean number of *P. polycephalum* cells. B) Mean surface area (cm^2) of the cells. C) Mean total surface area of the cells (cm^2). D) Mean total explored surface area of the cells (cm^2). E) Mean newly explored surface area (cm^2) of the cells. F) Mean normalized newly explored surface area (cm^2) of the cells (calculated as the newly explored surface area of the cells divided by the surface area of the cells). The solid lines represent the mean and the semi-transparent envelope represents the 95% confidence intervals, of the respective *P. polycephalum* exploration characteristics.

5.3.2 Simulation Results to Understand the Foraging Advantages of Splitting in *P. polycephalum*

<u>No food scenario</u>

We conducted simulation experiments in an environment with no food to understand the baseline behavior of the *P. polycephalum* agents. We used this

simulation to examine the change in proportion of simulation area covered by the agents as a function of the number of biomass and speed, for each value of total biomass area inputted into the simulation model. Figure 5.5 shows an example of the proportion of the simulation arena covered when the total biomass area was 2 cm^2. The results show that with the increase in the speed of movement, the proportion of area covered by the agents increased. Moreover, at higher speed values (i.e., when the speeds were 0.8 - 1.0 cm/min), the agents covered the whole surface area of the arena within the given simulation time period. However, at low and intermediate speed values the agents (i.e., when the speeds were 0.1 - 0.5 cm/min), the proportion of area covered by the agents increased with the increase in number of cells. The patterns observed were identical for the other values of the total biomass area (results shown in *Appendix* Figures C.1 – C.6). Overall, the results suggests that the *P. polycephalum* agents covered more surface area of the simulation arena with the increase in splitting and movement speed of the cells.

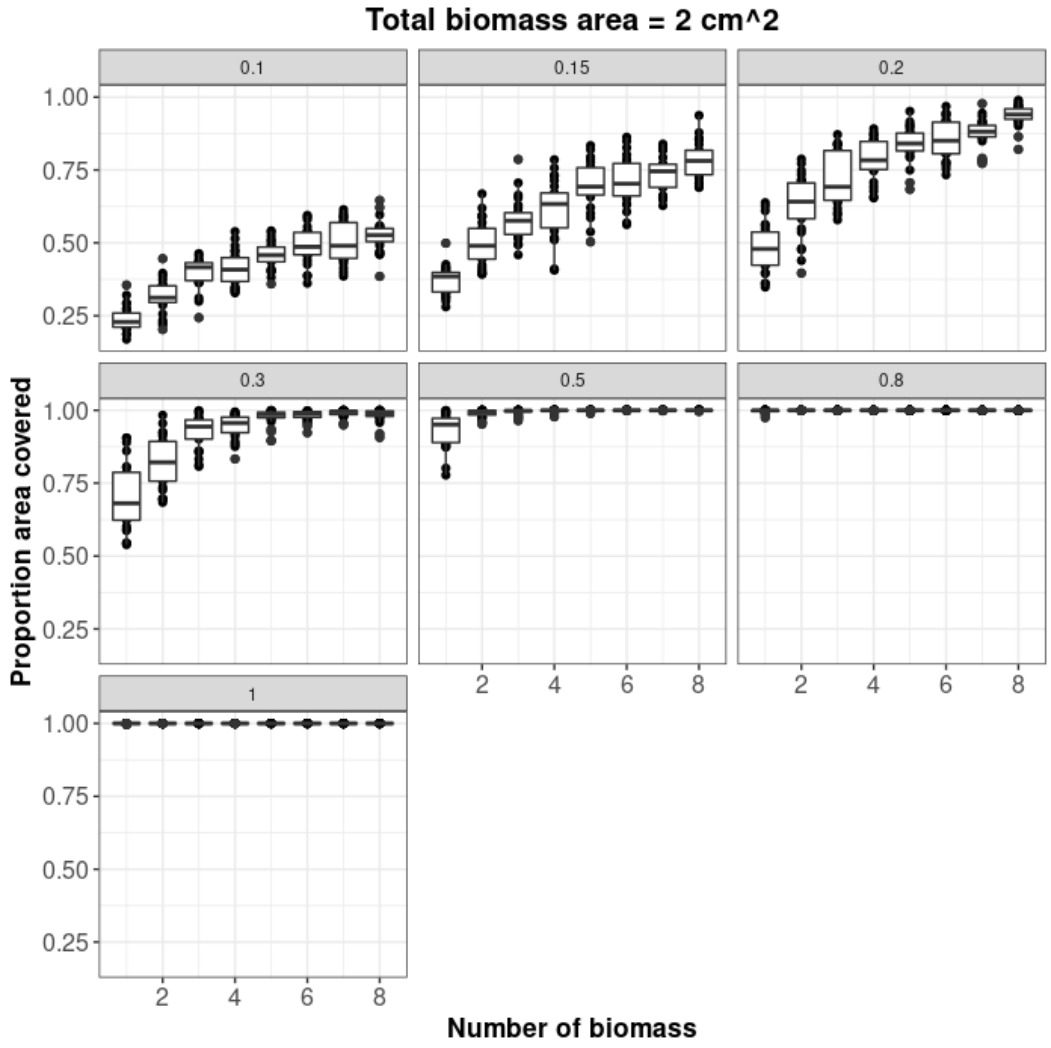

Figure 5.5 Shows the proportion of the simulation area covered as a function of number of biomass when the total biomass area was 2 cm^2. The plots are sectioned by the different speed values (units in cm/min) tested, and the values are given in the title of each plot.

Increasing probability profile

We used a GLM model with a beta error distribution and logit link function to analyze the relationship between the different model input parameters (i.e., the number of biomass, total biomass area, and speed), and the different combinations of interaction between the parameters (i.e., an interaction between number of biomass and total biomass area, number of biomass and speed, and total biomass

area and speed) on the time taken to find food. The model diagnostics and performance are given in Figure C.7 in the *Appendix*.

We found that, when all the other parameters values were set constant, then for every 1 unit increase in the number of biomass, the odds ratio (OR) of the time taken to find food decreases by a factor of -0.1827 (Figure 5.6A, 95% CI: -0.2076 to -0.1577, $p < 2e\text{-}16$). In other words, across all the experimental trials, the time taken to find food decreases with the increase in the number of biomass. Similarly, with the increase in total biomass area, the time taken to find food decreased (Figure 5.6B, OR: -0.07379, 95% CI: -0.0880 to -0.0595, and $p < 2e\text{-}16$). Furthermore, with the increase in speed, the time taken to find food decreased (Figure 5.6C, OR: -4.1658, 95% CI: -4.3862 to -3.9454, and $p < 2e\text{-}16$). In summary, with the increase in the number of biomass, total biomass area, and speed of the movement, the *P. polycephalum* agents were able to find food at an earlier time in the simulation time period.

The predictor variable comprising the interaction term between the number of biomass and total biomass area had a significant effect on the odds ratio of the time taken to find food (Figure 5.6D, OR: 0.003410, 95% CI: 0.0009 to 0.0058, $p = 0.00681$). The results show that when the total biomass area is low, then with the increase in the number of biomass, the time taken to find food decreases at a higher rate. Whereas, when the total biomass area is high, then with the increase in the number of biomass, the time taken to find food decreases at a lower rate. In summary, when the number of biomass increases, the reduction in the time taken to find food decreases, with the increase in total biomass area. To put it another

way, *P. polycephalum* agents with low total biomass area gain more in terms of foraging success with the increase in splitting, than compared to the agents with higher total biomass area.

The predictor variable comprising the interaction term between the number of biomass and speed has a significant effect on the time taken to find food (Figure 5.6E, OR: 0.1259, 95% CI: 0.09431 to 0.1574, $p < 5.62e-15$). This shows at lower speed values, as the number of biomass increases, the time taken to find food decreases at a higher rate. Conversely, at higher speed values and increasing number of biomass, the time taken to find food decreases at a lower rate. In summary, when the number of biomass increases, the reduction in time taken to find food decreases, with the increase in speed of movement of the agents. In particular, *P. polycephalum* agents with a lower speed of movement gain more in terms of foraging success, relative to the agents with high movement speed, with the increase in the number of biomass.

Lastly, the predictor variable comprising the interaction between total biomass area and speed also has a significant effect on the time taken to find food (Figure 5.6F, OR: 0.0418, 95% CI: 0.0236 to 0.0599, and $p < 6.12e-06$). This shows that, as the total biomass area increase, the time taken to find a food source decreases at a higher rate. In comparison, at higher speed values and increasing total biomass area, the time taken to find food decreases at a lower rate. In summary, when the total biomass area increases, the reduction in time taken to find food decreases, with the increase in speed of movement of the agents. This shows that the *P. polycephalum* agents with a lower speed of movement gain more

in terms of foraging success, relative to the ones with high movement speed, with the increase in the total biomass area.

Overall, the results are consistent with our expectations. The results show that splitting of *P. polycephalum* cells into autonomous subunits would help increase the foraging success of the cell to find food in the environment with an increasing probability profile. Moreover, the model predicts that increasing cell size and speed of movement would have a positive effect on the foraging success of the organism.

Decreasing probability profile

In the decreasing probability profile, we conducted the same analysis as in the increasing probability profile. The model diagnostics and performance are given in Figure C.8 in the *Appendix*.

The results show that the odds ratio (OR) of the time taken to find food decreases, when the number of biomass (Figure 5.7A, OR: -0.1799, 95% CI: -0.2069 to -0.1528, $p < 2e\text{-}16$), total biomass area (Figure 5.7B, OR: -0.1286, 95% CI: -0.1440 to -0.1132, $p < 2e\text{-}16$), speed (Figure 5.7C, OR: -3.001, 95% CI: -3.2883 to -2.774, $p < 2e\text{-}16$), increases independently. In other words, the *P. polycephalum* agents find food sooner with the increase in the number of biomass, total biomass area, and speed.

Moreover, the predictor variable comprising the interaction term between number of biomass and total biomass area (Figure 5.7D, OR: 0.1323, 95% CI: 0.0070 to 0.0122, $p = 5.61e\text{-}13$), number of biomass and speed (Figure 5.7E, OR:

0.1113, 95% CI: 0.0781 to 0.1446, p = 5.06e-11), and total biomass area and speed (Figure 5.7E, OR: 0.08317, 95% CI: 0.0641 to 0.1022, p < 2e-16), have a significant effect on the odds ratio of the time taken to find food. This shows that when the total biomass area and speed of movement is high, the time taken to find food decreases at a lower rate, with the increase in the number of biomass. Conversely, at low total biomass area and speed of movement, the time taken to find food decreases at a higher rate, with the increase in the number of biomass. In other words, the cells with a lower total biomass area and lower speed have greater foraging success with the increase in the splitting of the cells (Figures 5D and E). Additionally, when the speed of movement is high, the reduction in time taken to find food increases, the time taken to find food decreases at a higher rate, with the increase in biomass area. And conversely, at a low speed of movement, the reduction in time taken to find food decreases at a lower rate, with the increase in total biomass area (Figure 5F).

Overall, the results are contrary to our expectations. We expected the splitting of *P. polycephalum* agents would have a negative effect on the foraging success of the organism in the decreasing probability profile. However, our results show that splitting will increase foraging success in such environments. Additionally, the results show that an increase in biomass size and speed of movement will increase the foraging efficiency to find food in the environment.

5.4 Discussion

We examined and compared the exploratory behavior of *P. polycephalum* cells in two different physiological conditions, i.e., a high-energy condition (i.e., fed cells) and a low-energy condition (i.e., starved cells). We observed the starved cells split earlier in the experimental time period and into more autonomous subunits than the fed cells. Moreover, starved cells showed a higher propensity to explore new areas in the experimental environment. In order to understand the fitness advantages of splitting in *P. polycephalum* cells, we devised a conceptual agent-based model to test whether splitting can help improve the foraging success of *P. polycephalum* in finding food in the environment. In a simulation environment with *no food* present, we observed that splitting in *P. polycephalum* cells (i.e., agents in the model) helps cover more surface area of the simulation environment. In addition, in the *increasing and decreasing probability* profiles of the simulation environments, the splitting behavior of the *P. polycephalum* agents helped find food sooner within the simulation time period.

The simulation results show that splitting helps increase the foraging efficiency in both *increasing* and *decreasing probability profiles*. And therefore, the foraging advantages of *P. polycephalum* cells staying undivided are not understood clearly from our simulation experiments. In order to understand the foraging success of *P. polycephalum* cells in the undivided state, our future work would involve repeating the simulations in environments with probability profiles that are intermediary to the *increasing* and *decreasing probability profiles* used in this study.

Studies conducted by Kakiuchi et al. showed that *P. polycephalum* could split into multiple cells when exposed to low temperatures (*185*) and extreme light conditions (*186*). The studies found splitting to be transient (i.e., lasting around 6 - 8 hours), with the cells eventually fusing back to form a single organism. The authors found the subunits to be extremely small in size (i.e., the cell diameters were about 10 μm in diameter) and could not be visible using an unaided eye. Additionally, the studies did not explore the fitness consequences of such behaviors. However, in this study, we show that the autonomous subunits of *P. polycephalum* cells persist as autonomous subunits for relatively prolonged periods of time, and exist as macroscopic-sized entities. In addition, using a conceptual model, we show that *P. polycephalum* can increase its foraging success in finding food in the environment by splitting itself into multiple autonomous subunits.

In conclusion, our study shows a novel exploration strategy of splitting one's self into multiple autonomous parts in order to survive in difficult environmental conditions. We show using a conceptual model that splitting would help the organisms to discover food faster, in environments with random food distributions. Moreover, the increase in exploratory activity in *P. polycephalum* when in low-energy conditions is similar to that observed in brained organisms, such as in ants (*10*), flies (*187*), honey-bees (*188*), zebra finches (*189*). This suggests the presence of common adaptive strategies in organisms across disparate taxas.

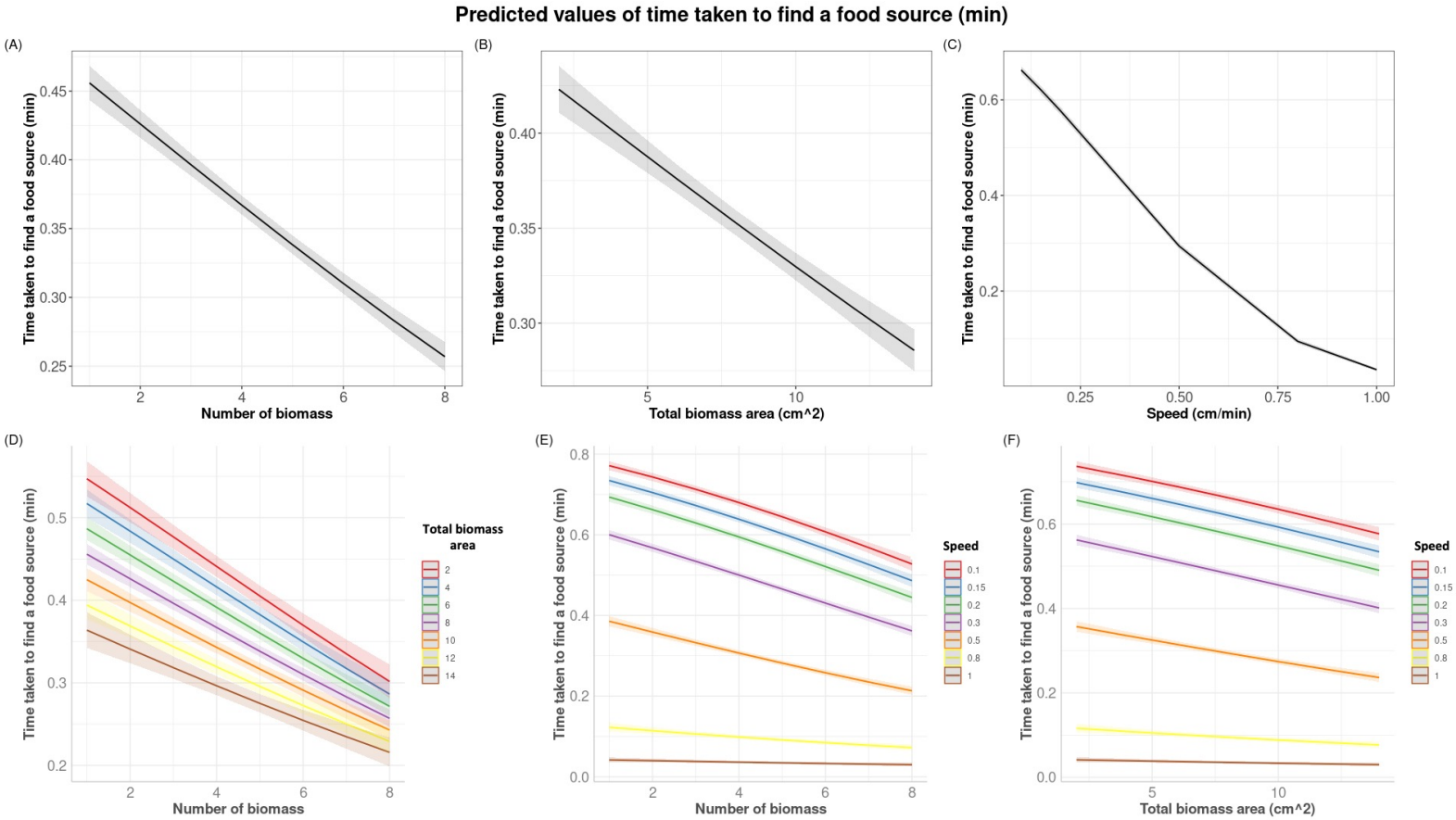

Figure 5.5 Plot of Time taken to find food (In *Increasing probability profile*) as function of the different input parameters, namely, A) Number of biomass, B) Total biomass area (cm^2), C) Speed of movement (cm/min), and the interaction terms between the input parameters, namely, D) Number of biomass and Total biomass area (cm^2), E) Number of biomass and Speed of movement (cm/min), and F) Total biomass area (cm^2) and Speed of movement (cm/min). The lines on each plot represents the predicted odd ratio (OR) of time taken to find food, and the semi-transparent line represents the 95% confidence interval. The data was analyzed using GLM model with beta error distribution and logit link function. The model results are mentioned in the text.

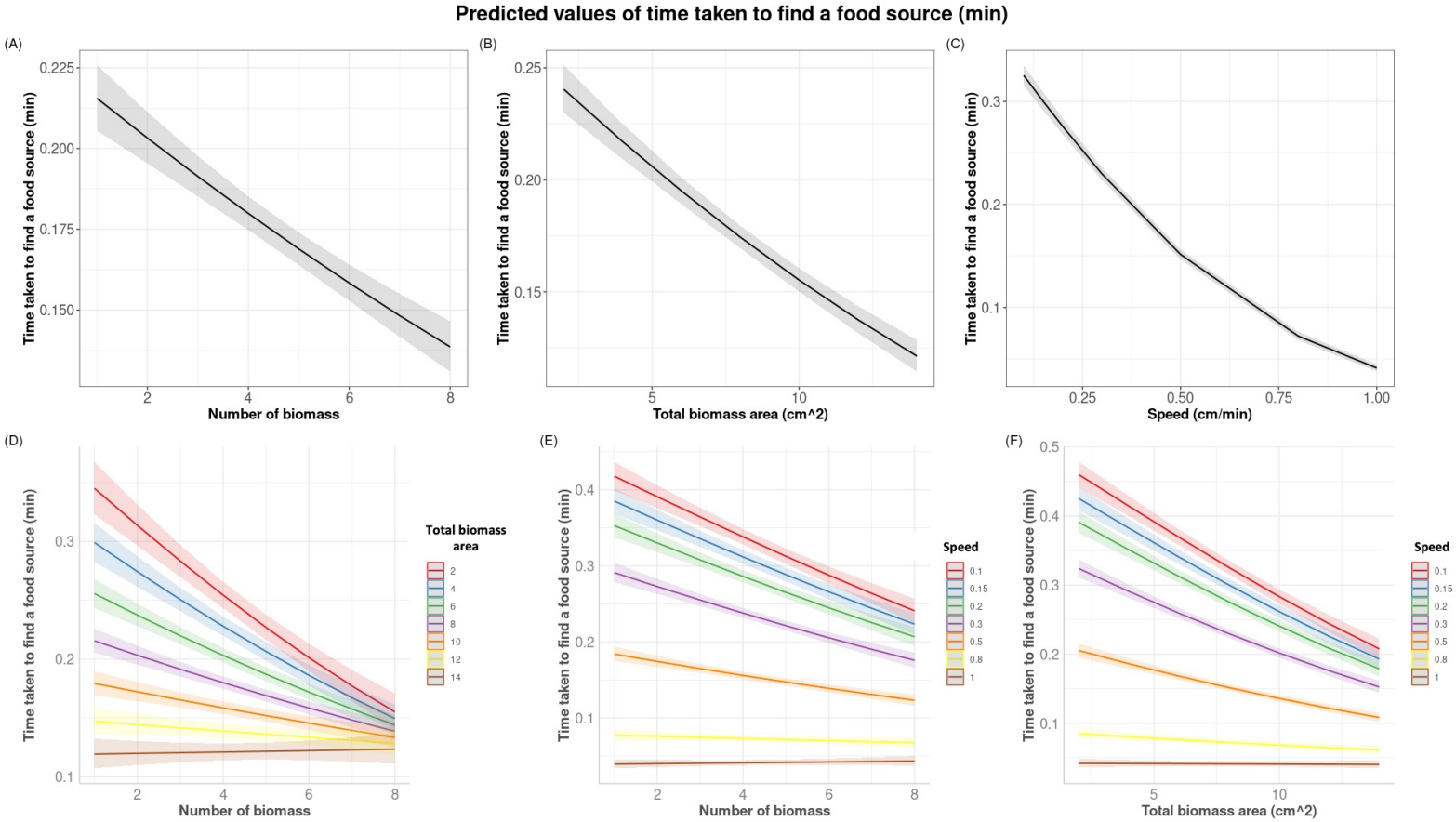

Figure 5.6 Plot of Time taken to find food (In *Decreasing probability profile*) as function of the different input parameters, namely, A) Number of biomass, B) Total biomass area (cm^2), C) Speed of movement (cm/min), and the interaction terms between the input parameters, namely, D) Number of biomass and Total biomass area (cm^2), E) Number of biomass and Speed of movement (cm/min), and F) Total biomass area (cm^2) and Speed of movement (cm/min). The lines on each plot represents the predicted odd ratio (OR) of time taken to find food, and the semi-transparent line represents the 95% confidence interval. The data was analyzed using GLM model with beta error distribution and logit link function. The model results are mentioned in the text.

CHAPTER 6

CONCLUSION

The big objective of this dissertation was to understand how environmental and physiological factors affect the adaptive behaviors of non-neuronal organisms. In order to answer this question, I used the acellular slime mold *Physarum polycephalum* as a model organism, as it combines the high experimental tractability of a macroscopic unicellular organism with the complex problem-solving behaviors of multi-cellular organisms. My dissertation focused on understanding the mechanisms adopted by *P. polycephalum* to explore and exploit resources in the physical environment using environmental and physiological information. To achieve this, in the first part of this dissertation (i.e., chapters 2 and 3), I studied the mechanisms used by *P. polycephalum* in exploiting resources when given a choice between two food sources. Additionally, in the second part of this dissertation, I studied the exploration strategy adopted by *P. polycephalum* in response to its past foraging experiences (i.e., chapter 4) and different physiological conditions (i.e., chapter 5). Overall, this dissertation shows that *P. polycephalum* can employ complex strategies that help integrate environmental and physiological information in order to exhibit problem-solving and adaptive behaviors.

Chapter 2 investigated the direction and amount of influence of different *P. polycephalum* cell regions on the contractile behavior of the whole cell while it was choosing between two food sources. The results show that the cell regions controlling the contractile behavior changed with the choice-making challenge

faced by the cell. Interestingly, when the two food sources presented to the cell were asymmetric in quality, the cell regions near the rejected food source were observed to act as the drivers of the cell's contractile behavior. To explain this result, my collaborators and I are currently working on a mechanistic model that suggests that the behavior of *P. polycephalum* may be driven by reduced contractile activity and stiffness in the cell region near the chosen food source. This creates a pressure differential within the cell, thereby generating a net flow of protoplasm and biomass accumulation towards the chosen food source. This model assumption is further supported by our finding that actin filaments are less polymerized in the cell region near the chosen food source. In summary, this work shows that choice-making in *P. polycephalum* can arise from the physical properties of the cell without requiring any form of communication between the different parts of the cell network. In my opinion, future efforts should be dedicated towards understanding the mechanisms used by *P. polycephalum* when choosing between three or more food sources and understanding the dynamics of the protoplasm movement through a 3-way tubular junction of a *P. polycephalum* cell network.

Chapter 3 introduced a generalized criterion to examine whether *P. polycephalum* could choose the best resource when presented with an option between two alternatives, and determine the time point when the cell made a choice. My criterion tested the null hypothesis that the relative difference in foraging effort distributed by *P. polycephalum* cells towards the most rewarding resource would be proportional to the relative difference in quality between the

available resources. In my experiments, *P. polycephalum* successfully chose the better alternative in all the tested conditions, except when the difference in quality between the food sources was low. In this case, the experimental time period was insufficient to choose the better resource. This result suggests the existence of a comparative valuation process (also referred to as the “tug-of-war” model of decision-making by Kacelnik et al. (2010) (*190*)) in *P. polycephalum*, as the choice-making time increased with the increase in the closeness of the option values.

Chapter 4 tested the capability of *P. polycephalum* to alter its exploratory behavior in response to the foraging experiences gathered in the past. The results show a weak correlation between different *P: polycephalum* exploratory network properties and the past foraging environment. Since *P. polycephalum* has been shown to have a form of an internal memory, I believe repeating the experiments with lower *P. polycephalum* biomass would show a strong relationship between the different exploratory network properties and past foraging environments. However, if observed, the differences in the exploratory network properties can result from the differences in the fed state and not because of the differences in the distribution of the food sources. Therefore, I recommend the experiments be repeated by changing the distribution of food sources in each experimental treatment but keeping the total food content constant between the treatments.

Chapter 5 examined whether *P. polycephalum* can employ different exploratory strategies in different physiological states. In this chapter, I show that *P. polycephalum* can split into multiple autonomous subunits to explore its environment when starved for 24 hours. I further show that this property of splitting

into multiple subunits helps increase the chances of, at least one subunit, finding food in its environment. Moreover, the results show that the starved cells become denser and more compact after splitting. This suggests that *P. polycephalum* cells can demonstrate autophagy when under starvation stress. Previous literature has suggested that autophagy under starvation stress helps in homeostasis (*191*); however, I recommend that future research be dedicated to examining the adaptive value of autophagy in *P. polycephalum* when starved and uncovering the involved cellular processes.

This dissertation shows that *P. polycephalum* can employ strategies that help them achieve the same fitness objectives as neuronal organisms. The information processing system used in exhibiting such adaptive behaviors is decentralized and driven by a plethora of complex, dynamic interactions occurring between molecules, such as genes, proteins, ions, and metabolites (*12*, *192*). Such a cognitive architecture, i.e., one lacking a stable structure and static elements, has led some studies to refer to as “liquid” brains (*193*). However, our knowledge of the mechanisms used by such dynamic systems to achieve computation and the capability to encode and retrieve memory, is very limited. Therefore, in my opinion, uncovering such mechanisms should be the subject of scientific investigations aiming to understand problem-solving in non-neuronal organisms.

APPENDIX A

SUPPLIMENTARY INFORMATION FOR PHYSARUM POLYCEPHALUM CHOICE-MAKING IN CHAPTER 3

This appendix provides the supplementary information to the results described in Chapter 3.

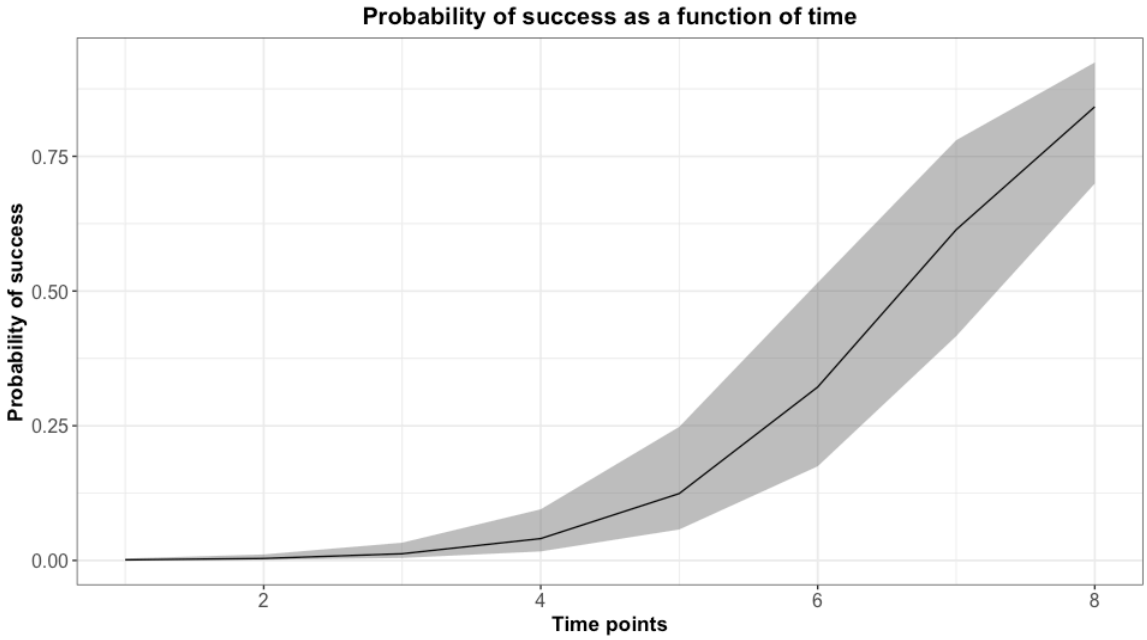

Figure A.1 The figure shows the plot of the probability of success vs the time points. The relationship was found to be significant (OR:1.8924, 95% CI: 1.57 to 2.21, and p < 2e-16). That is, with every one-unit increase in the time point, the odds of the probability of success increased by a factor of 1.8924.

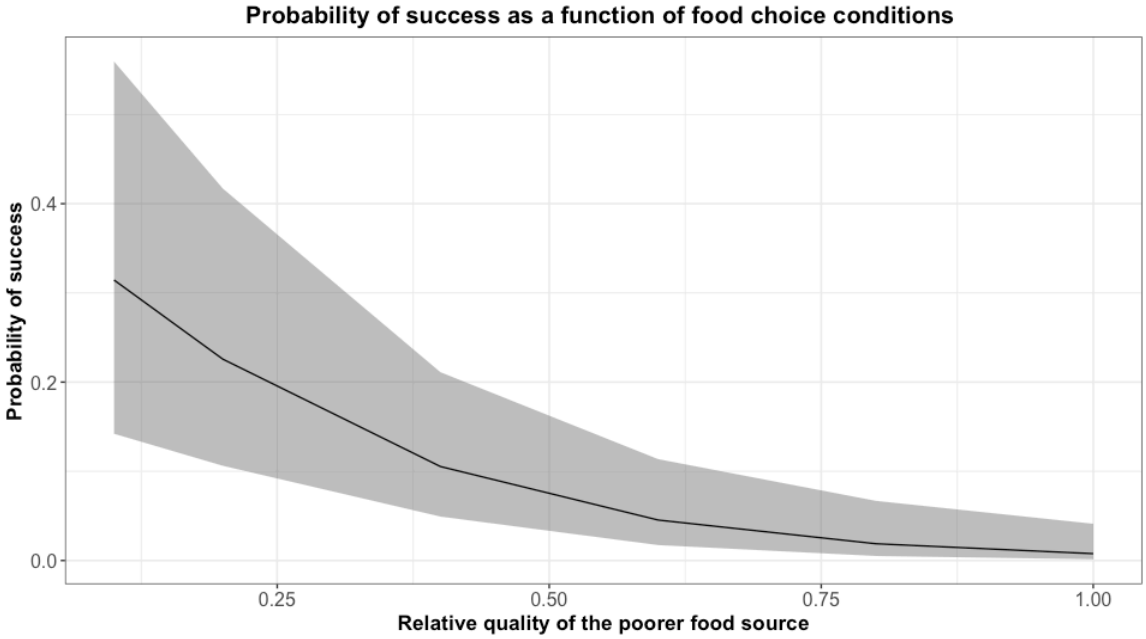

Figure A.2 The figure shows the plot of the probability of success vs relative quality of the poorer food source. The relationship was found to be non significant (OR = 1.7612, p = 0.197).

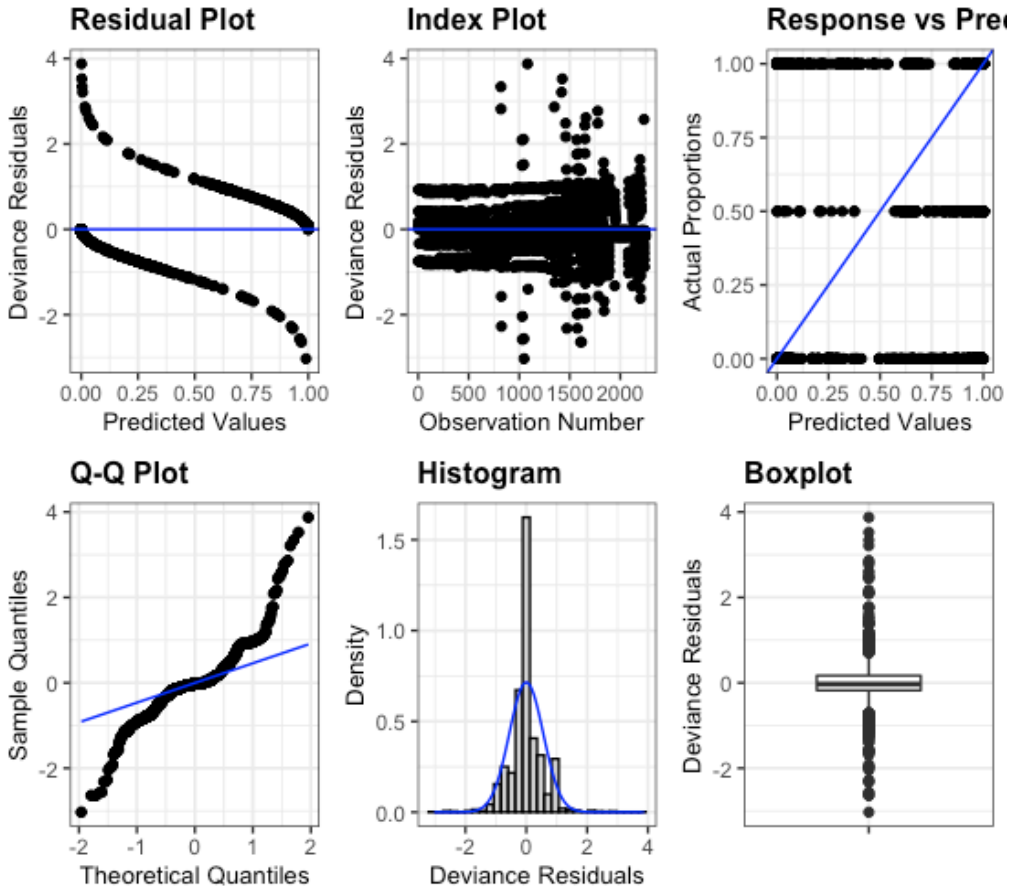

Figure A.3 Model diagnostics of using GLMM with binomial error distribution, logit link function, when analyzing the relationship between the relative quality of the poorer food source, time points, and interaction between the relative quality of the poorer food source and time points, on the probability of observing distinguishable growth on the better food source (i.e., the probability of success).

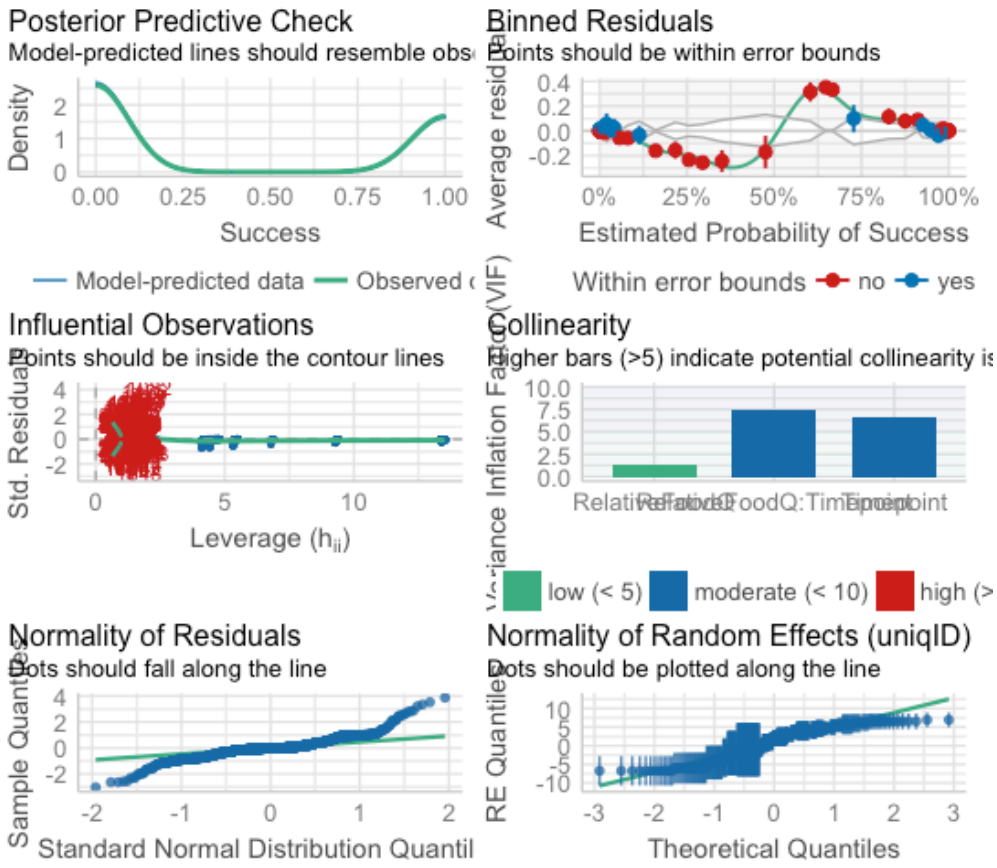

Figure A.4 Model performance of using GLMM with binomial error distribution, logit link function, when analyzing the relationship between the relative quality of the poorer food source, time points, and interaction between the relative quality of the poorer food source and time points, on the probability of observing distinguishable growth on the better food source (i.e., the probability of success).

APPENDIX B

SUPPLIMENTARY INFORMATION FOR PHYSARUM POLYCEPHALUM EXPLORATORY NETWORK METRICS IN CHAPTER 4

This appendix provides the supplementary information to the *P.* polycephalum exploratory network metrics described in Chapter 4.

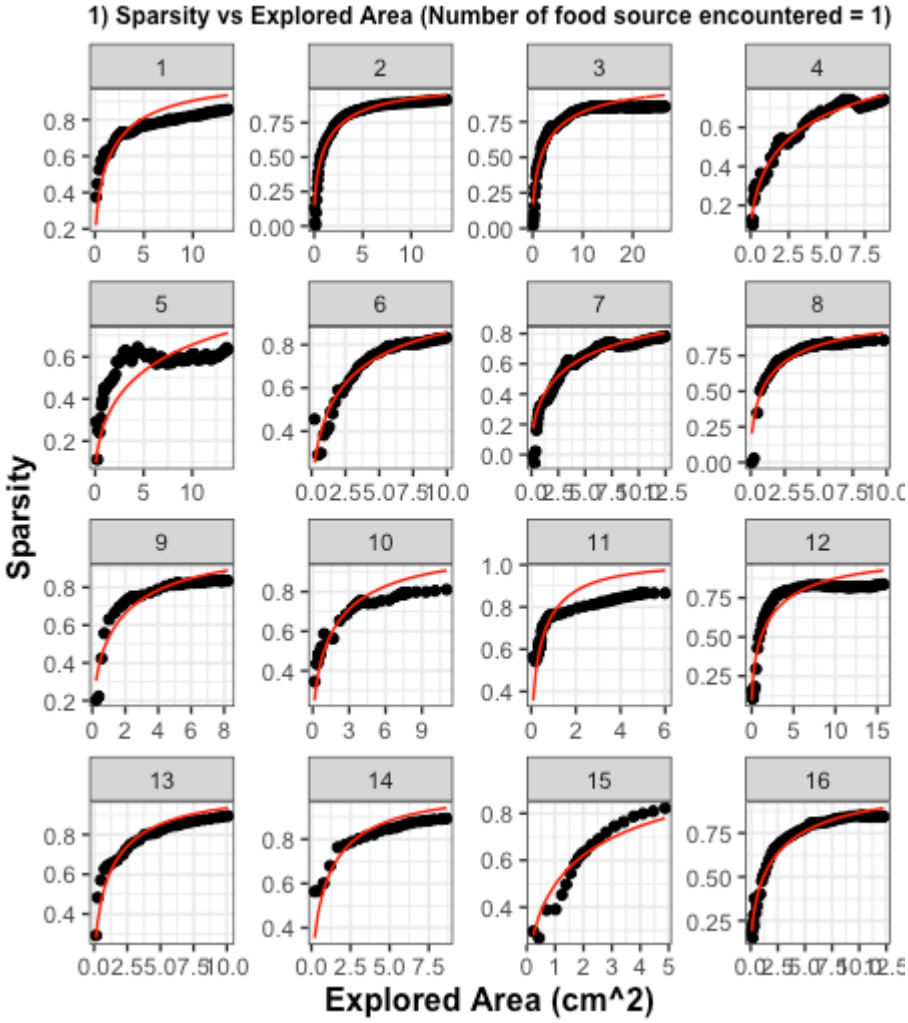

Figure B.1 Plot showing asymptotic fit on *Sparsity* data for experimental condition 1 (i.e., number of food sources encountered = 1). The black dots represent the *Sparsity* values and the red curve shows the asymptotic fit. The numbers on the title of the plots show the replicate numbers of the experiments conducted for the specific experimental condition.

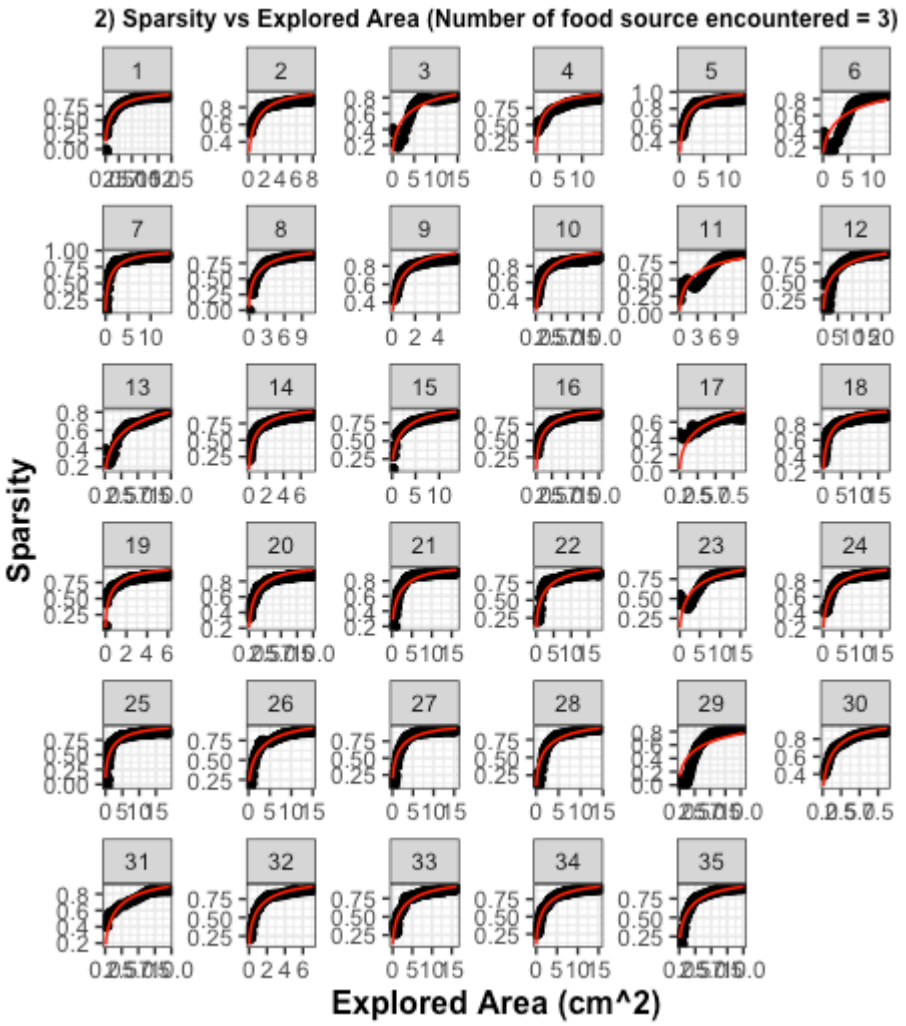

Figure B.2 Plot showing asymptotic fit on *Sparsity* data for experimental condition 2 (i.e., number of food sources encountered = 3). The black dots represent the *Sparsity* values and the red curve shows the asymptotic fit. The numbers on the title of the plots show the replicate numbers of the experiments conducted for the specific experimental condition.

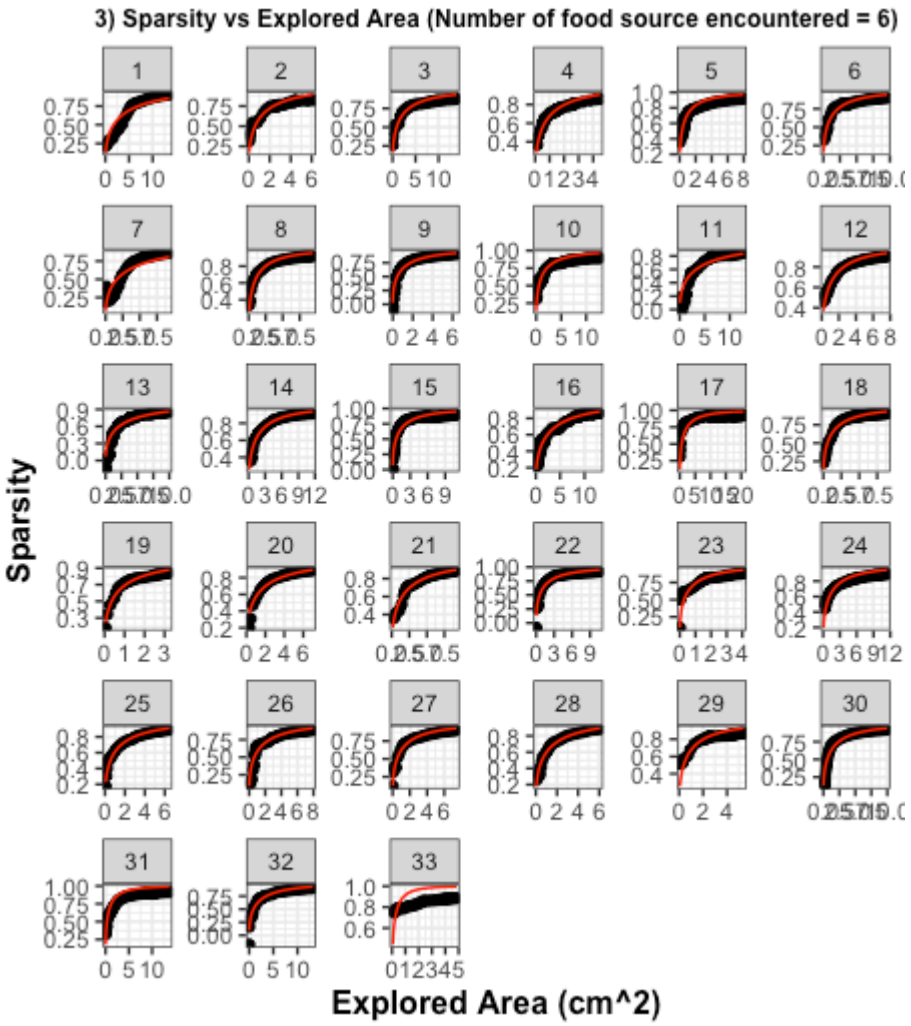

Figure B.3 Plot showing asymptotic fit on *Sparsity* data for experimental condition 3 (i.e., number of food sources encountered = 6). The black dots represent the *Sparsity* values and the red curve shows the asymptotic fit. The numbers on the title of the plots show the replicate numbers of the experiments conducted for the specific experimental condition.

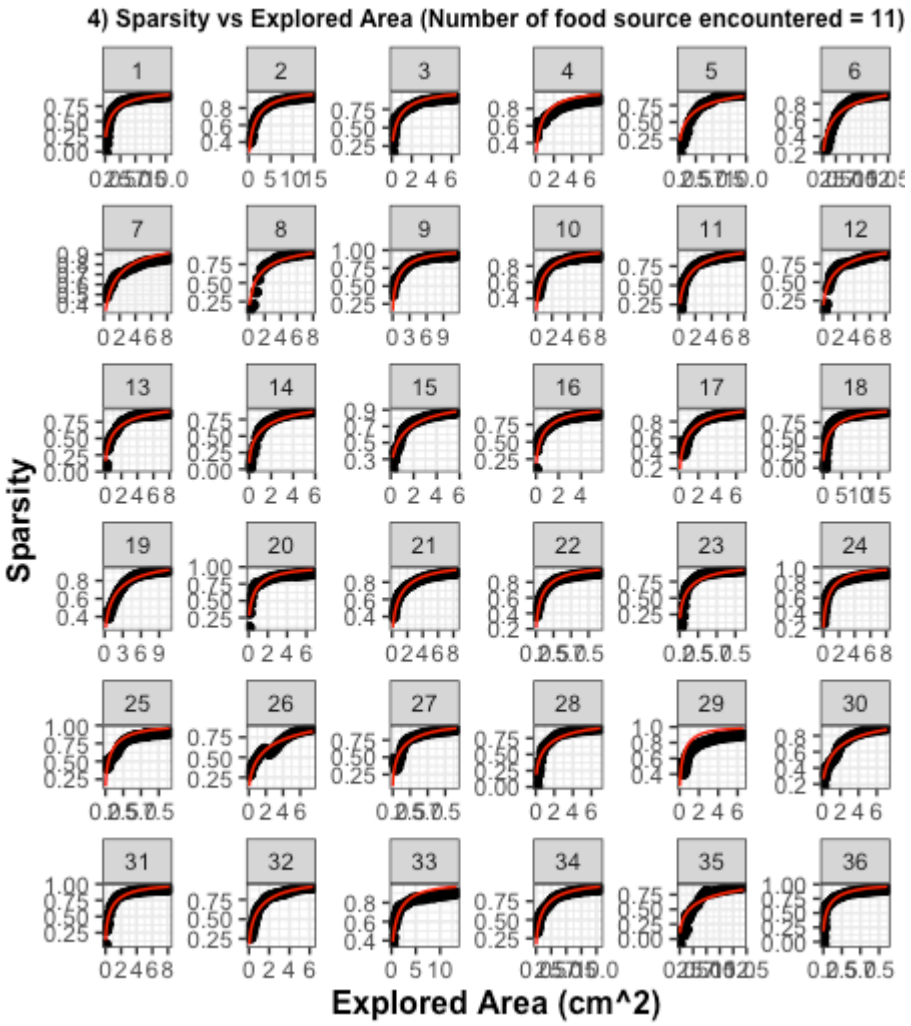

Figure B.4 Plot showing asymptotic fit on *Sparsity* data for experimental condition 4 (i.e., number of food sources encountered = 11). The black dots represent the *Sparsity* values and the red curve shows the asymptotic fit. The numbers on the title of the plots show the replicate numbers of the experiments conducted for the specific experimental condition.

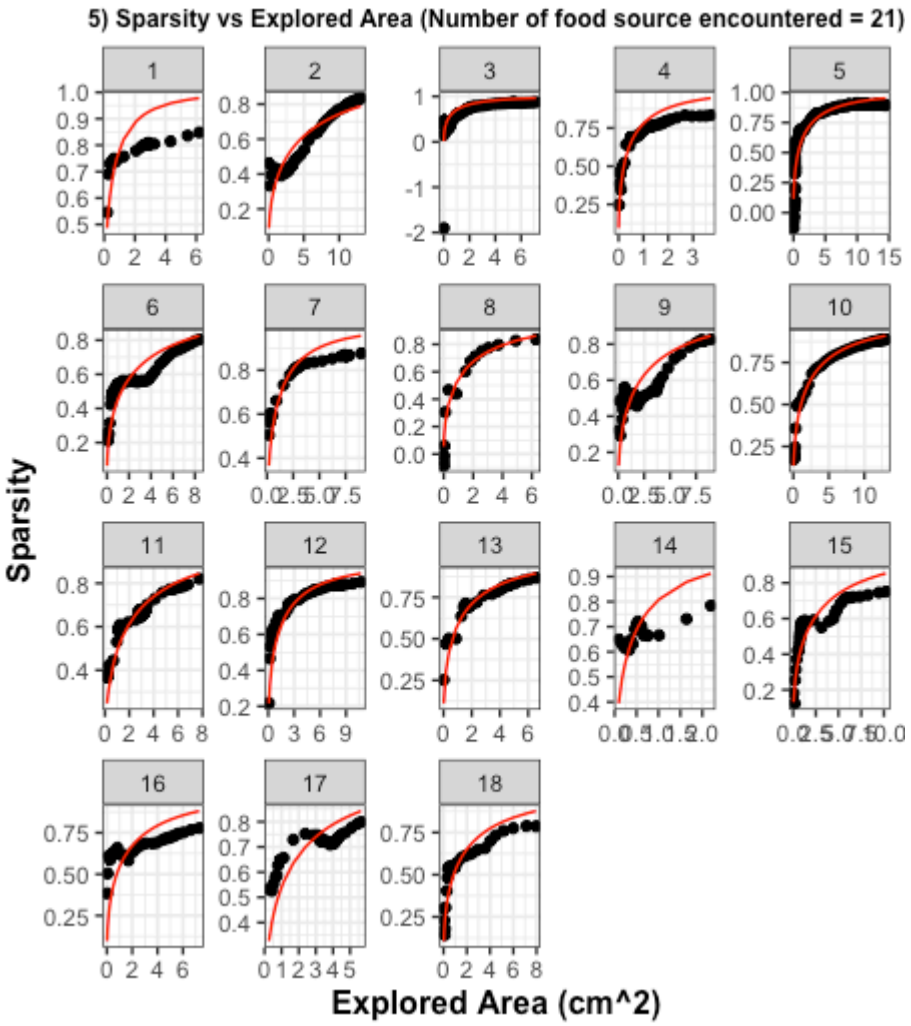

Figure B.5 Plot showing asymptotic fit on *Sparsity* data for experimental condition 5 (i.e., number of food sources encountered = 21). The black dots represent the *Sparsity* values and the red curve shows the asymptotic fit. The numbers on the title of the plots show the replicate numbers of the experiments conducted for the specific experimental condition.

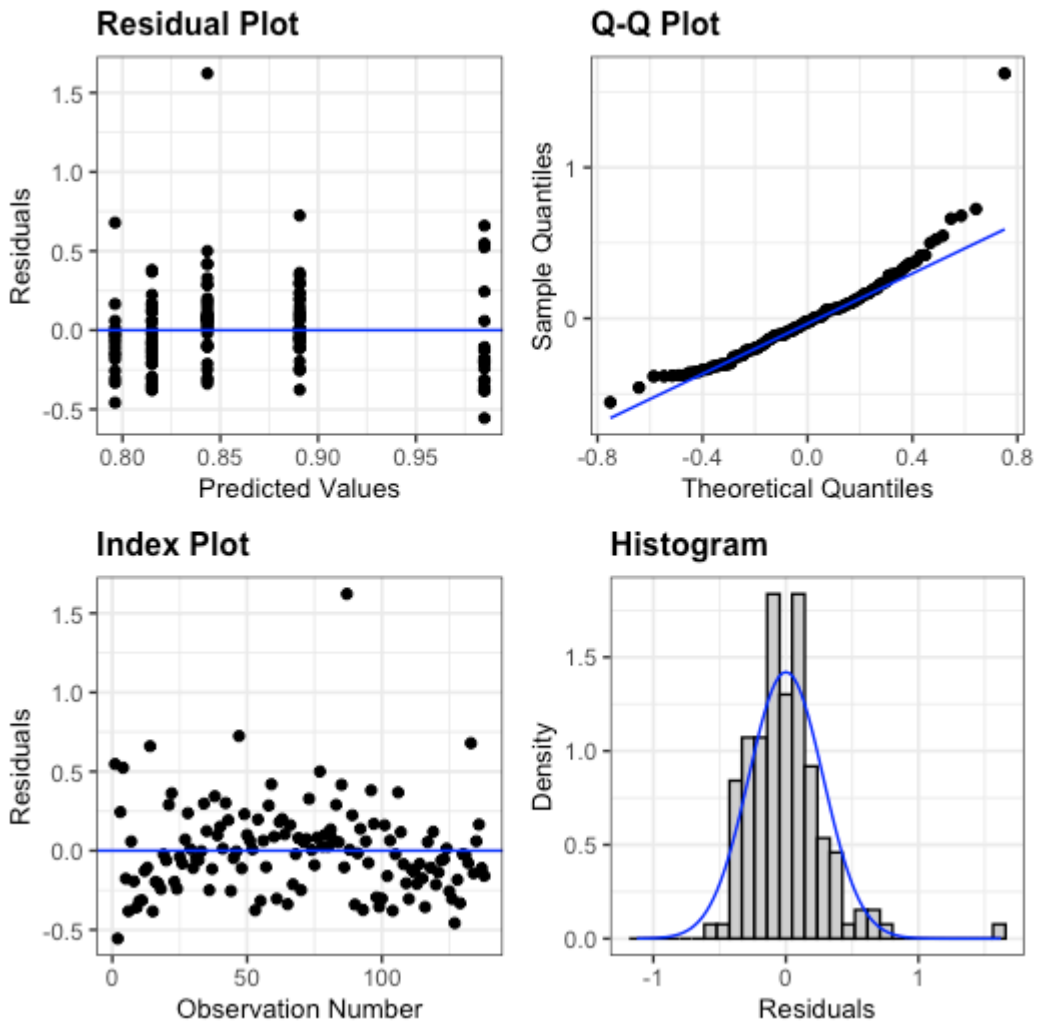

Figure B.6 Residual plots of fitting a linear model to the rate of change of Sparsity vs Number of food source data.

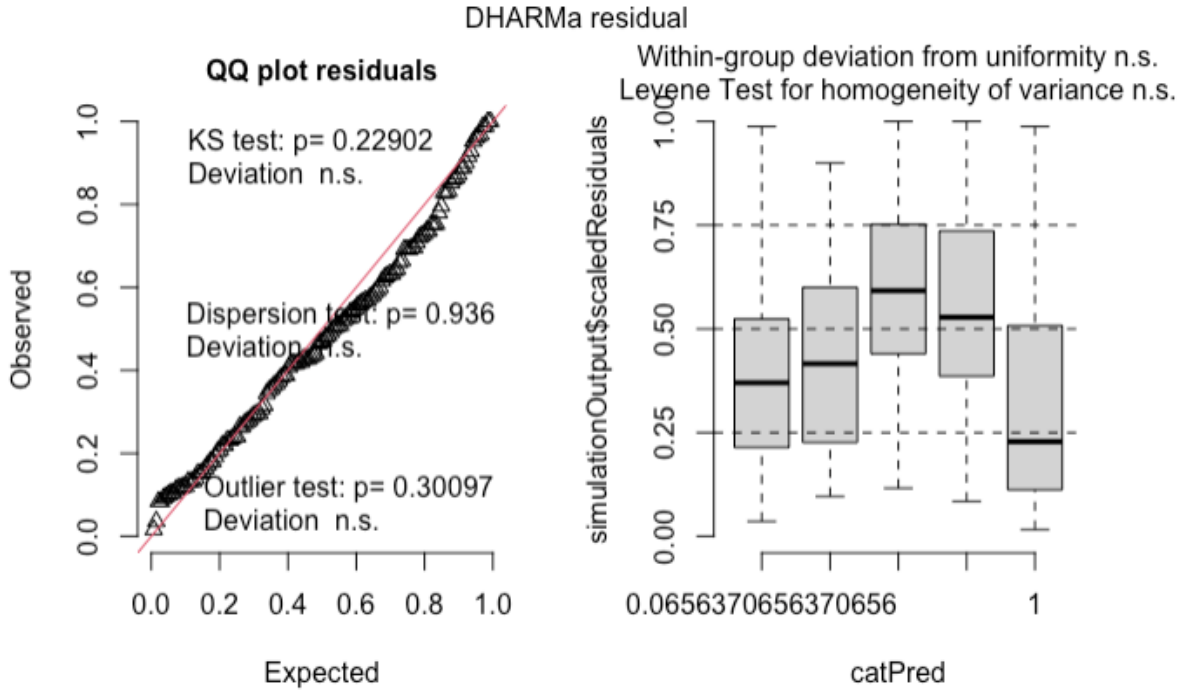

Figure B.7 Performance of the linear model fit on the change of Sparsity vs Number of food source data using DHARMa R package. The Q-Q plot of the DHARMa R package looks different from the one shown in the previous plot, as the DHARMa R package normalizes the Observed and Expected quantiles between 0 and 1.

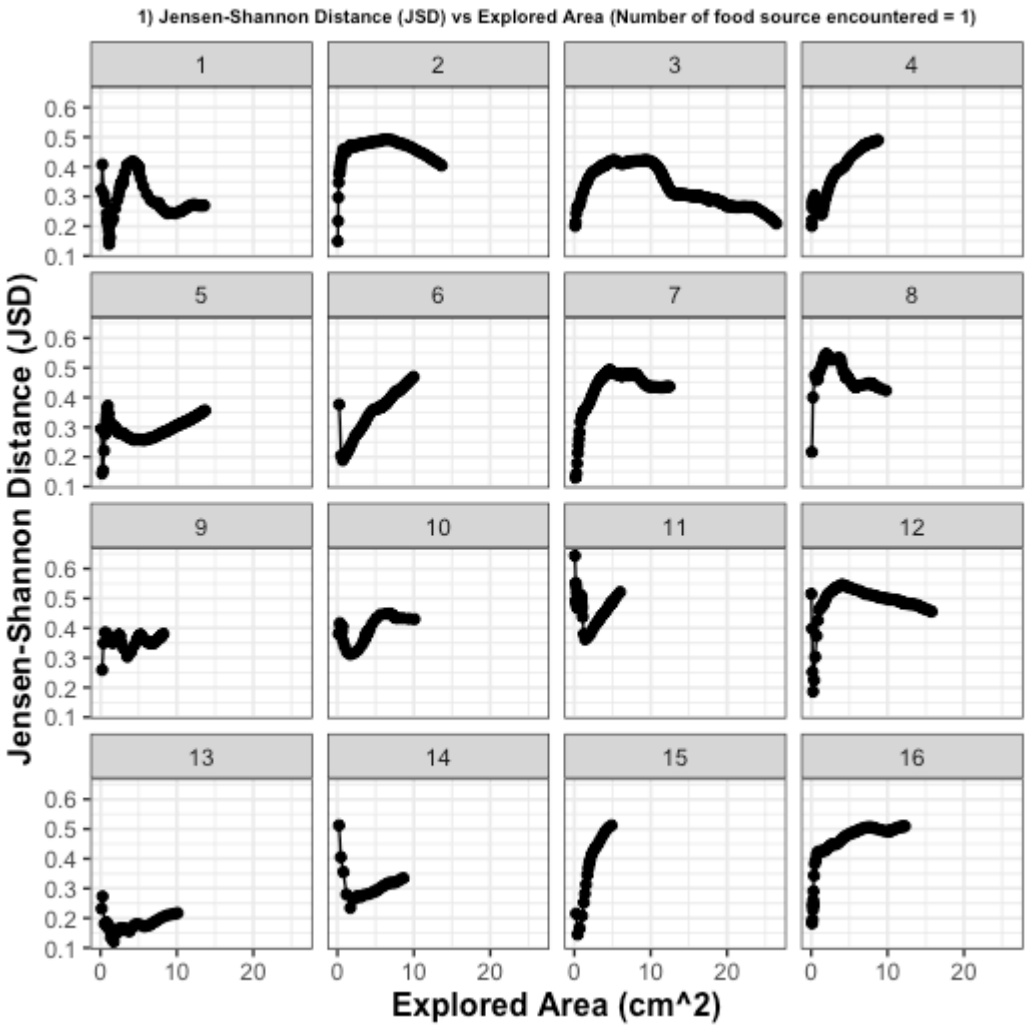

Figure B.8 Plot showing the changes in the Jensen-Shannon index (JSD) as function of area explored for experimental condition 1 (i.e., number of food sources encountered = 1). The black dots in the figure represent JSD values. The numbers on the title of the plots show the replicate numbers of the experiments conducted for the specific experimental condition.

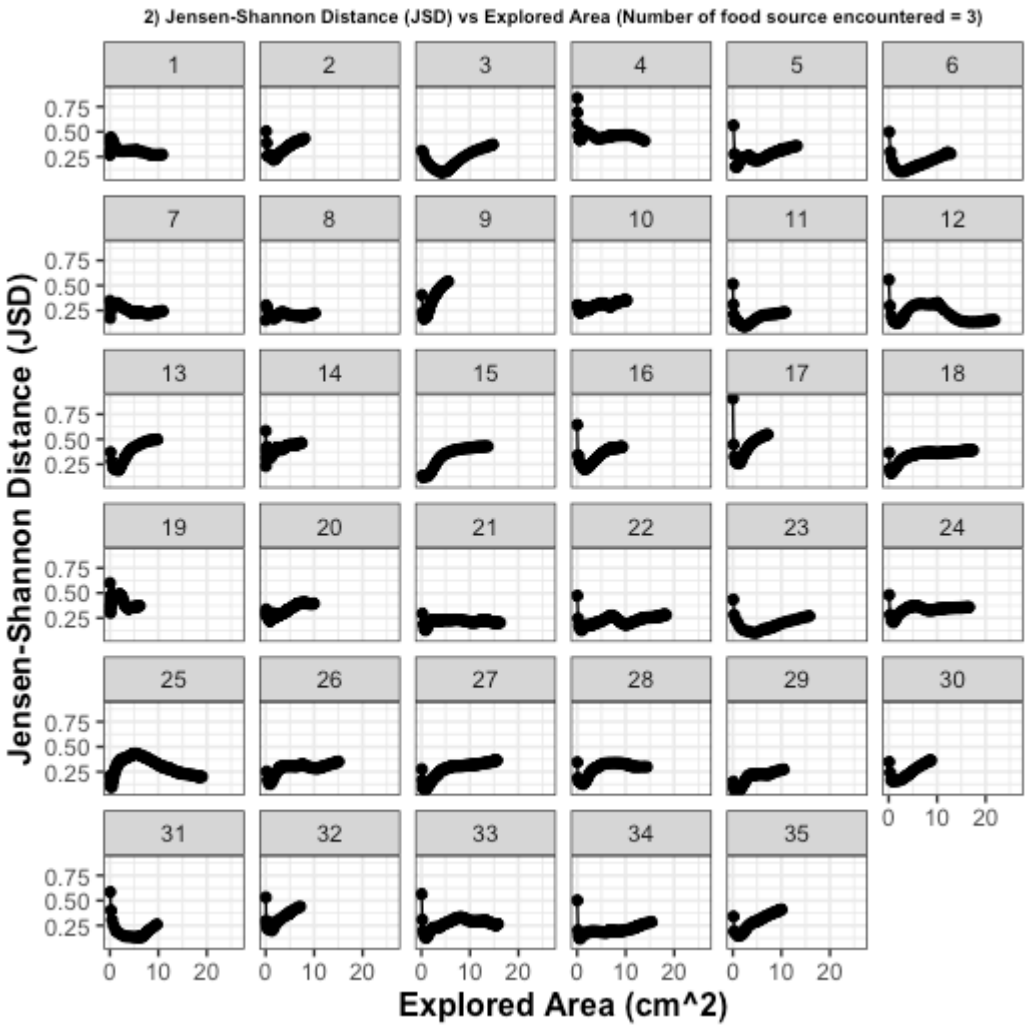

Figure B.9 Plot showing the changes in the Jensen-Shannon index (JSD) as function of area explored for experimental condition21 (i.e., number of food sources encountered = 3). The black dots in the figure represent JSD values. The numbers on the title of the plots show the replicate numbers of the experiments conducted for the specific experimental condition.

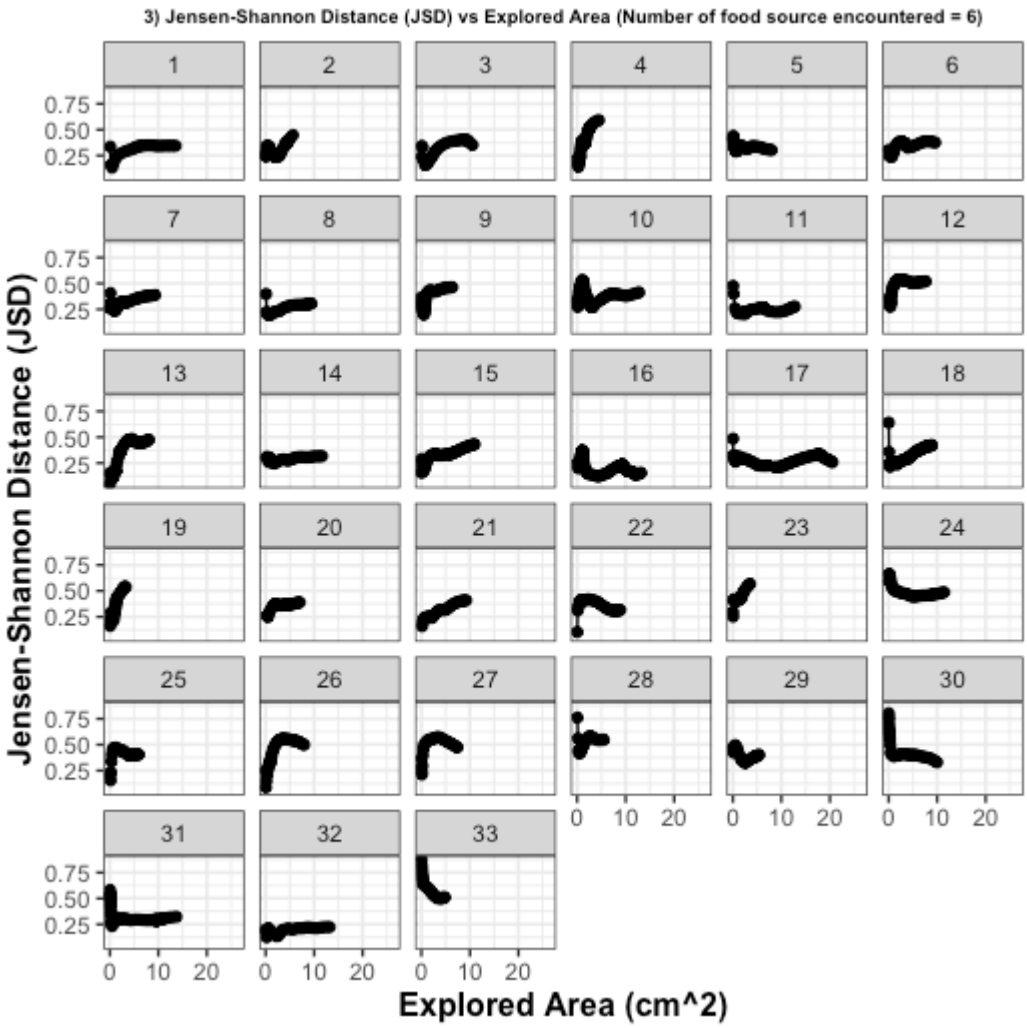

Figure B.10 Plot showing the changes in the Jensen-Shannon index (JSD) as function of area explored for experimental condition 3 (i.e., number of food sources encountered = 6). The black dots in the figure represent JSD values. The numbers on the title of the plots show the replicate numbers of the experiments conducted for the specific experimental condition.

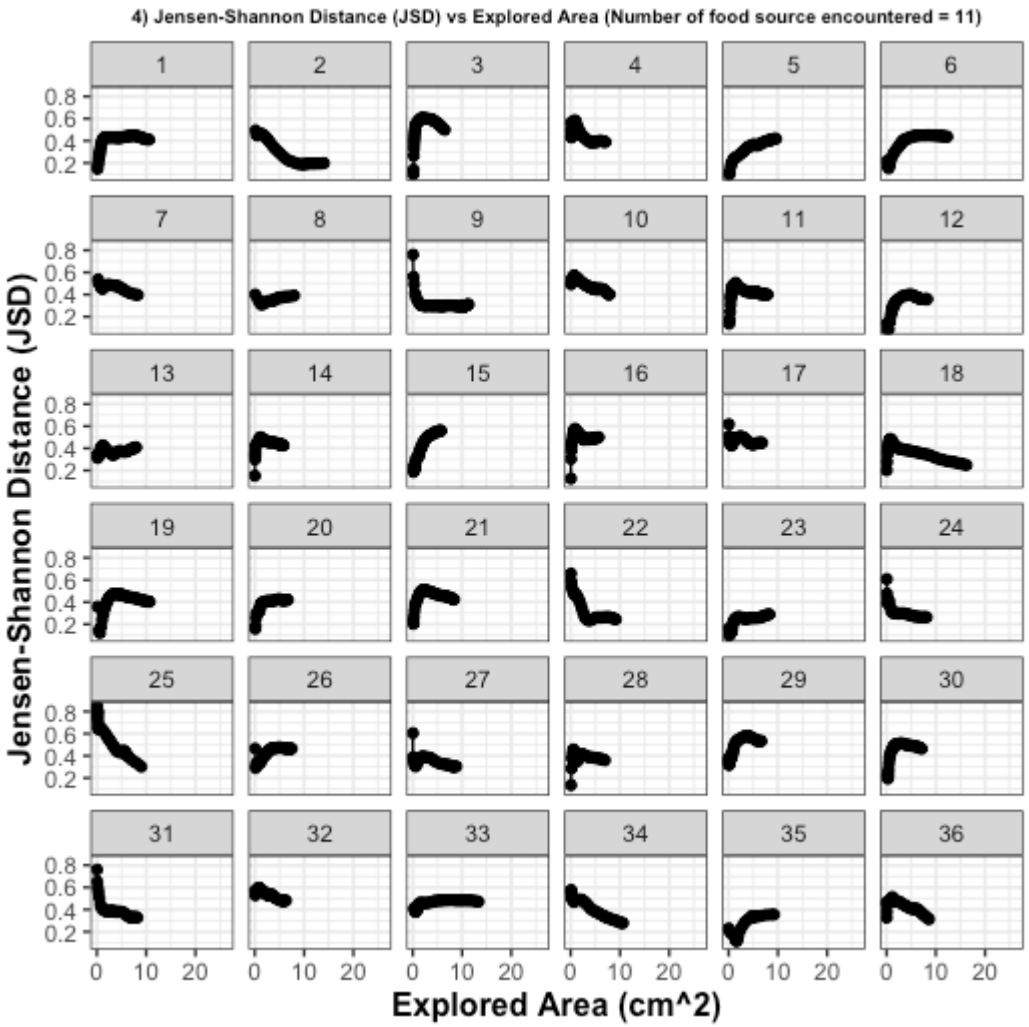

Figure B.11 Plot showing the changes in the Jensen-Shannon index (JSD) as function of area explored for experimental condition 4 (i.e., number of food sources encountered = 11). The black dots in the figure represent JSD values. The numbers on the title of the plots show the replicate numbers of the experiments conducted for the specific experimental condition.

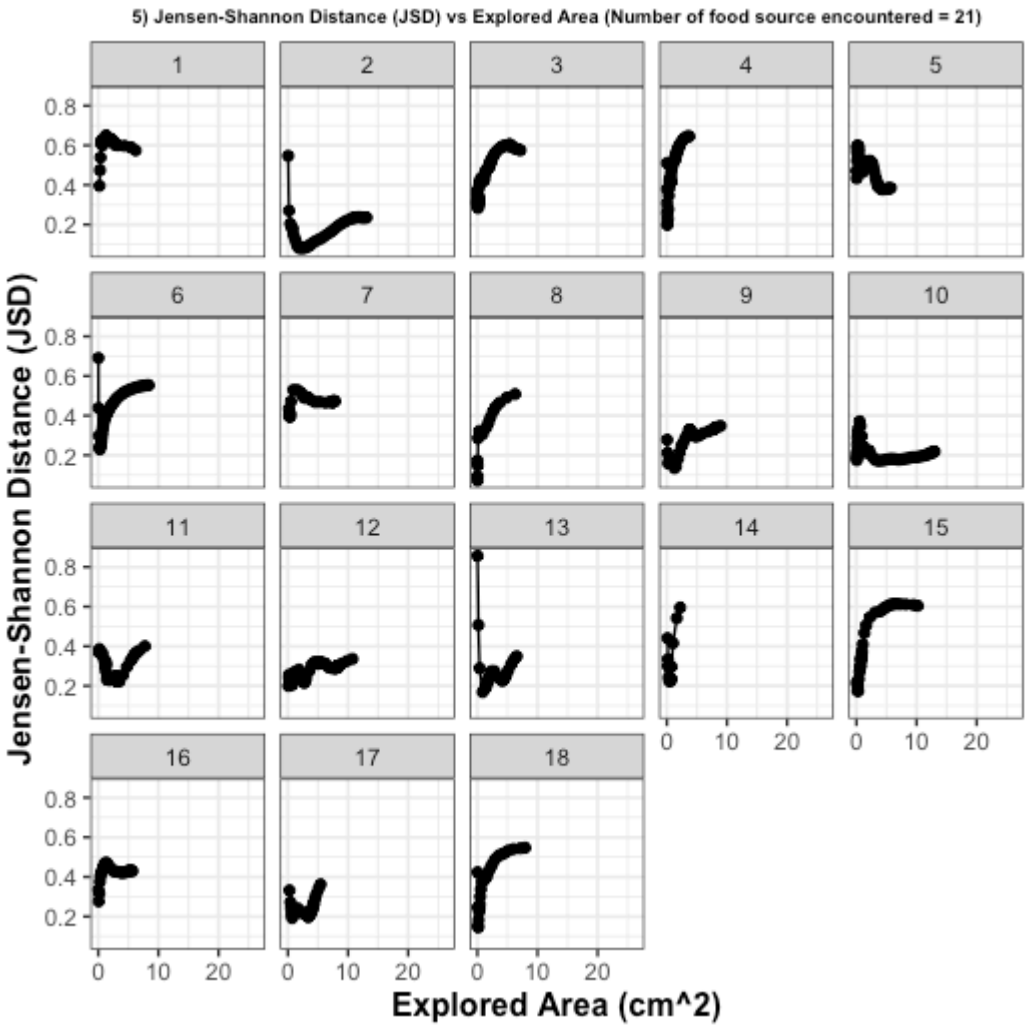

Figure B.12 Plot showing the changes in the Jensen-Shannon index (JSD) as function of area explored for experimental condition 5 (i.e., number of food sources encountered = 21). The black dots in the figure represent JSD values. The numbers on the title of the plots show the replicate numbers of the experiments conducted for the specific experimental condition.

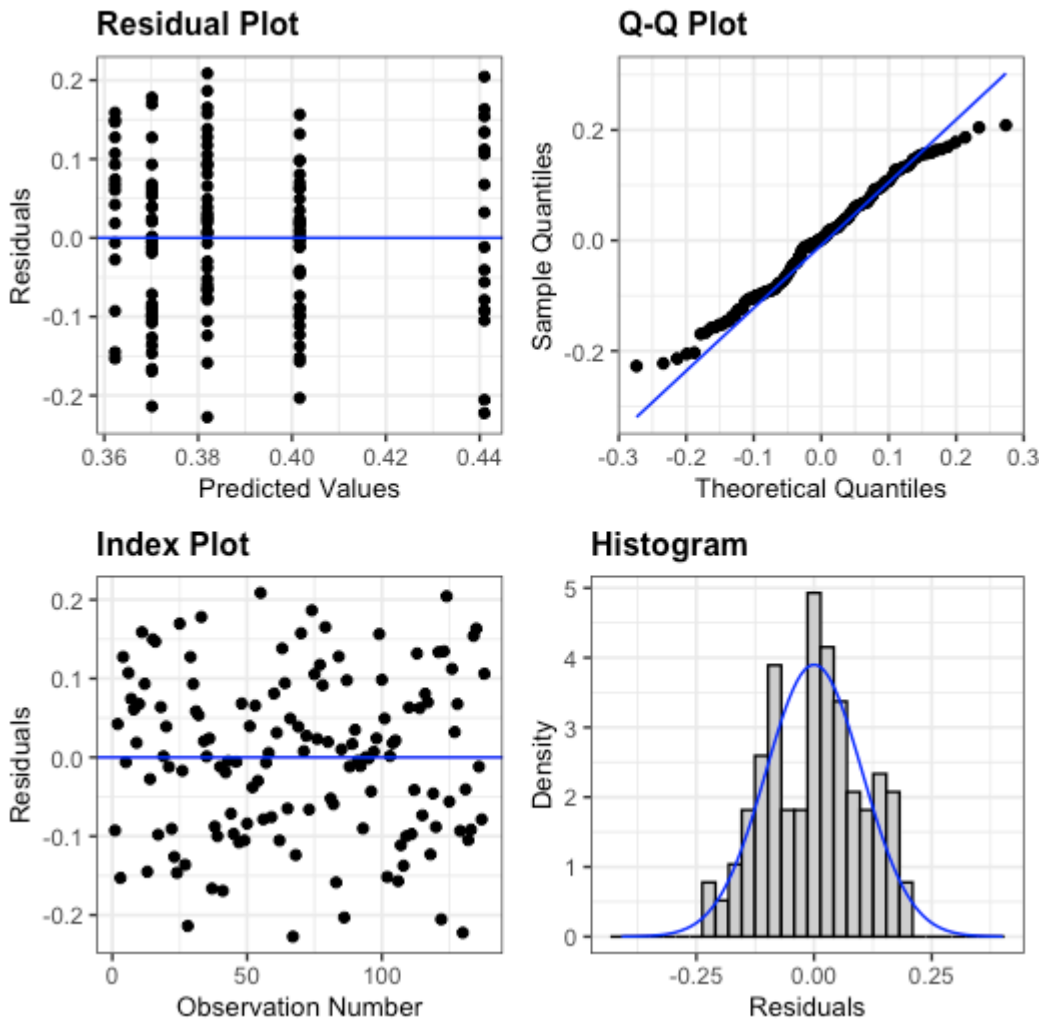

Figure B.13 Residual plots of the linear model fit to the Final Isotropy vs Number of food sources.

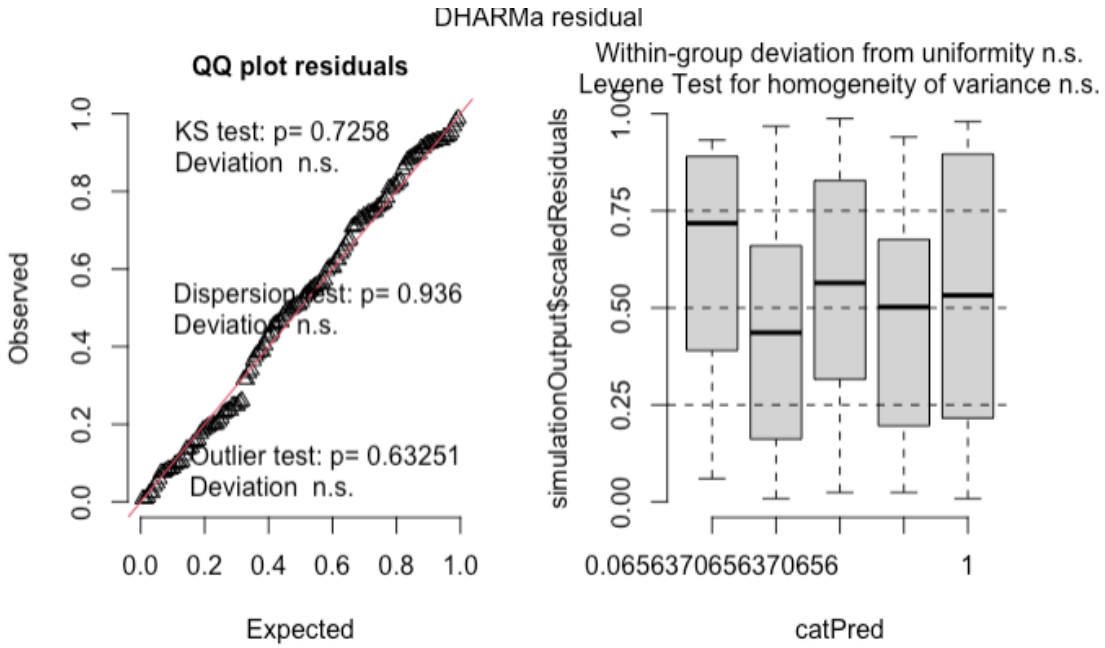

Figure B.14 Performance of the linear model fit on the Final Isotropy vs Number of food source data using DHARMa R package. The Q-Q plot of the DHARMa R package looks different from the one shown in the previous plot, as the DHARMa R package normalizes the Observed and Expected quantiles between 0 and 1.

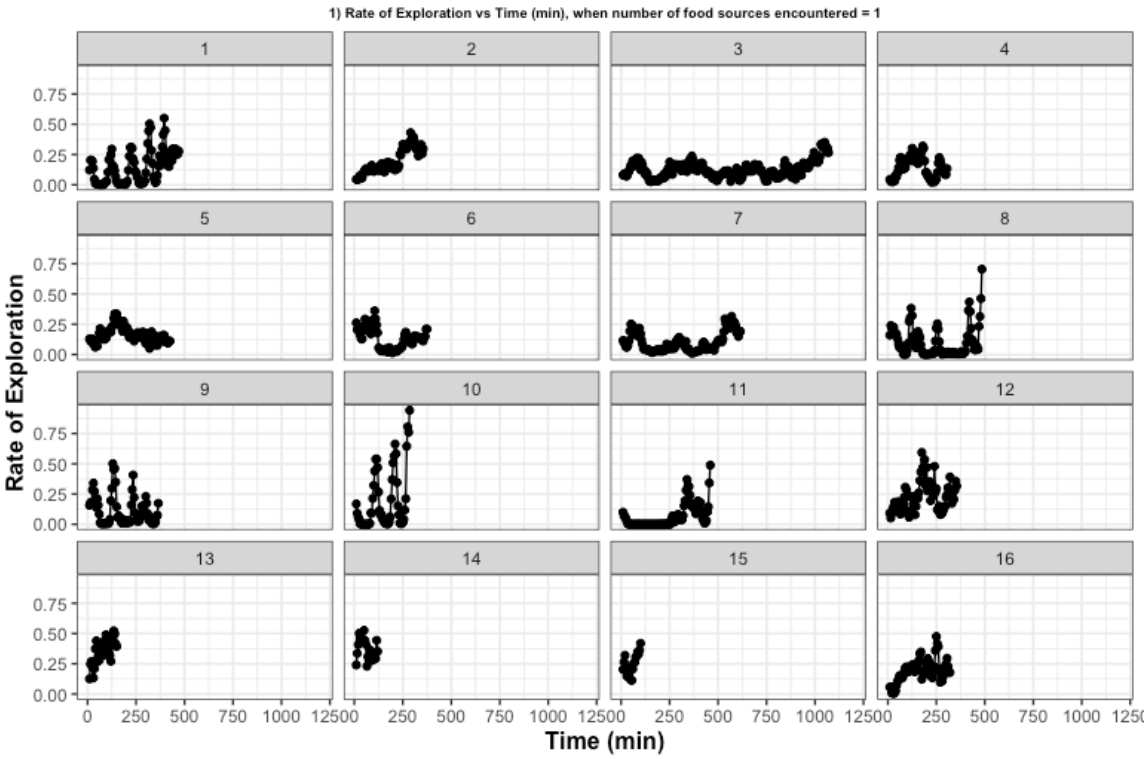

Figure B.15 Plot showing the changes in the rate of exploration index as function of time for experimental condition 1 (i.e., number of food sources encountered = 1). The black dots in the figure represent the rate of exploration values. The numbers on the title of the plots show the replicate numbers of the experiments conducted for the specific experimental condition.

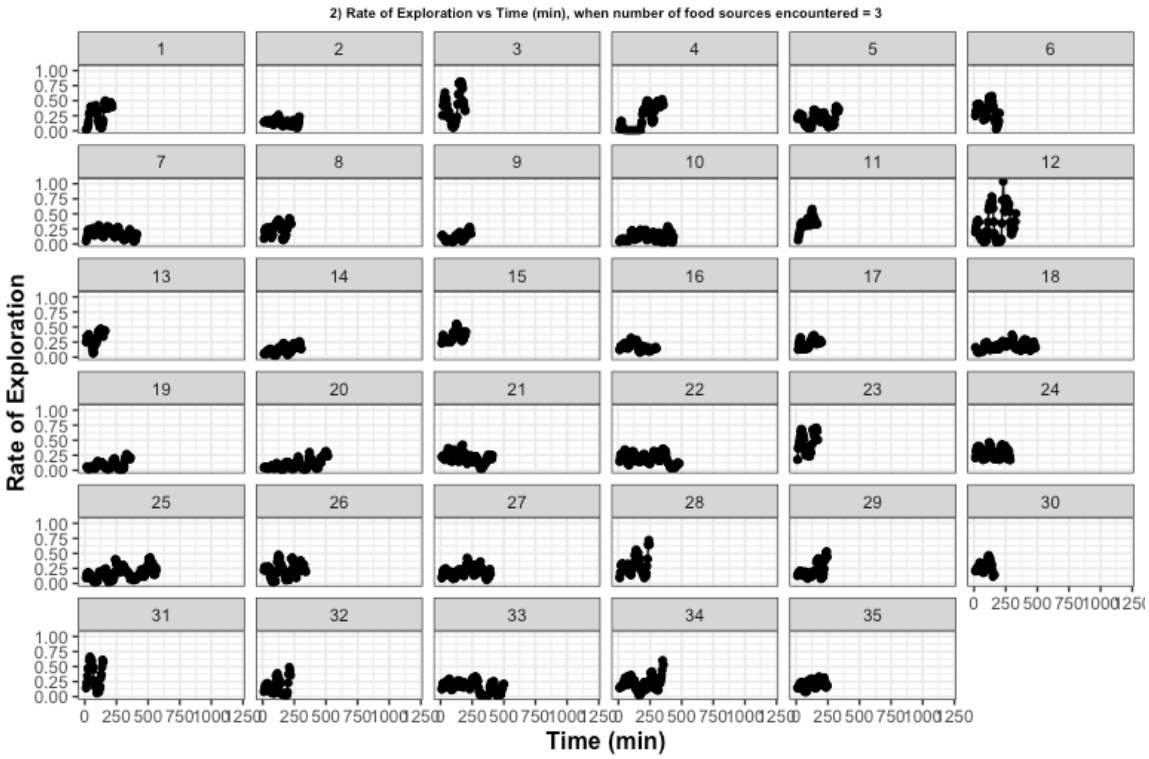

Figure B.16 Plot showing the changes in the rate of exploration index as function of time for experimental condition 2 (i.e., number of food sources encountered = 3). The black dots in the figure represent the rate of exploration values. The numbers on the title of the plots show the replicate numbers of the experiments conducted for the specific experimental condition.

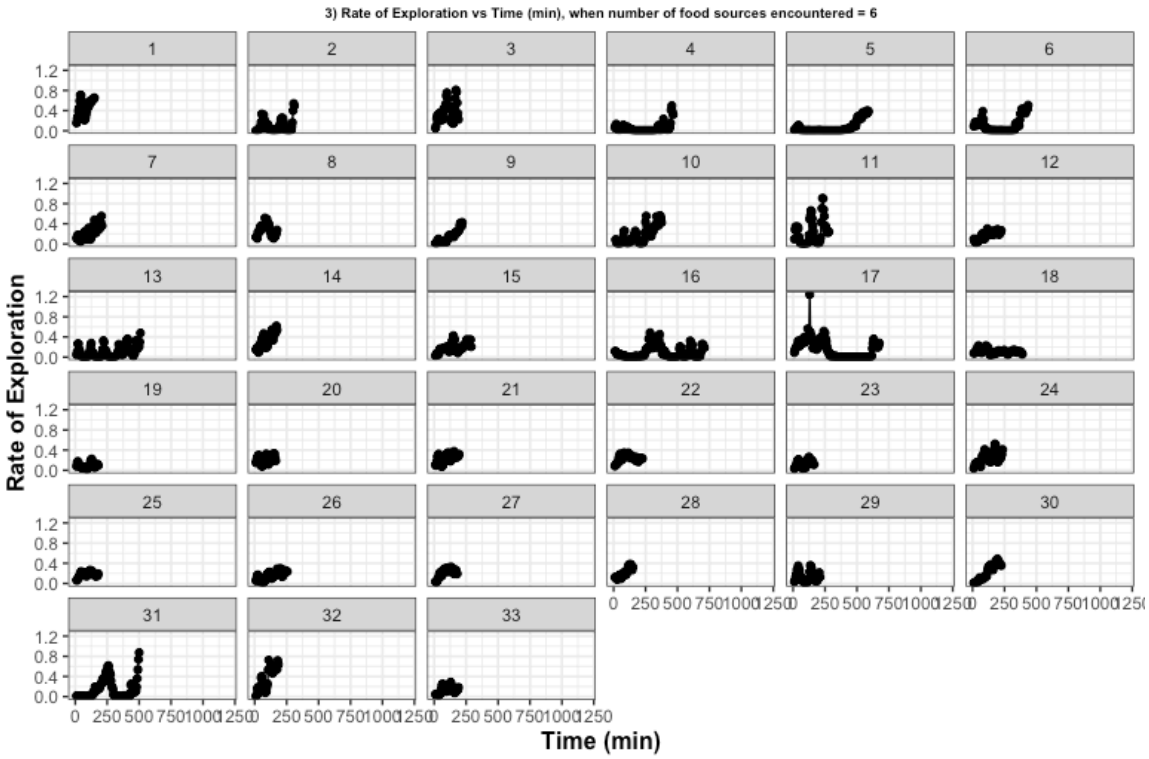

Figure B.17 Plot showing the changes in the rate of exploration index as function of time for experimental condition 3 (i.e., number of food sources encountered = 6). The black dots in the figure represent the rate of exploration values. The numbers on the title of the plots show the replicate numbers of the experiments conducted for the specific experimental condition.

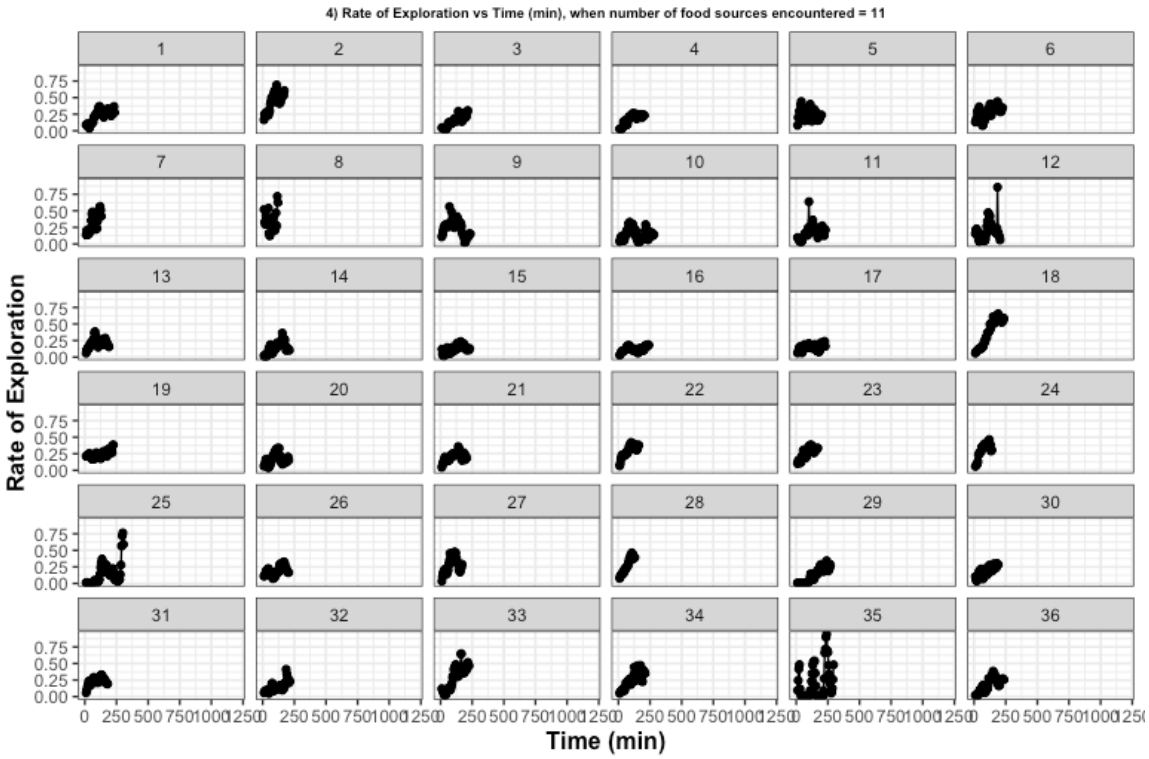

Figure B.18 Plot showing the changes in the rate of exploration index as function of time for experimental condition 4 (i.e., number of food sources encountered = 11). The black dots in the figure represent the rate of exploration values. The numbers on the title of the plots show the replicate numbers of the experiments conducted for the specific experimental condition.

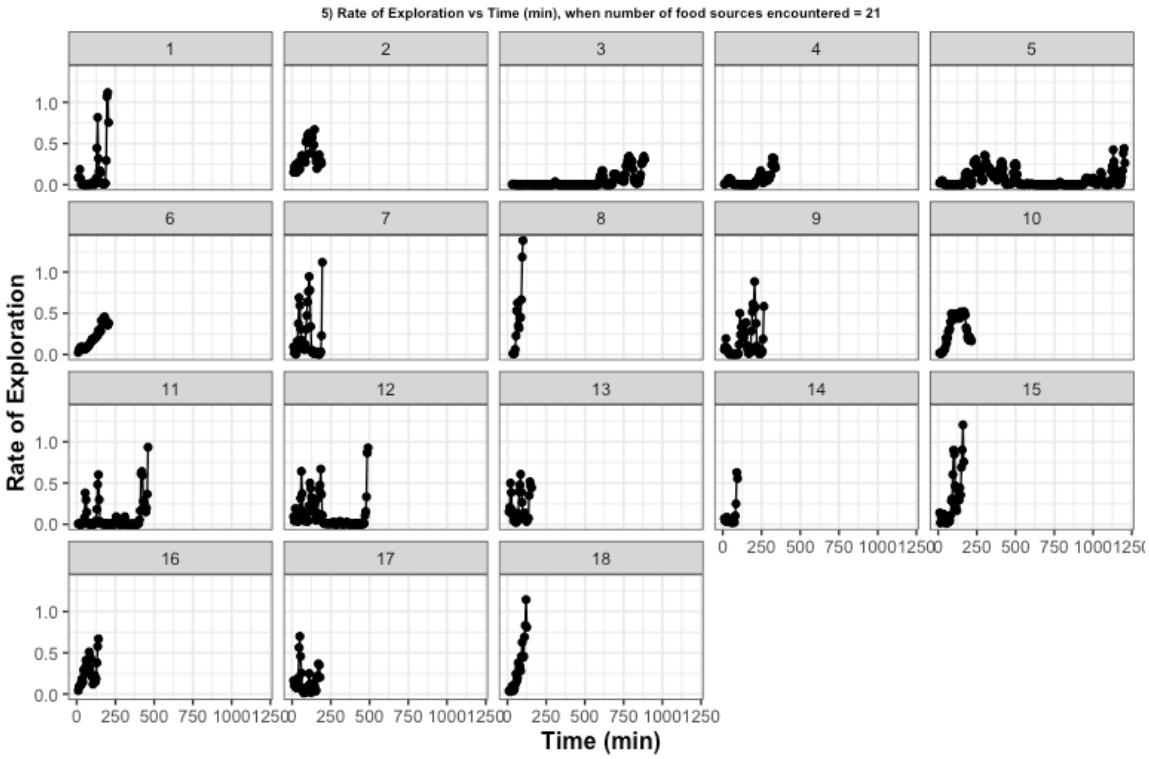

Figure B.19 Plot showing the changes in the rate of exploration index as function of time for experimental condition 5 (i.e., number of food sources encountered = 21). The black dots in the figure represent the rate of exploration values. The numbers on the title of the plots show the replicate numbers of the experiments conducted for the specific experimental condition.

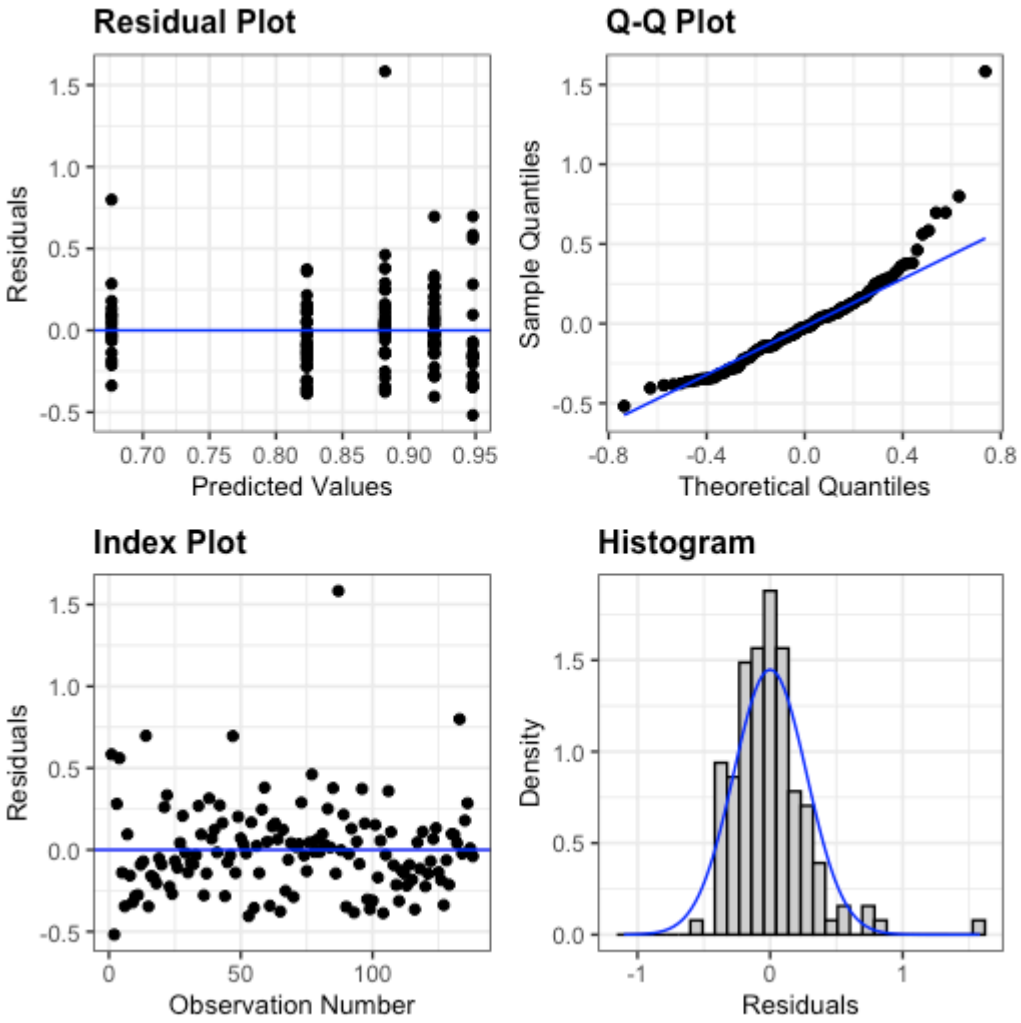

Figure B.20 Residual plots of fitting a linear model to the Mean rate of exploration vs Number of food sources.

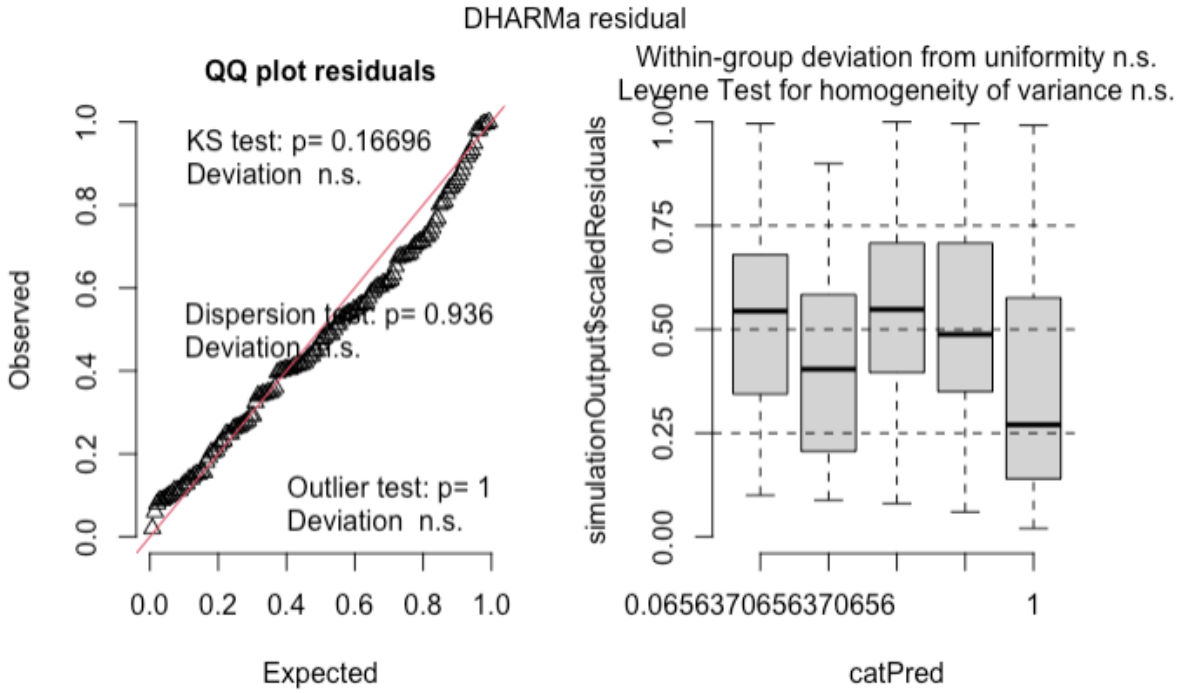

Figure B.21 Performance of the linear model fit on the Mean rate of exploration vs Number of food source data using DHARMa R package. The Q-Q plot of the DHARMa R package looks different from the one shown in the previous plot, as the DHARMa R package normalizes the Observed and Expected quantiles between 0 and 1.

APPENDIX C

SUPPLIMENTARY INFORMATION FOR FED VS STARVED CELL EXPLORATORY BEHAVIOR SIMULATION STUDY IN CHAPTER 5

This appendix provides the information to the analysis of simulation conducted in Chapter 5.

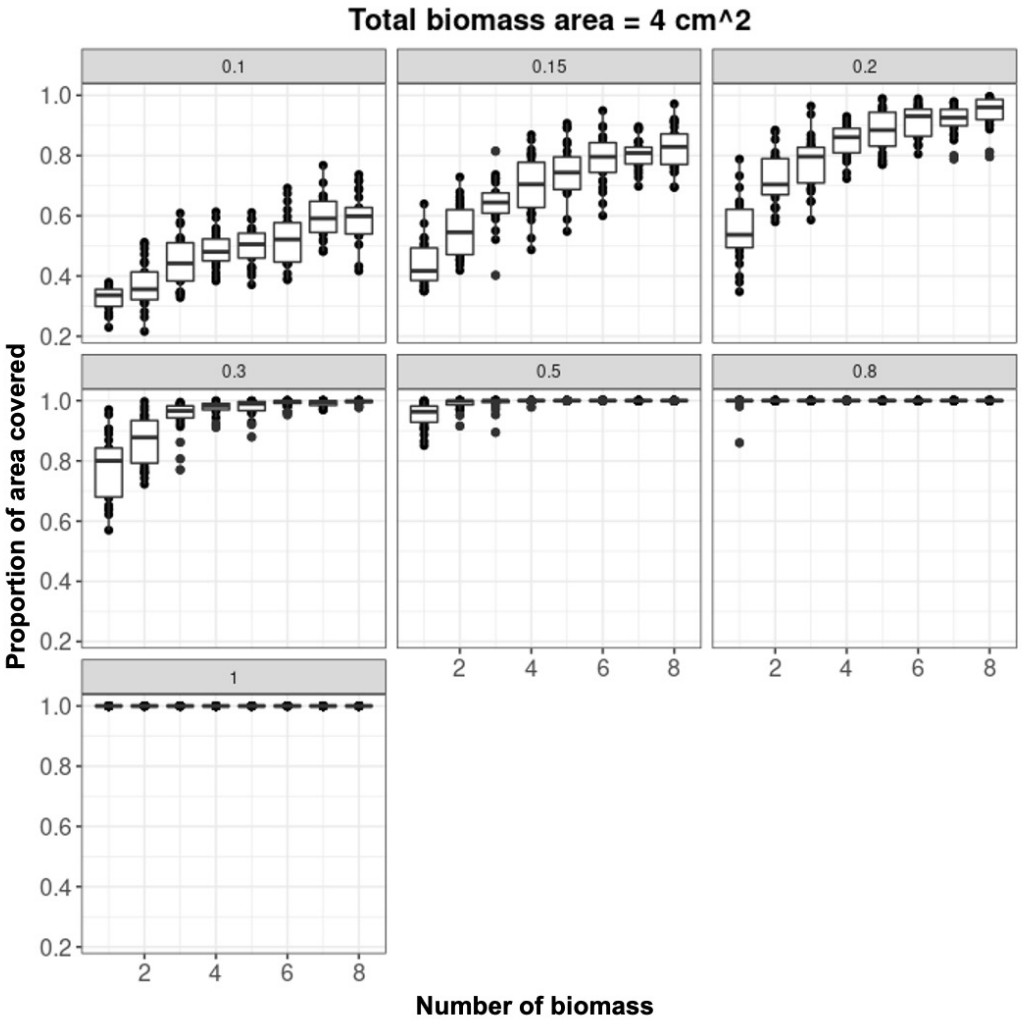

Figure C.1 Proportion of the simulation area covered as function of Number of biomass when the total biomass area was 4 cm^2. The plot is sectioned by the different speed values (units in cm/min). The speed values are given in the title of each subplot.

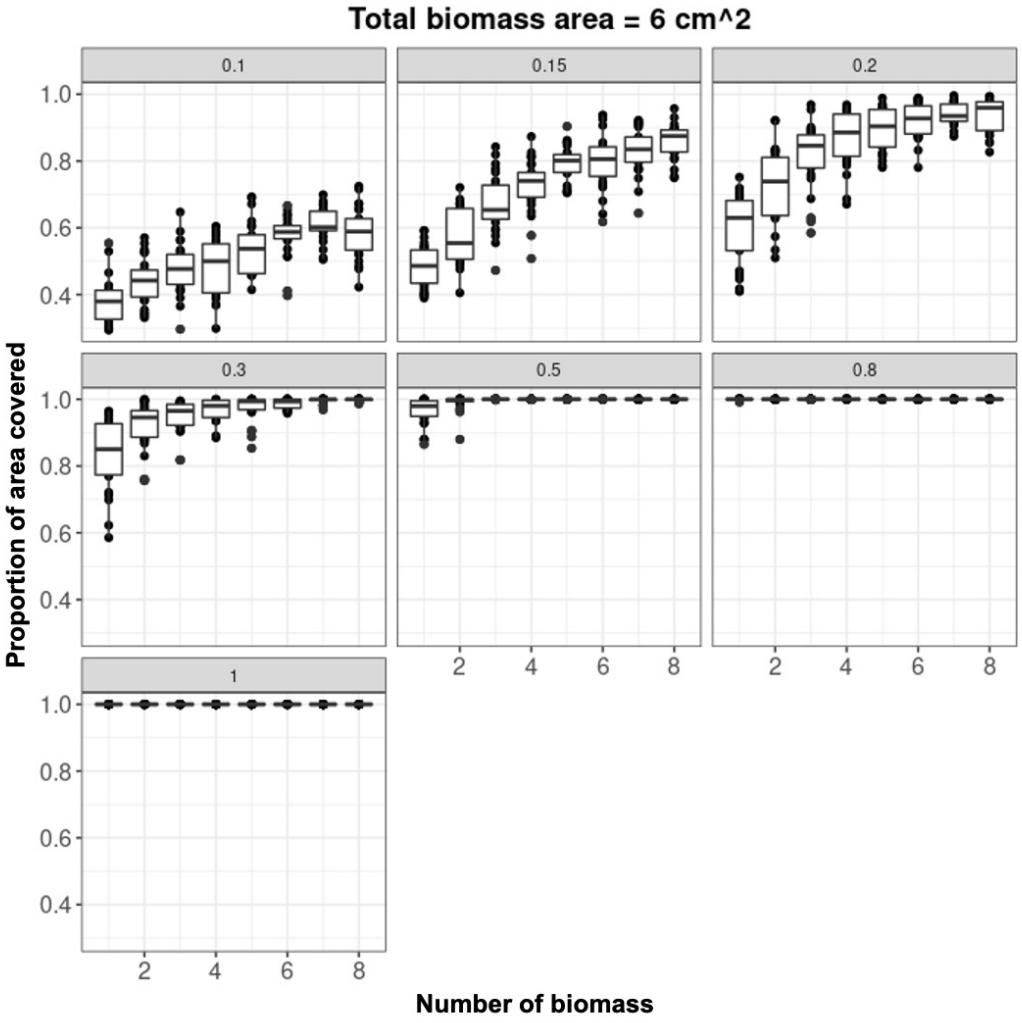

Figure C.2 Proportion of the simulation area covered as function of Number of biomass when the total biomass area was 6 cm^2. The plot is sectioned by the different speed values (units in cm/min). The speed values are given in the title of each subplot.

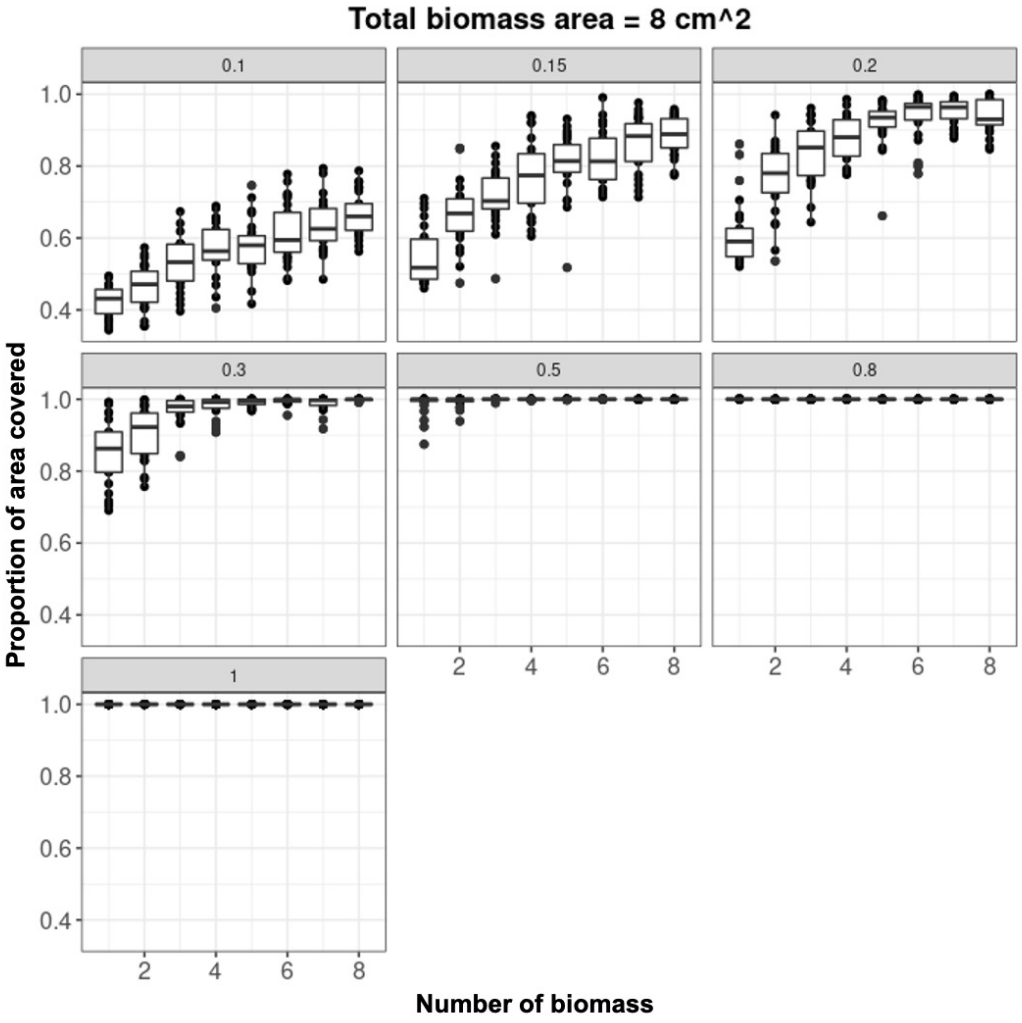

Figure C.3 Proportion of the simulation area covered as function of Number of biomass when the total biomass area was 8 cm^2. The plot is sectioned by the different speed values (units in cm/min). The speed values are given in the title of each subplot.

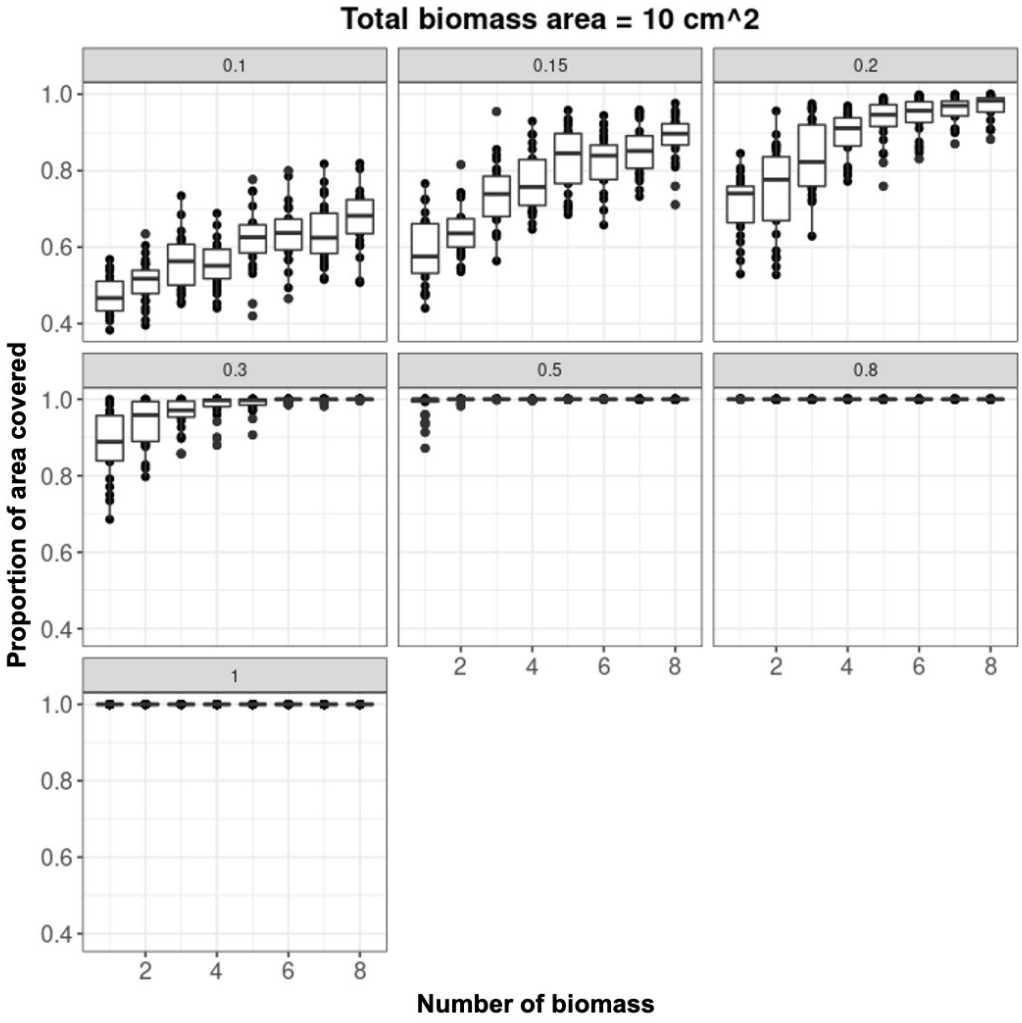

Figure C.4 Proportion of the simulation area covered as function of Number of biomass when the total biomass area was 10 cm^2. The plot is sectioned by the different speed values (units in cm/min). The speed values are given in the title of each subplot.

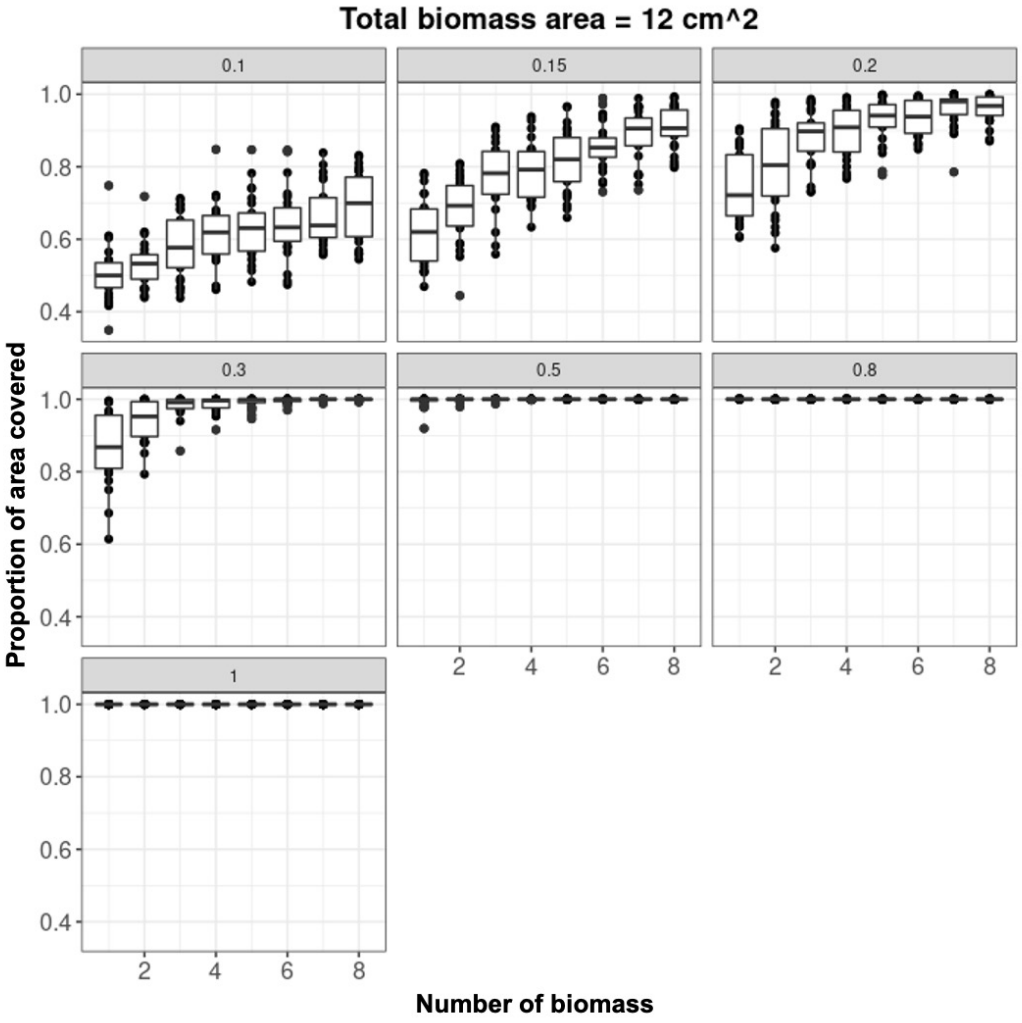

Figure C.5 Proportion of the simulation area covered as function of Number of biomass when the total biomass area was 12 cm^2. The plot is sectioned by the different speed values (units in cm/min). The speed values are given in the title of each subplot.

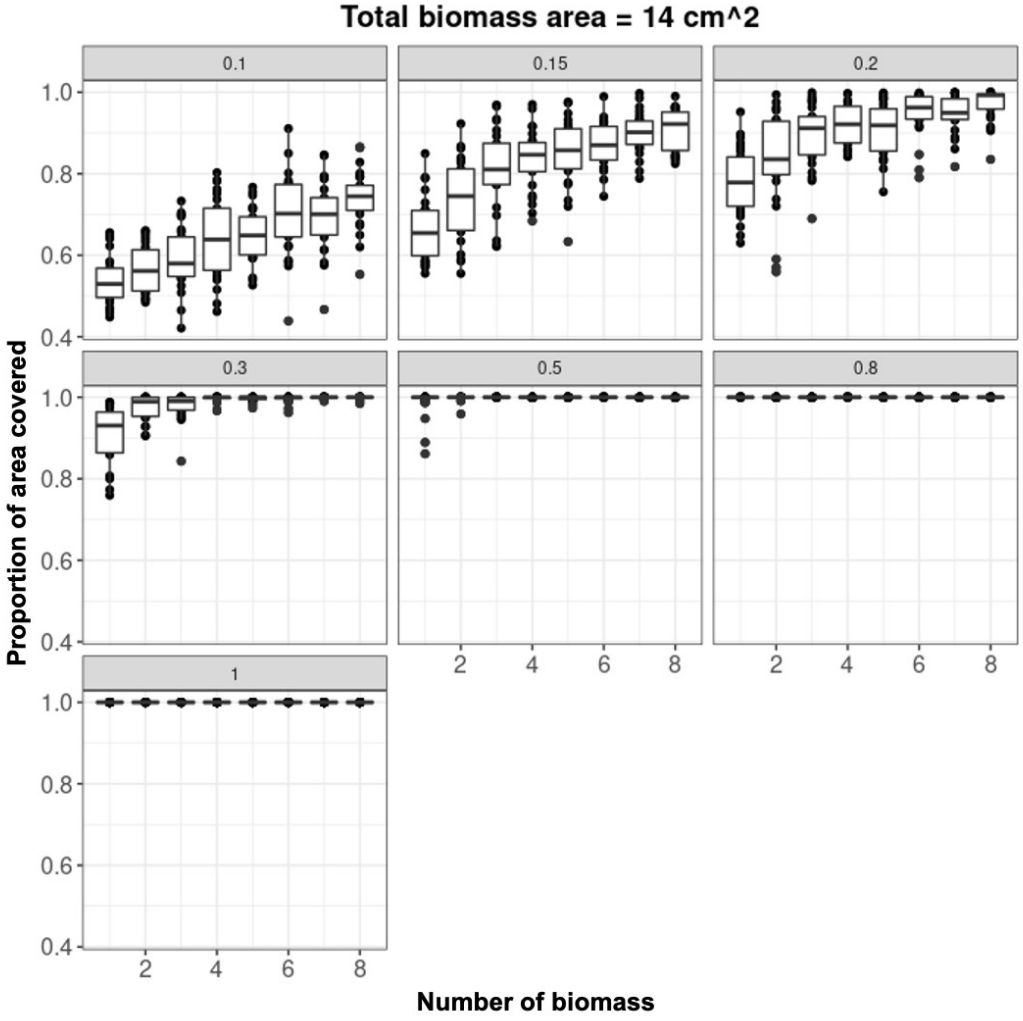

Figure C.6 Proportion of the simulation area covered as function of Number of biomass when the total biomass area was 14 cm^2. The plot is sectioned by the different speed values (units in cm/min). The speed values are given in the title of each subplot.

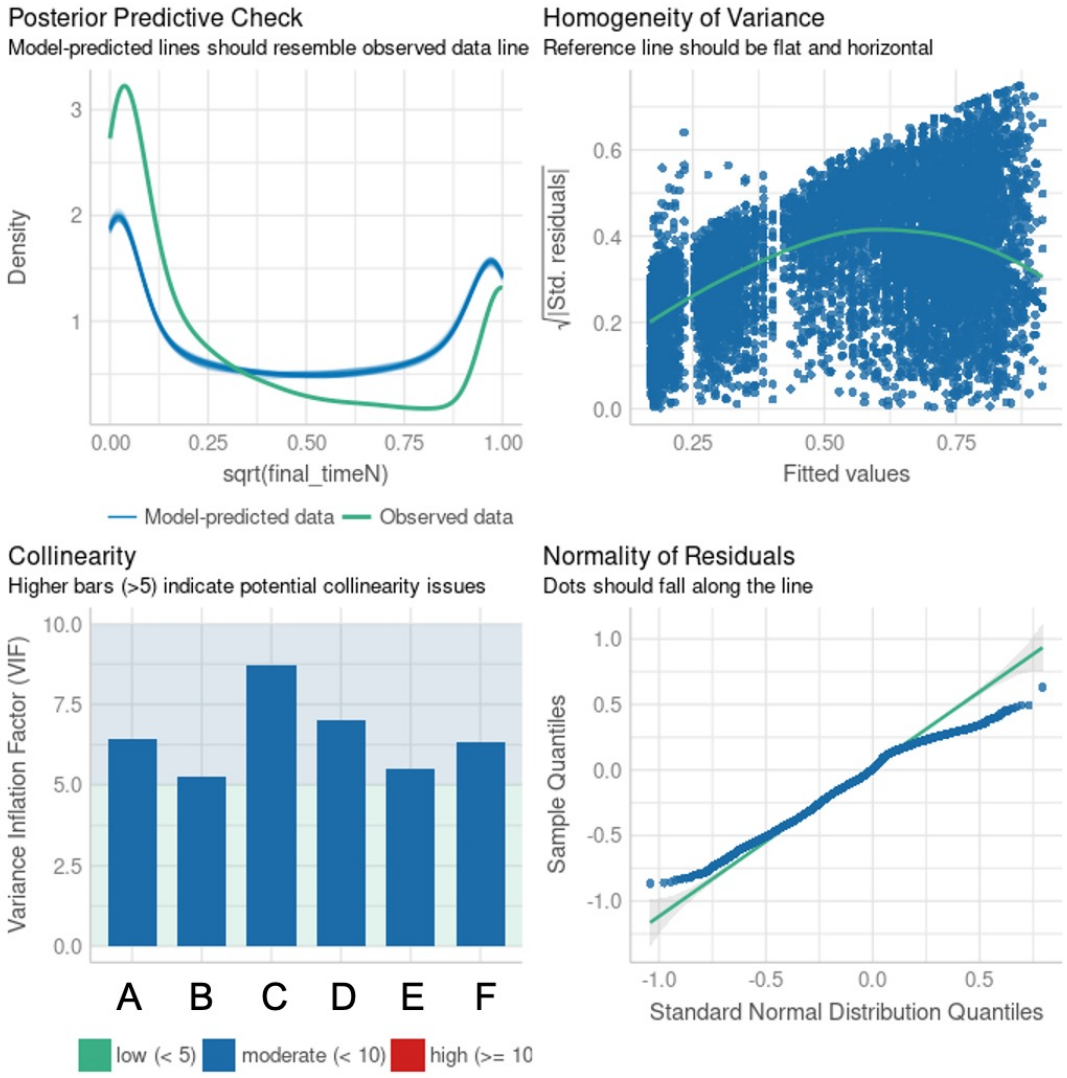

Figure C.7 Model diagnostics and performance for the Increasing probability profile. Each bar of the of the Variance Inflation Factor (VIF) plot reads in the sequence as follows: A) Number of biomass, B) Number of biomass:Speed, C) Number of biomass:Total biomass area, D) Speed, E) Speed:Total biomass area, and F) Total biomass area.

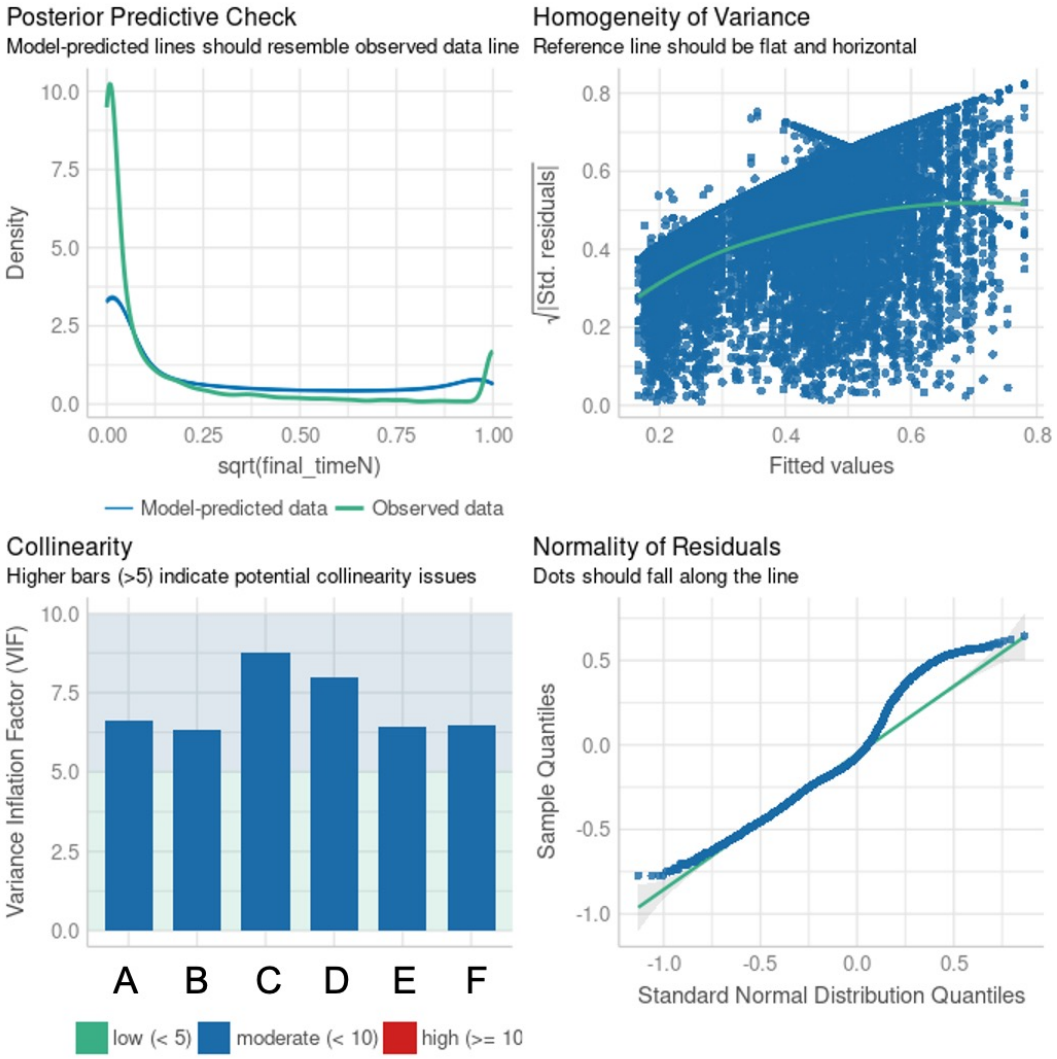

Figure C.8 Model diagnostics and performance for the Increasing probability profile Each bar of the of the Variance Inflation Factor (VIF) plot reads in the sequence as follows: A) Number of biomass, B) Number of biomass:Speed, C) Number of biomass:Total biomass area, D) Speed, E) Speed:Total biomass area, and F) Total biomass area.

REFERENCES

1. G. M. Viswanathan, V. Afanasyev, S. V. Buldyrev, E. J. Murphy, P. A. Prince, H. E. Stanley, Lévy flight search patterns of wandering albatrosses. *Nature*. **381**, 413–415 (1996).

2. G. Ramos-Fernández, J. L. Mateos, O. Miramontes, G. Cocho, H. Larralde, B. Ayala-Orozco, Lévy walk patterns in the foraging movements of spider monkeys (*Ateles geoffroyi*). *Behav. Ecol. Sociobiol.* **55**, 223–230 (2004).

3. R. P. D. Atkinson, C. J. Rhodes, D. W. Macdonald, R. M. Anderson, Scale-free dynamics in the movement patterns of jackals. *Oikos*. **98**, 134–140 (2002).

4. N. Saleh, L. Chittka, Traplining in bumblebees (*Bombus impatiens*): a foraging strategy's ontogeny and the importance of spatial reference memory in short-range foraging. *Oecologia*. **151**, 719–730 (2007).

5. A. T. Hurly, Spatial memory in rufous hummingbirds: memory for rewarded and non-rewarded sites. *Anim. Behav.* **51**, 177–183 (1996).

6. J. S. E. Garrison, C. L. Gass, Response of a traplining hummingbird to changes in nectar availability. *Behav. Ecol.* **10**, 714–725 (1999).

7. J. A. Merkle, D. Fortin, J. M. Morales, A memory-based foraging tactic reveals an adaptive mechanism for restricted space use. *Ecol. Lett.* **17**, 924–931 (2014).

8. P. Sandhu, O. Shura, R. L. Murray, C. Guy, Worms make risky choices too: the effect of starvation on foraging in the common earthworm (*Lumbricus terrestris*). *Can. J. Zool.* **96**, 1278–1283 (2018).

9. D. M. Weary, E. A. Pajor, B. K. Thompson, D. Fraser, Risky behaviour by piglets: a trade off between feeding and risk of mortality by maternal crushing? *Anim. Behav.* **51**, 619–624 (1996).

10. A.-C. Mailleux, C. Devigne, J.-L. Deneubourg, C. Detrain, Impact of starvation on *Lasius niger* exploration. *Ethology*. **116**, 248–256 (2010).

11. Y. M. Bar-On, R. Phillips, R. Milo, The biomass distribution on Earth. *Proc. Natl. Acad. Sci. U. S. A.* **115**, 6506–6511 (2018).

12. F. Baluška, M. Levin, On Having No Head: cognition throughout biological systems. *Front. Psychol.* **7**, 902 (2016).

13. S. L. Baldauf, W. F. Doolittle, Origin and evolution of the slime molds (Mycetozoa). *Proc. Natl. Acad. Sci. U. S. A.* **94**, 12007–12012 (1997).

14. D. Kessler, Plasmodial structure and motility. *Cell biology of Physarum and Didymium,* Sydney, Australia: Academic Press.

15. O. R. Collins, E. F. Haskins, Genetics of somatic fusion in *Physarum polycephalum*: the Ppii Strain. *Genetics*. **71**, 63–71 (1972).

16. W.F. Dove, H.P. Rusch, *Growth and Differentiation in Physarum polycephalum*, Princeton, New Jersey: Princeton University Press.

17. T. Nakagaki, H. Yamada, A. Tóth, Maze-solving by an amoeboid organism. *Nature*. **407**, 470 (2000).

18. A. Tero, S. Takagi, T. Saigusa, K. Ito, D. P. Bebber, M. D. Fricker, K. Yumiki, R. Kobayashi, T. Nakagaki, Rules for biologically inspired adaptive network design. *Science*. **327**, 439–442 (2010).

19. A. Dussutour, T. Latty, M. Beekman, S. J. Simpson, Amoeboid organism solves complex nutritional challenges. *Proc. Natl. Acad. Sci. U. S. A.* **107**, 4607–4611 (2010).

20. C. R. Reid, M. Beekman, Solving the towers of Hanoi - how an amoeboid organism efficiently constructs transport networks. *J. Exp. Biol.* **216**, 1546–1551 (2013).

21. T. Saigusa, A. Tero, T. Nakagaki, Y. Kuramoto, Amoebae anticipate periodic events. *Phys. Rev. Lett.* **100**, 018101 (2008).

22. C. R. Reid, T. Latty, A. Dussutour, M. Beekman, Slime mold uses an externalized spatial “memory” to navigate in complex environments. *Proc. Natl. Acad. Sci. U. S. A.* **109**, 17490–17494 (2012).

23. R. P. Boisseau, D. Vogel, A. Dussutour, Habituation in non-neural organisms: evidence from slime moulds. *Proc. Biol. Sci.* **283** (2016), doi:10.1098/rspb.2016.0446.

24. D. Vogel, A. Dussutour, Direct transfer of learned behaviour via cell fusion in non-neural organisms. *Proc. Biol. Sci.* **283** (2016), doi:10.1098/rspb.2016.2382.

25. T. Latty, M. Beekman, Irrational decision-making in an amoeboid organism: transitivity and context-dependent preferences. *Proc. Biol. Sci.* **278**, 307–312 (2011).

26. T. Latty, M. Beekman, Food quality and the risk of light exposure affect patch-choice decisions in the slime mold *Physarum polycephalum*. *Ecology*. **91**, 22–27 (2010).

27. T. Nakagaki, M. Iima, T. Ueda, Y. Nishiura, T. Saigusa, A. Tero, R. Kobayashi, K. Showalter, Minimum-risk path finding by an adaptive amoebal network. *Phys. Rev. Lett.* **99**, 068104 (2007).

28. T. Latty, M. Beekman, Speed-accuracy trade-offs during foraging decisions in the acellular slime mould Physarum polycephalum. *Proceedings of the Royal Society B: Biological Sciences*. **278**, 539–545 (2011).

29. C. R. Reid, H. MacDonald, R. P. Mann, J. A. R. Marshall, T. Latty, S. Garnier, Decision-making without a brain: how an amoeboid organism solves the two-armed bandit. *J. R. Soc. Interface*. **13**, 20160030 (2016).

30. M. Beekman, T. Latty, Brainless but Multi-Headed: Decision Making by the acellular slime mould *Physarum polycephalum*. *J. Mol. Biol.* **427**, 3734–3743 (2015).

31. P. Schaap, I. Barrantes, P. Minx, N. Sasaki, R. W. Anderson, M. Bénard, K. K. Biggar, N. E. Buchler, R. Bundschuh, X. Chen, C. Fronick, L. Fulton, G. Golderer, N. Jahn, V. Knoop, L. F. Landweber, C. Maric, D. Miller, A. A. Noegel, R. Peace, G. Pierron, T. Sasaki, M. Schallenberg-Rüdinger, M. Schleicher, R. Singh, T. Spaller, K. B. Storey, T. Suzuki, C. Tomlinson, J. J. Tyson, W. C. Warren, E. R. Werner, G. Werner-Felmayer, R. K. Wilson, T. Winckler, J. M. Gott, G. Glöckner, W. Marwan, The *Physarum polycephalum* genome reveals extensive use of prokaryotic two-Component and metazoan-type tyrosine kinase signaling. *Genome Biol. Evol.* **8**, 109–125 (2015).

32. M. Haindl, E. Holler, Use of the giant multinucleate plasmodium of *Physarum polycephalum* to study RNA interference in the myxomycete. *Anal. Biochem.* **342**, 194–199 (2005).

33. S. C. Materna, W. Marwan, Estimating the number of plasmids taken up by a eukaryotic cell during transfection and evidence that antisense RNA abolishes gene expression in *Physarum polycephalum*. *FEMS Microbiol. Lett.* **243**, 29–35 (2005).

34. C. R. Reid, S. Garnier, M. Beekman, T. Latty, Information integration and multiattribute decision making in non-neuronal organisms. *Anim. Behav.* **100**, 44–50 (2015).

35. M. Kim, T. Kim, Diffusion-based and long-range concentration gradients of multiple chemicals for bacterial chemotaxis assays. *Anal. Chem.* **82**, 9401–9409 (2010).

36. M. J. Sackett, J. P. Armitage, E. E. Sherwood, T. P. Pitta, Photoresponses of the purple nonsulfur bacteria *Rhodospirillum centenum* and *Rhodobacter sphaeroides*. *J. Bacteriol.* **179**, 6764–6768 (1997).

37. M. T. Keating, J. T. Bonner, Negative chemotaxis in cellular slime molds. *J. Bacteriol.* **130**, 144–147 (1977).

38. K. Katsura, Y. Miyata, Swimming behavior of *Phytophthora capsic*i zoospores. *Morphol & Biochem Events in Plant parasite Interaction* (1971) (available at http://agris.fao.org/agris-search/search.do?recordID=US201302389449).

39. R. M. Harshey, Bacterial motility on a surface: many ways to a common goal. *Annu. Rev. Microbiol.* **57**, 249–273 (2003).

40. E. Ben-Jacob, H. Levine, Self-engineering capabilities of bacteria. *J. R. Soc. Interface*. **3**, 197–214 (2006).

41. J. F. Cahill Jr, G. G. McNickle, J. J. Haag, E. G. Lamb, S. M. Nyanumba, C. C. St Clair, Plants integrate information about nutrients and neighbors. *Science*. **328**, 1657 (2010).

42. D. P. Bebber, J. Hynes, P. R. Darrah, L. Boddy, M. D. Fricker, Biological solutions to transport network design. *Proc. Biol. Sci.* **274**, 2307–2315 (2007).

43. R. Martínez-García, C. E. Tarnita, Seasonality can induce coexistence of multiple bet-hedging strategies in *Dictyostelium discoideum* via storage effect. *J. Theor. Biol.* **426**, 104–116 (2017).

44. C. Oettmeier, K. Brix, H.-G. Doebereiner, Physarum polycephalum-a new take on a classic model system. *J. Phys. D Appl. Phys.* (2017) (available at http://iopscience.iop.org/article/10.1088/1361-6463/aa8699/meta).

45. H. C. Aldrich, J. W. Daniel, *Cell Biology of Physarum and Didymium Volume 1: Organisms, Nucleus, and Cell Cycle* (Academic Press Inc., New York, New York, 1982).

46. K. Matsumoto, T. Ueda, Y. Kobatake, Propagation of phase wave in relation to tactic responses by the plasmodium of *Physarum polycephalum*. *J. Theor. Biol.* **122**, 339–345 (1986).

47. K. Matsumoto, T. Ueda, Y. Kobatake, Reversal of thermotaxis with oscillatory stimulation in the plasmodium of *Physarum polycephalum*. *J. Theor. Biol.* **131**, 175–182 (1988).

48. K. E. Wohlfarth-Bottermann, Oscillating contractions in protoplasmic strands of Physarum: simultaneous tensiometry of longitudinal and radial rhythms, periodicity analysis and temperature dependence. *J. Exp. Biol.* **67**, 49–59 (1977).

49. G. Isenberg, K. E. Wohlfarth-Bottermann, Transformation of cytoplasmic actin importance for the organization of the contractile gel reticulnm and the contraction — relaxation cycle of cytoplasmic actomyosin. *Cell Tissue Res.* **173**, 495–528 (1976).

50. K. Alim, G. Amselem, F. Peaudecerf, M. P. Brenner, A. Pringle, Random network peristalsis in *Physarum polycephalum* organizes fluid flows across an individual. *Proc. Natl. Acad. Sci. U. S. A.* **110**, 13306–13311 (2013).

51. W. W. Tso, T. E. Mansour, Thermotaxis in a slime mold, *Physarum polycephalum*. *Behav. Biol.* **14**, 499–504 (1975).

52. A. C. Durham, E. B. Ridgway, Control of chemotaxis in *Physarum polycephalum*. *J. Cell Biol.* **69**, 218–223 (1976).

53. K. E. Wohlfarth-Bottermann, I. Block, The pathway of photosensory transduction in *Physarum polycephalum*. *Cell Biol. Int. Rep.* **5**, 365–373 (1981).

54. Y. Miyake, H. Tada, M. Yano, H. Shimizu, Relationship between intracellular period modulation and external environment change in *Physarum plasmodium*. *Cell Struct. Funct.* **19**, 363–370 (1994).

55. K. Alim, N. Andrew, A. Pringle, M. P. Brenner, Mechanism of signal propagation in *Physarum polycephalum*. *Proc. Natl. Acad. Sci. U. S. A.*, 201618114 (2017).

56. Y. Miyake, S. Tabata, H. Murakami, M. Yano, H. Shimizu, Environment-dependent self-organization of positional information field in chemotaxis of *Physarum Plasmodium*. *J. Theor. Biol.* **178**, 341–353 (1996).

57. S. Camazine, J.-L. Deneubourg, N. R. Franks, J. Sneyd, E. Bonabeau, G. Theraula, *Self-organization in Biological Systems* (Princeton University Press, 2003).

58. A. Strandburg-Peshkin, C. R. Twomey, N. W. F. Bode, A. B. Kao, Y. Katz, C. C. Ioannou, S. B. Rosenthal, C. J. Torney, H. S. Wu, S. A. Levin, I. D. Couzin, Visual sensory networks and effective information transfer in animal groups. *Curr. Biol.* **23**, R709-11 (2013).

59. M. Toyota, D. Spencer, S. Sawai-Toyota, W. Jiaqi, T. Zhang, A. J. Koo, G. A. Howe, S. Gilroy, Glutamate triggers long-distance, calcium-based plant defense signaling. *Science*. **361**, 1112–1115 (2018).

60. C. E. Shannon, A mathematical theory of communication. *The Bell System Technical Journal*. **27**, 379–423 (1948).

61. T. Schreiber, Measuring information transfer. *Phys. Rev. Lett.* **85**, 461–464 (2000).

62. J. T. Lizier, M. Prokopenko, Differentiating information transfer and causal effect. *Eur. Phys. J. B*. **73**, 605–615 (2010).

63. N. Orange, N. Abaid, A transfer entropy analysis of leader-follower interactions in flying bats. *Eur. Phys. J. Spec. Top.* **224**, 3279–3293 (2015).

64. S. Butail, V. Mwaffo, M. Porfiri, Model-free information-theoretic approach to infer leadership in pairs of zebrafish. *Phys Rev E*. **93**, 042411 (2016).

65. S. Butail, F. Ladu, D. Spinello, M. Porfiri, Information Flow in Animal-Robot Interactions. *Entropy* . **16**, 1315–1330 (2014).

66. A. G. Dimitrov, A. A. Lazar, J. D. Victor, Information theory in neuroscience. *J. Comput. Neurosci.* **30**, 1–5 (2011).

67. N. M. Timme, S. Ito, M. Myroshnychenko, S. Nigam, M. Shimono, F.-C. Yeh, P. Hottowy, A. M. Litke, J. M. Beggs, High-degree neurons feed cortical computations. *PLoS Comput. Biol.* **12**, e1004858 (2016).

68. G. Valentini, D. G. Moore, J. R. Hanson, T. P. Pavlic, S. C. Pratt, S. I. Walker, Transfer of information in collective decisions by artificial agents. *The 2018 Conference on Artificial Life: A Hybrid of the European Conference on Artificial Life (ECAL) and the International Conference on the Synthesis and Simulation of Living Systems (ALIFE)*, 641–648 (2018).

69. O. Kwon, J. -S. Yang, Information flow between stock indices. *Europhys. Lett.* **82**, 68003 (2008).

70. J. P. Crutchfield, The calculi of emergence. *Physica D*. **75**, 11–54 (1994).

71. W. S. Cleveland, Robust Locally Weighted regression and smoothing scatterplots. *J. Am. Stat. Assoc.* **74**, 829–836 (1979).

72. E. B. Wilson, Probable inference, the law of succession, and statistical inference. *J. Am. Stat. Assoc.* **22**, 209–212 (1927).

73. D. G. Moore, G. Valentini, S. I. Walker, M. Levin, Inform: Efficient information-theoretic analysis of collective behaviors. *Front. Robot. AI*. **5**, 60 (2018).

74. R Core Team, R: A language and environment for statistical computing. R Foundation for Statistical Computing, Vienna, Austria (2018).

75. W. Korohoda, Z. Shraideh, Z. Baranowski, K. E. Wohlfarth-Bottermann, Energy metabolic regulation of oscillatory contraction activity in *Physarum polycephalum*. *Cell Tissue Res.* **231**, 675–691 (1983).

76. Y. Yoshimoto, F. Matsumura, N. Kamiya, Simultaneous oscillations of Ca2+ efflux and tension generation in the permealized plasmodial strand of *Physarum*. *Cell Motil.* **1**, 433–443 (1981).

77. N. B. Matveeva, V. A. Teplov, S. I. Beylina, Suppression of the autooscillatory contractile activity of *Physarum polycephalum* plasmodium by the inhibitor of the IP3-Induced Ca2 release, 2-aminoethoxydiphenyl borate. *Biochem. Suppl. Ser*. **4**, 70–76 (2010).

78. N. B. Matveeva, V. A. Teplov, S. I. Beylina, Coupling of phospholipase C and PI3K/PTEN signaling pathways in *Physarum polycephalum*: the action of U73122 on motile and autooscillatory activity of plasmodium. *Biochemistry (Moscow) Supplement Series A: Membrane and Cell Biology*. **6**, 255–264 (2012).

79. H. Kim, P. Davies, S. I. Walker, New scaling relation for information transfer in biological networks. *J. R. Soc. Interface*. **12**, 20150944 (2015).

80. D. Vogel, A. Dussutour, J.-L. Deneubourg, Symmetry breaking and inter-clonal behavioural variability in a slime mould. *Biol. Lett.* **14**, 20180504 (2018).

81. A. Dussutour, Q. Ma, D. Sumpter, Phenotypic variability predicts decision accuracy in unicellular organisms. *Proc. Biol. Sci.* **286**, 20182825 (2019).

82. R Core Team, R: A language and environment for statistical computing. R Foundation for Statistical Computing, Vienna, Austria (2021).

83. D. Bates, M. Mächler, B. Bolker, S. Walker, Fitting linear mixed-effects models using lme4. *J. Stat. Soft.*. **67** (2015), pp. 1–48.

84. S. K. Ray, G. Valentini, P. Shah, A. Haque, C. R. Reid, G. F. Weber, S. Garnier, Information transfer during food choice in the slime mold *Physarum polycephalum*. *Frontiers in Ecology and Evolution*. **7**, 67 (2019).

85. J. P. Gould, Risk, stochastic preference, and the value of information. *J. Econ. Theory*. **8**, 64–84 (1974).

86. G. H. Pyke, Optimal foraging theory: A critical review. *Annu. Rev. Ecol. Syst.* **15**, 523–575 (1984).

87. S. R. X. Dall, L.-A. Giraldeau, O. Olsson, J. M. McNamara, D. W. Stephens, Information and its use by animals in evolutionary ecology. *Trends Ecol. Evol.* **20**, 187–193 (2005).

88. S. Benhamou, Spatial memory and searching efficiency. *Anim. Behav.* **47**, 1423–1433 (1994).

89. T. Avgar, R. Deardon, J. M. Fryxell, An empirically parameterized individual based model of animal movement, perception, and memory. *Ecol. Modell.* **251**, 158–172 (2013).

90. J. D. Thomson, Trapline foraging by bumblebees: I. Persistence of flight-path geometry. *Behav. Ecol.* **7**, 158–164 (1996).

91. L. Comba, Patch use by bumblebees (Hymenoptera Apidae): temperature, wind, flower density and traplining. *Ethol. Ecol. Evol.* **11**, 243–264 (1999).

92. P. A. Garber, Foraging decisions during nectar feeding by Tamarin monkeys (*Saguinus mystax* and *Saguinus fuscicollis*, *Callitrichidae*, Primates) in Amazonian Peru. *Biotropica*. **20**, 100–106 (1988).

93. T. A. Morrison, J. A. Merkle, J. G. C. Hopcraft, E. O. Aikens, J. L. Beck, R. B. Boone, A. B. Courtemanch, S. P. Dwinnell, W. S. Fairbanks, B. Griffith, A. D. Middleton, K. L. Monteith, B. Oates, L. Riotte-Lambert, H. Sawyer, K. T. Smith, J. A. Stabach, K. L. Taylor, M. J. Kauffman, Drivers of site fidelity in ungulates. *J. Anim. Ecol.* **90**, 955–966 (2021).

94. M. A. Edwards, J. A. Nagy, A. E. Derocher, Low site fidelity and home range drift in a wide-ranging, large Arctic omnivore. *Anim. Behav.* **77**, 23–28 (2009).

95. D. Moore, P. Doherty, Acquisition of a time-memory in forager honey bees. *J. Comp. Physiol. A Neuroethol. Sens. Neural Behav. Physiol.* **195**, 741–751 (2009).

96. S. G. Reebs, M. Lague, Daily food-anticipatory activity in golden shiners. A test of endogenous timing mechanisms. *Physiol. Behav.* **70**, 35–43 (2000).

97. C. Waitt, H. M. Buchanan-Smith, What time is feeding?: How delays and anticipation of feeding schedules affect stump-tailed macaque behavior. *Appl. Anim. Behav. Sci.* **75**, 75–85 (2001).

98. P. Arranz, K. J. Benoit-Bird, B. L. Southall, J. Calambokidis, A. S. Friedlaender, P. L. Tyack, Risso's dolphins plan foraging dives. *J. Exp. Biol.* **221** (2018), doi:10.1242/jeb.165209.

99. A. Mitchell, G. H. Romano, B. Groisman, A. Yona, E. Dekel, M. Kupiec, O. Dahan, Y. Pilpel, Adaptive prediction of environmental changes by microorganisms. *Nature*. **460**, 220–224 (2009).

100. M. Alejandra Guzmán, A. Delgado, J. De Carvalho, A novel multiobjective optimization algorithm based on bacterial chemotaxis. *Eng. Appl. Artif. Intell.* **23**, 292–301 (2010).

101. G. Roth, in *The Long Evolution of Brains and Minds* (Springer, Dordrecht, 2013), pp. 69–77.

102. E. J. Bottone, N. Nagarsheth, K. Chiu, Evidence of self-inhibition by filamentous fungi accounts for unidirectional hyphal growth in colonies. *Can. J. Microbiol.* **44**, 390–393 (1998).

103. P. Louâpre, A.-K. Bittebière, B. Clément, J.-S. Pierre, C. Mony, How past and present influence the foraging of clonal plants? *PLoS One*. **7**, e38288 (2012).

104. T. Latty, M. Beekman, Food quality affects search strategy in the acellular slime mould, *Physarum polycephalum*. *Behav. Ecol.* **20**, 1160–1167 (2009).

105. S. Benhamou, Efficiency of area-concentrated searching behaviour in a continuous patchy environment. *J. Theor. Biol.* **159**, 67–81 (1992).

106. P. A. Zollner, S. L. Lima, Search Strategies for Landscape-Level Interpatch Movements. *Ecology*. **80**, 1019–1030 (1999).

107. D. Fortin, Optimal searching behaviour: the value of sampling information. *Ecol. Modell.* **153**, 279–290 (2002).

108. A. E. Martin, D. Jørgensen, C. C. Gates, Costs and benefits of straight versus tortuous migration paths for Prairie Rattlesnakes (*Crotalus viridis viridis*) in seminatural and human-dominated landscapes. *Can. J. Zool.* **95**, 921–928 (2017).

109. Y. P. Papastamatiou, D. P. Cartamil, C. G. Lowe, C. G. Meyer, B. M. Wetherbee, K. N. Holland, Scales of orientation, directed walks and movement path structure in sharks. *J. Anim. Ecol.* **80**, 864–874 (2011).

110. M. del M. Delgado, V. Penteriani, V. O. Nams, L. Campioni, Changes of movement patterns from early dispersal to settlement. *Behav. Ecol. Sociobiol.* **64**, 35–43 (2009).

111. L. Campioni, M. del M. Delgado, R. Lourenço, G. Bastianelli, N. Fernández, V. Penteriani, Individual and spatio-temporal variations in the home range behaviour of a long-lived, territorial species. *Oecologia*. **172**, 371–385 (2013).

112. H. J. de Knegt, G. M. Hengeveld, F. van Langevelde, W. F. de Boer, K. P. Kirkman, Patch density determines movement patterns and foraging efficiency of large herbivores. *Behav. Ecol.* **18**, 1065–1072 (2007).

113. O. R. Anderson, Fine structure observations of phagotrophic activity by plasmodia of *Physarum polycephalum*. *J. Eukaryot. Microbiol.* **40**, 67–71 (1993).

114. Y. Yoshimoto, N. Kamiya, Studies on contraction rhythm of the plasmodial strand I. Synchronization of local rhythms. *Protoplasma*. **95**, 89–99 (1978).

115. J. Lin, Divergence measures based on the Shannon entropy. *IEEE Trans. Inf. Theory*. **37**, 145–151 (1991).

116. S. Kullback, *Information Theory and Statistics* (Courier Corporation, 1997).

117. F. Hartig, Residual diagnostics for hierarchical (multi-Level / mixed) regression models [R package DHARMa version 0.4.5] (2022) (available at https://CRAN.R-project.org/package=DHARMa).

118. C. R. Reid, M. Beekman, T. Latty, A. Dussutour, Amoeboid organism uses extracellular secretions to make smart foraging decisions. *Behav. Ecol.* **24**, 812–818 (2013).

119. J. Smith-Ferguson, T. C. Burnham, M. Beekman, Experience shapes future foraging decisions in a brainless organism. *Adapt. Behav.*, 105971232199468 (2021).

120. J. Minderman, J. M. Reid, M. Hughes, M. J. H. Denny, S. Hogg, P. G. H. Evans, M. J. Whittingham, Novel environment exploration and home range size in starlings *Sturnus vulgaris*. *Behav. Ecol.* **21**, 1321–1329 (2010).

121. M. Videlier, C. Bonneaud, R. Cornette, A. Herrel, Exploration syndromes in the frog Xenopus (Silurana) tropicalis : correlations with morphology and performance? *J. Zool.* . **294**, 206–213 (2014).

122. B. Farnworth, R. Meitern, J. Innes, J. R. Waas, Increasing predation risk with light reduces speed, exploration and visit duration of invasive ship rats (Rattus rattus). *Sci. Rep.* **9**, 3739 (2019).

123. P. Šmilauer, M. Šmilauerová, M. Kotilínek, J. Košnar, Foraging speed and precision of arbuscular mycorrhizal fungi under field conditions: An experimental approach. *Mol. Ecol.* **29**, 1574–1587 (2020).

124. C. Mettke-Hofmann, H. Winkler, B. Leisler, The significance of ecological factors for exploration and neophobia in parrots. *Ethology*. **108**, 249–272 (2002).

125. D. W. Stephens, J. S. Brown, R. C. Ydenberg, *Foraging: Behavior and Ecology* (University of Chicago Press, 2008).

126. M. McClure, L. Morcos, E. Despland, Collective choice of a higher-protein food source by gregarious caterpillars occurs through differences in exploration. *Behav. Ecol.* **24**, 113–118 (2013).

127. J. A. Stamps, The effect of familiarity with a neighborhood on territory acquisition. *Behav. Ecol. Sociobiol.* **21**, 273–277 (1987).

128. C. Mettke-Hofmann, M. Wink, M. Braun, H. Winkler, Residency and a broad feeding spectrum are related to extensive spatial exploration in Parrots. *Behav. Ecol.* **23**, 1365–1371 (2012).

129. G. Cowlishaw, The role of vigilance in the survival and reproductive strategies of desert baboons. *Behaviour*. **135**, 431–452 (1998).

130. S. L. Lima, L. M. Dill, Behavioral decisions made under the risk of predation: a review and prospectus. *Can. J. Zool.* **68**, 619–640 (1990).

131. A. J. Wirsing, M. R. Heithaus, L. M. Dill, Living on the edge: dugongs prefer to forage in microhabitats that allow escape from rather than avoidance of predators. *Anim. Behav.* **74**, 93–101 (2007).

132. Y. Lubin, S. Ellner, M. Kotzman, Web relocation and habitat selection in desert widow spider. *Ecology*. **74**, 1915–1928 (1993).

133. J. S. Brown, B. P. Kotler, Hazardous duty pay and the foraging cost of predation. *Ecol. Lett.* **7**, 999–1014 (2004).

134. A. Kacelnik, A. I. Houston, Some effects of energy costs on foraging strategies. *Anim. Behav.* **32**, 609–614 (1984).

135. J. H. Fewell, Energetic and time costs of foraging in harvester ants, Pogonomyrmex occidentalis. *Behav. Ecol. Sociobiol.* **22**, 401–408 (1988).

136. A. L. Bryan, M. C. Coulter, C. J. Pennycuick, Foraging strategies and energetic costs of foraging flights by breeding wood storks. *Condor*. **97**, 133–140 (1995).

137. K. A. Nagy, G. L. Kooyman, P. J. Ponganis, Energetic cost of foraging in free-diving emperor penguins. *Physiol. Biochem. Zool.* **74**, 541–547 (2001).

138. B. Naef-Daenzer, Patch time allocation and patch sampling by foraging great and blue tits. *Anim. Behav.* **59**, 989–999 (2000).

139. E. Cunningham, C. Janson, Integrating information about location and value of resources by white-faced saki monkeys (*Pithecia pithecia*). *Anim. Cogn.* **10**, 293–304 (2007).

140. R. B. McKane, L. C. Johnson, G. R. Shaver, K. J. Nadelhoffer, E. B. Rastetter, B. Fry, A. E. Giblin, K. Kielland, B. L. Kwiatkowski, J. A. Laundre, G. Murray, Resource-based niches provide a basis for plant species diversity and dominance in arctic tundra. *Nature*. **415**, 68–71 (2002).

141. N. H. C. Fraser, N. B. Metcalfe, J. E. Thorpe, Temperature-dependent switch between diurnal and nocturnal foraging in salmon. *Proceedings of the Royal Society of London. Series B: Biological Sciences*. **252**, 135–139 (1993).

142. G. M. Viswanathan, S. V. Buldyrev, S. Havlin, M. G. da Luz, E. P. Raposo, H. E. Stanley, Optimizing the success of random searches. *Nature*. **401**, 911–914 (1999).

143. F. Bartumeus, M. G. E. da Luz, G. M. Viswanathan, J. Catalan, Animal search strategies: A quantitative random-walk analysis. *Ecology*. **86**, 3078–3087 (2005).

144. A. Mårell, J. P. Ball, A. Hofgaard, Foraging and movement paths of female reindeer: insights from fractal analysis, correlated random walks, and Lévy flights. *Can. J. Zool.* **80**, 854–865 (2002).

145. A. M. Reynolds, M. A. Frye, Free-flight odor tracking in Drosophila is consistent with an optimal intermittent scale-free search. *PLoS One*. **2**, e354 (2007).

146. A. M. Reynolds, Extending Lévy search theory from one to higher dimensions: Lévy walking favours the blind. *Proc. Math. Phys. Eng. Sci.* **471**, 20150123 (2015).

147. P. V. Switzer, Site fidelity in predictable and unpredictable habitats. *Evol. Ecol.* **7**, 533–555 (1993).

148. K. C. Hamer, R. A. Phillips, J. K. Hill, S. Wanless, A. G. Wood, Contrasting foraging strategies of gannets *Morus bassanus* at two North Atlantic colonies: foraging trip duration and foraging area fidelity. *Mar. Ecol. Prog. Ser.* **224**, 283–290 (2001).

149. J. Nauta, Y. Khaluf, P. Simoens, Hybrid foraging in patchy environments using spatial memory. *J. R. Soc. Interface*. **17**, 20200026 (2020).

150. N. P. Moran, A. Sánchez-Tójar, H. Schielzeth, K. Reinhold, Poor nutritional condition promotes high-risk behaviours: a systematic review and meta-analysis. *Biol. Rev. Camb. Philos. Soc.* **96**, 269–288 (2021).

151. J. H. Lammers, K. Warburton, B. W. Cribb, Anti-predator strategies in relation to diurnal refuge usage and exploration in the australian freshwater prawn, *Macrobrachium australiense*. *J. Crustacean Biol.* **29**, 175–182 (2009).

152. M. de la Flor, L. Chen, C. Manson-Bishop, T.-C. Chu, K. Zamora, D. Robbins, G. Gunaratne, G. Roman, Drosophila increase exploration after visually detecting predators. *PLoS One*. **12**, e0180749 (2017).

153. O. Lapiedra, T. W. Schoener, M. Leal, J. B. Losos, J. J. Kolbe, Predator-driven natural selection on risk-taking behavior in anole lizards. *Science*. **360**, 1017–1020 (2018).

154. C. Schradin, N. Pillay, Female striped mice (*Rhabdomys pumilio*) change their home ranges in response to seasonal variation in food availability. *Behav. Ecol.* **17**, 452–458 (2006).

155. G. J. M. Rickbeil, J. A. Merkle, G. Anderson, M. P. Atwood, J. P. Beckmann, E. K. Cole, A. B. Courtemanch, S. Dewey, D. D. Gustine, M. J. Kauffman, D. E. McWhirter, T. Mong, K. Proffitt, P. J. White, A. D. Middleton, Plasticity in elk migration timing is a response to changing environmental conditions. *Glob. Chang. Biol.* **25**, 2368–2381 (2019).

156. J. F. Duquette, J. L. Belant, C. M. Wilton, N. Fowler, B. W. Waller, D. E. Beyer Jr, N. J. Svoboda, S. L. Simek, J. Beringer, Black bear (*Ursus americanus*) functional resource selection relative to intraspecific competition and human risk. *Can. J. Zool.* **95**, 203–212 (2017).

157. A. Lepik, M. Abakumova, J. Davison, K. Zobel, M. Semchenko, Spatial mapping of root systems reveals diverse strategies of soil exploration and resource contest in grassland plants. *J. Ecol.* **109**, 652–663 (2021).

158. A. G. Marr, R. J. Harvey, W. C. Trentini, Growth and division of *Escherichia coli*. *J. Bacteriol.* **91**, 2388–2389 (1966).

159. J. T. Staley, Prosthecomicrobium and Ancalomicrobium: new prosthecate freshwater bacteria. *J. Bacteriol.* **95**, 1921–1942 (1968).

160. S. Chiewchanvit, P. Mahanupab, P. Hirunsri, N. Vanittanakom, Cutaneous manifestations of disseminated *Penicillum marneffei* mycosis in five HIV-infected patients. *Mycoses*. **34**, 245–249 (2009).

161. J. Vávra, A. Horák, D. Modrý, J. Lukes, B. Koudela, *Trachipleistophora extenrec* n. sp. a new microsporidian (fungi: microsporidia) infecting mammals. *J. Eukaryot. Microbiol.* **53**, 464–476 (2006).

162. M. T. Cushion, Are members of the fungal genus pneumocystis (a) commensals; (b) opportunists; (c) pathogens; or (d) all of the above? *PLoS Pathog.* **6**, e1001009 (2010).

163. K. Hanamura, H. Endoh, Binary fission and encystation of opalina sp. in Axenic Medium. *jzoo*. **18**, 381–387 (2001).

164. J. H. Gregg, Developmental potential of isolated *Dictyostelium* rnyxamoebae'. *Dev. Biol.* **26**, 478–485 (1971).

165. T. Y. Kingma Boltjes, Über *Hyphomicrobium vulgare* Stutzer et Hartleb. *Archiv für Mikrobiologie*. **7**, 188–205 (1936).

166. N. Pfennig, G. cohen-Bazire, Some properties of the green bacterium *Pelodictyon clathratiforme*. *Arch. Mikrobiol.* **59**, 226–236 (1967).

167. E. Duchow, H. C. Douglas, *Rhodomicrobium vannielii*, a new photoheterotrophic bacterium. *Journal of Bacteriology*. **58**, 409–416 (1949).

168. J. L. Shannon, A. H. Rothman, Transverse septum formation in budding cells of the yeastlike fungus *Candida albicans*. *J. Bacteriol.* **106**, 1026–1028 (1971).

169. A. B. Herrero, M. C. López, L. Fernández-Lago, A. Domínguez, *Candida albicans* and *Yarrowia lipolytica* as alternative models for analysing budding patterns and germ tube formation in dimorphic fungi. *Microbiology*. **145 (Pt 10)**, 2727–2737 (1999).

170. L. H. Hartwell, *Saccharomyces cerevisiae* cell cycle. *Bacteriol. Rev.* **38**, 164–198 (1974).

171. A. B. Fischer, D. K. Hofmann, Budding, bud morphogenesis, and regeneration in *Carybdea marsupialis* Linnaeus, 1758 (Cnidaria: Cubozoa). *Hydrobiologia*. **530–531**, 331–337 (2004).

172. H. Van Iten, R. S. Cox, Evidence of clonal budding in a radial cluster of *Paraconularia crustula* (White) (Pennsylvanian: Cnidaria). *Lethaia*. **25**, 421–426 (1992).

173. R. H. Kessin, *Dictyostelium: Evolution, Cell Biology, and the Development of Multicellularity* (Cambridge University Press, 2001).

174. A. Driks, Overview: Development in bacteria: spore formation in *Bacillus subtilis*. *Cell. Mol. Life Sci.* **59**, 389–391 (2002).

175. T. T. Wyatt, H. A. B. Wösten, J. Dijksterhuis, in *Advances in Applied Microbiology*, S. Sariaslani, G. M. Gadd, Eds. (Academic Press, 2013), vol. 85, pp. 43–91.

176. M. Huang, C. M. Hull, Sporulation: how to survive on planet Earth (and beyond). *Curr. Genet.* **63**, 831–838 (2017).

177. F.-P. J. Martin, N. Sprenger, I. K. S. Yap, Y. Wang, R. Bibiloni, F. Rochat, S. Rezzi, C. Cherbut, S. Kochhar, J. C. Lindon, E. Holmes, J. K. Nicholson, Panorganismal gut microbiome-host metabolic crosstalk. *J. Proteome Res.* **8**, 2090–2105 (2009).

178. P. Schnupf, V. Gaboriau-Routhiau, P. J. Sansonetti, N. Cerf-Bensussan, Segmented filamentous bacteria, Th17 inducers and helpers in a hostile world. *Curr. Opin. Microbiol.* **35**, 100–109 (2017).

179. C. P. Davis, D. C. Savage, Habitat, succession, attachment, and morphology of segmented, filamentous microbes indigenous to the murine gastrointestinal tract. *Infect. Immun.* **10**, 948–956 (1974).

180. J. Dighton, J. White, P. Oudemans, *The fungal community: its organization and role in the ecosystem, Second Edition* (CRC Press, 1992).

181. R. Garilleti, V. Mazimpaka, F. Lara, New *Ulota* species with multicellular spores from southern South America. *bryo*. **115**, 585–600 (2012).

182. R. Nathan, E. Klein, J. J. Robledo-Arnuncio, E. Revilla, in *Dispersal Ecology and Evolution*, J. Clobert, M. Baguette, T. G. Benton, J. M. Bullock, Eds. (OUP Oxford, 2012).

183. J. Bezanson, A. Edelman, S. Karpinski, V. B. Shah, Julia: A fresh approach to numerical computing. *SIAM Rev.* **59**, 65–98 (2017).

184. M. E. Brooks, K. Kristensen, K. J. van Benthem, A. Magnusson, C. W. Berg, A. Nielsen, H. J. Skaug, M. Maechler, B. M. Bolker, glmmTMB Balances speed and flexibility among packages for zero-inflated generalized linear mixed modeling. *The R Journal*. **9** (2017), pp. 378–400.

185. Y. Kakiuchi, T. Ueda, Fragmentation of the plasmodium into equally sized pieces by low temperatures in the true slime mold *Physarum polycephalum*: A new morphogenesis. *Protoplasma*. **206**, 131–136 (1999).

186. Y. Kakiuchi, T. Takahashi, A. Murakami, T. Ueda, Light irradiation induces fragmentation of the Plasmodium, a novel photomorphogenesis in the true slime mold *Physarum polycephalum*: Action spectra and evidence for involvement of the phytochrome¶. *Photochem. Photobiol.* **73**, 324–329 (2007).

187. D. Mahishi, T. Triphan, R. Hesse, W. Huetteroth, The Panopticon-assessing the effect of starvation on prolonged fly activity and place preference. *Front. Behav. Neurosci.* **15**, 640146 (2021).

188. C. Mayack, D. Naug, Individual energetic state can prevail over social regulation of foraging in honeybees. *Behav. Ecol. Sociobiol.* **67**, 929–936 (2013).

189. O. L. Crino, K. L. Buchanan, L. Trompf, M. C. Mainwaring, S. C. Griffith, Stress reactivity, condition, and foraging behavior in zebra finches: effects on boldness, exploration, and sociality. *Gen. Comp. Endocrinol.* **244**, 101–107 (2017).

190. A. Kacelnik, M. Vasconcelos, T. Monteiro, J. Aw, Darwin's "tug-of-war" vs. starlings' "horse-racing": how adaptations for sequential encounters drive simultaneous choice. *Behav. Ecol. Sociobiol.* **65**, 547–558 (2011).

191. C. He, D. J. Klionsky, Regulation mechanisms and signaling pathways of autophagy. *Annu. Rev. Genet.* **43**, 67–93 (2009).

192. H. V. Westerhoff, A. N. Brooks, E. Simeonidis, R. García-Contreras, F. He, F. C. Boogerd, V. J. Jackson, V. Goncharuk, A. Kolodkin, Macromolecular networks and intelligence in microorganisms. *Front. Microbiol.* **5**, 379 (2014).

193. R. Solé, M. Moses, S. Forrest, Liquid brains, solid brains. *Philos. Trans. R. Soc. Lond. B Biol. Sci.* **374**, 20190040 (2019).